Genetics and Kinetics of Fetal Cell Microchimerism

A thesis submitted by

Stephanie Pritchard

In partial fulfillment of the requirements for the degree of

Doctor of Philosophy

in Genetics

TUFTS UNIVERSITY

Sackler School of Graduate Biomedical Sciences

May 2013

Advisor: Diana W. Bianchi, M.D.

ABSTRACT

During each pregnancy, cells from the fetus travel into the maternal circulation and organs, resulting in the development of life-long microchimerism. It is currently uncertain whether persistent fetal cells have beneficial or harmful effects on maternal health, or whether they have any effect at all. Evidence from multiple laboratories suggests that microchimeric fetal cells contribute to maternal tissue repair after injury. A deeper understanding of their phenotype and postpartum trafficking patterns of fetal cells would permit better understanding of possible mechanisms by which they affect maternal health. The research presented here aimed to close these knowledge gaps.

Using a mouse model in which a wild type female is mated to a male homozygous for the *Egfp* transgene, fetal cells in the maternal organs were easily identified by their green fluorescence using high-speed flow cytometery. Small numbers of fetal cells were flow-sorted from the maternal lung in both syngeneic and allogeneic matings, facilitating discovery-driven gene expression analysis. Multidimensional gene expression microarray analysis of these fetal cells suggests that fetal cells in the murine maternal lung are a mixed population during pregnancy, consisting of trophoblasts, mesenchymal stem cells (MSCs) and cells of the immune system. Further characterization of fetal MSCs and immune cells in the maternal organs was limited by the small number of cells present. These results underscore the challenges of working with these rare cells. Functional significance of these cell types was further explored in two different injury models, contact hypersensitivity and unilateral pneumonectomy.

Previous work has shown that the maternal lungs contain the greatest number of fetal cells, and that their levels increase throughout gestation. These findings were augmented through analysis in this dissertation of the natural history of fetal cells in the

postpartum maternal lungs and bone marrow. The results showed that fetal cells persist in these organs until at least three months postpartum in healthy female mice. A two-stage decline was observed, with an initial two and a half-week rapid clearance followed by a trend of gradual decrease. Additionally, an increase in the ratio of live to dead cells within the lung over time suggests that these cells may replicate in vivo.

In conclusion, in this work we demonstrate that low numbers of fetal cells can be flow-sorted from the maternal organs and reproducible gene expression information can be obtained from them. In syngeneic pregnancy, fetal cells in the maternal lung are primarily trophoblasts, mesenchymal stem cells, and cells of the immune system. In allogeneic pregnancies, fetal cells appear to be less differentiated. We recommend that future mouse studies of fetal cell microchimerism should use allogeneic matings wherever possible, to more closely reflect the heterogeneity found in human reproduction. We also show that fetal cell clearance in postpartum maternal organs is a two-stage process. Future murine injury experiments investigating the potential postpartum effects of fetal cells on maternal tissue repair should start at a minimum of 17-18 days after delivery to be certain that the initial clearance stage has been completed.

ACKNOWLEDGMENTS

It would not have been possible to write this doctoral thesis without the help and support of many people, only some of whom it is possible to give particular mention here.

This thesis would not have been possible without the support, guidance and patience of my mentor, Dr. Diana Bianchi. I am especially grateful for her constant and unwavering encouragement to see the strengths of my work. She taught me, both consciously and unconsciously, what it means to be a physician-scientist. I look forward to continuing our relationship throughout my career.

Dr. Kirby Johnson, Ms. Helene Stroh, Dr. Lisa Kallenbach, Dr. Jill Maron, and Ms. Jessica Dietz all taught me critical laboratory skills, and helped me remain optimistic in the face of “failed” experiments.

Dr. Lisa Hui and Dr. Lillian Zwemer were both instrumental in the latter parts of this work, not only for discussion of laboratory techniques, assistance with data analysis, and critical reading of this thesis, but also for offering a listening ear and reassurance.

Ms. Heather Wick performed the microarray normalization and some of the associated analyses, often under a looming, not-too-distant deadline. Without her enthusiasm and commitment I could not have accomplished all that I did. Merely saying “thank you” does not appropriately convey the depth of my gratitude.

I would like to thank the other members of the Bianchi Laboratory, both past and present, including Dr. Lauren Massingham, Dr. Andrea Edlow, Dr. Elizabeth Taglauer, Dr. Faycal Guedj, and Ms. Sarah Hwang, for providing stimulating conversations, friendly company, and taste-testers for the results of my baking experiments.

Mr. Stephen Kwok and Mr. Allen Parmelee of the Tufts University Flow Cytometry Core Facility both went above and beyond to provide assistance with FACS. We have spent many hours together staring at a computer screen hoping for green cells to appear. This project would not have been possible without their dedication and flexibility.

Dr. Andrew Hoffman and Ms. Airiel Davis provided expertise in the surgical, physiologic and analytical aspects of the mouse lung. I am greatly appreciative of their vital collaboration on the pneumonectomy injury model.

My thesis committee, Dr. Peter Brodeur, Dr. Gordon Huggins, and Dr. Janis Lem, provided essential guidance throughout the project for which I am indebted to them. I would also like to express my gratitude to Dr. Keelin O'Donoghue for agreeing to examine this thesis.

I would like to acknowledge the financial, academic and technical support of the Genetics Program and Tufts University, particularly the Sackler Dean's Fellowship and the Provost Fund, which provided financial support for this research. Thank you also to Dean Naomi Rosenberg and Dr. Jim Schwob for guidance and advice throughout my time at Tufts.

I received additional financial support from the NIH training grant T32 HD049341, which provided my stipend for one year.

Amongst my fellow graduate students, I would like to especially thank Christina Binder, Karyn Austin, Marina Freytsis, Laura Gainey and Samuel Stampfer for their friendship, advice, and invariable willingness to meet for a beer, a run, or seaweed facemasks.

Finally, to my mom and dad, my sister, and Rich, my other half: thank you for protecting my mental sanity. Working on the PhD has been a wonderful, but often overwhelming and frustrating task. Without your encouragement, hugs and cooking, this process would have been even more challenging. I cannot thank you enough.

TABLE OF CONTENTS

TABLE OF TABLES

TABLE OF FIGURES

LIST OF PUBLICATIONS

Pritchard S, Hoffman AM, Johnson KL, Bianchi DW. 2011. Pregnancy-associated progenitor cells: An under-recognized potential source of stem cells in maternal lung. *Placenta* 32 Suppl 4:S298-303

Pritchard S and Bianchi DW. 2012. Fetal cell microchimerism in the maternal heart: Baby gives back**.** *Circulation Research* 110: 3-5

Pritchard S, Wick HC, Slonim DK, Johnson KL, Bianchi DW. 2012. Comprehensive analysis of genes expressed by rare microchimeric fetal cells in the maternal mouse lung. *Biology of Reproduction* 87(2):42,1-6

Pritchard S, Peter I, Johnson KL, Bianchi DW. 2012. The natural history of fetal cells in postpartum murine maternal lung and bone marrow: A two stage phenomenon. *Chimerism* 3(3):59-64

CO-AUTHOR CONTRIBUTIONS

Diana W. Bianchi, MD

Mother Infant Research Institute, Floating Hospital at Tufts Medical Center, Boston, Massachusetts

Dr. Bianchi provided guidance for study design, data analysis and interpretation, and project development. She supervised the data analysis, provided guidance on the general direction of this thesis, and critically reviewed all manuscripts.

Kirby L. Johnson, PhD

Mother Infant Research Institute, Floating Hospital at Tufts Medical Center, Boston, Massachusetts

Dr. Johnson provided support with laboratory training, experimental design, data analysis and interpretation, and manuscript preparation.

Heather C. Wick, BS

Department of Computer Science, Tufts University, Medford, Massachusetts

Ms. Wick normalized microarray gene expression datasets and assisted with statistical analysis for all microarray experiments.

Donna K. Slonim, PhD

Department of Computer Science, Tufts University, Medford, Massachusetts

Dr. Slonim provided advice and collaboration on development of the computational methods used for determination of fetal cell phenotype, statistical expertise on multiple testing adjustments, and pre-processing and normalization of data. She performed the

BioGPS analysis for tissue-specific probes for the syngeneic lung gene expression project.

Inga Peter, PhD

Department of Genetics and Genomic Sciences, Mount Sinai School of Medicine, New York, New York

Dr. Peter performed the statistical analysis for the postpartum fetal cell kinetics project.

Andrew M. Hoffman, PhD

Department of Clinical Sciences, Cummings School of Veterinary Medicine at Tufts University, North Grafton, Massachusetts

Dr. Hoffman helped develop, supervise and analyze the pneumonectomy study.

Airiel M. Davis

Department of Clinical Sciences, Cummings School of Veterinary Medicine at Tufts University, North Grafton, Massachusetts

Ms. Davis helped develop the pneumonectomy study, performed the surgeries and handled postsurgical animal care.

ABBREVIATIONS USED IN THIS DISSERTATION

BH: Benjamini-Hochberg

BSA: Bovine serum albumin

CHS: Contact hypersentitivity

DMEM: Dulbecco modified eagle medium

DPBS: Dulbecco phosphate buffered saline

Egfp: Enhanced green fluorescent protein

EPCs: Endothelial progenitor cells

FACS: Fluorescence-activated cell sorting

GEO: Gene Expression Omnibus

GFP: Green fluorescent protein

HLA: Human leukocyte antigen

HSCs: Hematopoietic stem cells

IPA: Ingenuity Pathway Analysis

MSCs: Mesenchymal stem cells

MHC: Major histocompatibility complex

MoM: Multiples of the median

PCA: Principal component analysis

PI: Propidium iodide

qRT-PCR: Quantitative reverse transcriptase polymerase chain reaction

RSA: Recurrent spontaneous abortion

vWF: von Willibrand factor

INTRODUCTION

Over 90% of women in the United States experience at least one pregnancy in their lifetime (Chandra et al., 2005). Transplacental bidirectional trafficking of cells from the fetus to the mother occurs in all human pregnancies (Ariga et al., 2001; Michaelsson et al., 2006; O'Donoghue et al., 2004). Although the exact purpose of this cellular exchange is unknown, it is thought to be important in development of immune tolerance of the mother to the fetus and vice versa (Michaelsson et al., 2006; Mold et al., 2008; Nijagal et al., 2011; Taglauer et al., 2010). Substantial numbers of fetal cells persist in the maternal circulation and tissues without evidence of immune rejection. This has given rise to the term fetal cell microchimerism (Liegeois et al., 1981). Fetal cells can be identified for decades after the pregnancy (Bianchi et al., 1996; Lissauer et al., 2007; O'Donoghue et al., 2004). Therefore, as a result of pregnancy, females acquire populations of cells that have unknown effects on their health.

Despite years of research, the maternal health implications of fetal microchimeric cells remains unknown (Lee et al., 2010). The intrinsic phenotypic properties of these cells may affect their impact on health. For example, if they have stem cell-like properties, they may contribute to maternal tissue repair. If instead they are more mature, their presence could trigger autoimmune disease due to co-expression of maternal antigens (Johnson and Bianchi, 2004). The work described in this thesis sought to identify potential maternal health implications of fetal cell microchimerism by determining the phenotype of fetal cells in maternal organs as well as the kinetics of fetal cell clearance in the postpartum period. This introduction will explore the history, discovery and biological function of fetal cell microchimerism; discuss its potential role in disease; and highlight gaps in knowledge.

DISCOVERY OF FETOMATERNAL CELL TRAFFICKING IN HUMANS

The first report of fetal cells in the maternal organs occurred in 1893. German pathologist Georg Schmorl observed multi-nucleated giant cells in the pulmonary circulation of women who had died of eclampsia (Lapaire et al., 2007). The cells were adherent to the capillary walls and within the lumen of the vessels. He surmised that the placenta was the source of these cells due to their morphology and consistent presence in all of the women studied. He further hypothesized that fetomaternal cell trafficking might also occur in normal pregnancies, although his own investigations on this matter were unsuccessful.

Schmorl's discovery was not revisited for another 70 years. Starting in the late 1950s, multiple investigators reported on the presence of fetal erythrocytes in the maternal circulation in the peripartum period (Bromberg et al., 1956; Clayton et al., 1962; Cohen et al., 1964; Zipursky et al., 1959). Fetal erythrocytes were identified by fetal hemoglobin staining using the Kleihauer-Betke test. These red blood cells were thought to enter the maternal circulation through fetomaternal hemorrhage, especially during labor and delivery.

This notion was dispelled a few years later. Examining the circulating lymphocytes of pregnant women, researchers noticed cells with an additional small acrocentric chromosome, consistent with a 46,XY karyotype (Walknows.J et al., 1969). Fetal leukocytes were found in nineteen of twenty-two women who subsequently gave birth to males. Two of eight women who delivered females had XY cells, which were presumed to be derived from prior pregnancies with male fetuses. This was the first hint of long-term postpartum persistence of fetal cells. Due to discordance between the ratio of fetal erythrocytes and lymphocytes in maternal versus fetal blood, the authors

concluded that mechanisms other than leakage of blood must have been responsible for fetal lymphocyte transplacental passage. They suggested that lymphocytes cross to the maternal circulation in a fashion similar to their migration through vascular endothelium.

Research over the next decade focused on whether these fetal cells could be used for non-invasive determination of fetal sex. Male fetal cells were identified by maternal peripheral blood culture and detection of nuclei containing a Y chromosome. Using microscopic analysis and quinacrine fluorescence, it was estimated that 0.1-0.5% of lymphocytes in the blood of pregnant women were fetal (Schroder and Chapelle, 1972). This method, however, resulted in many false negatives, as it required examination of thousands of cells and identification of only a few XY cells. Due to the highly subjective nature of this process, many physicians and scientists remained skeptical of fetomaternal cell trafficking (Schroder, 1975). Herzenberg and colleagues (Herzenberg et al., 1979) developed a more objective method by using antibodies to paternally-inherited HLA-A2 and fluorescence-activated cell sorting (FACS) to collect fetal cells from maternal blood.

Improved sensitivity allowed detection of progressively lower concentrations of fetal cells in the maternal circulation. Initially fetal cells were thought to be cleared immediately following pregnancy. Then persistence of fetal cells in maternal blood was shown at one (Schroder et al., 1974) and five (Ciaranfi et al., 1977) years postpartum. A turning point occurred in 1996 when it was first discovered that human fetal cells could be detected in maternal blood for several decades postpartum (Bianchi et al., 1996). Since then, fetal cells have been found up to 50 years postpartum (O'Donoghue et al., 2004), suggesting lifelong persistence in the mother.

The potential clinical implications of long-term microchimerism gained more importance after these discoveries. The priorities for subsequent research included determining whether fetal cells replicated within maternal organs, whether fetal cell

trafficking was physiologically necessary for a successful pregnancy, and investigation of the relationship of fetal cells to postpartum maternal health. Most human studies on fetal microchimerism are restricted to qualitative studies of the presence or absence of fetal cells in various tissues and diseases. Confounding these studies is the fact that women may receive male cells from other sources, such as blood transfusions or a male twin. It has even been suggested that a female fetus could acquire cells or DNA from an older male sibling as a result of microchimerism in the mother (Dawe et al., 2007; Nelson, 2003). Research involving human samples is associated with other challenges, including limited access to tissues in living subjects and lack of complete reproductive history (including miscarriages and elective terminations) for deceased subjects (Khosrotehrani and Bianchi, 2005; Lee et al., 2010). Animal models of fetal microchimerism have therefore made a valuable contribution to our current understanding of this phenomenon. Such studies allow greater access to tissues, complete control of reproductive history and more in-depth studies of the dynamics of microchimerism. Additionally, animal experiments can be designed to investigate the potential mechanistic role of fetal cells in disease and establish causality.

ANIMAL MODELS

One of the most popular animal models is the mouse. Mice are commonly used for many reasons including the relative ease of housing and ability for genetic manipulation. Obvious differences exist between murine and human pregnancies, most notably the length of gestation and the number of fetuses per pregnancy. Slight distinctions also exist between the developmental timing and structure of murine and human placentas (Dawe et al., 2007; Georgiades et al., 2002; Malassine et al., 2003). Despite these differences anatomical observations and descriptive gene expression

studies suggest comparable function between them, permitting researchers to draw conclusions about humans from mouse models (Georgiades et al., 2002).

Similar to human studies that focus on identification of the Y chromosome in the mother, animal models use a paternally inherited marker to identify microchimeric fetal cells. These markers range from extra chromosomes (Liegeois et al., 1977; Liegeois et al., 1981) to fluorescent markers like green fluorescent protein (GFP) (Fujiki et al., 2008b) and luciferase (Bou-Gharios et al., 2011; Dubernard et al., 2009). Fluorescent markers may be under the control of either a ubiquitiously-expressed promoter, such as that for ß-actin (Fujiki et al., 2008a; Fujiki et al., 2008b; Fujiki et al., 2009), or a specific promoter to highlight only the fetal cells expressing a specific gene (Dubernard et al., 2009; Huu et al., 2007).

The use of animal models has permitted a deeper understanding of fetal cell kinetics in the mother during and following pregnancy. As fetal cells are rare, it was initially important to determine the natural history of their presence in maternal blood and organs before determining their function. Several groups have now demonstrated that fetal cell microchimerism starts early in gestation and increases progressively, peaking immediately prior to delivery (Fujiki et al., 2008a; Sunami et al., 2010; Vernochet et al., 2007). Furthermore, the maternal lung contains the greatest concentration of fetal cells (Fujiki et al., 2008a; Kallenbach et al., 2011a; Khosrotehrani et al., 2005). The spleen, liver, blood and kidney also contain a large number of fetal cells. Fewer are found in the bone marrow, heart, brain and thymus (Fujiki et al., 2008a).

Fetal cells have also been detected in the uterine draining lymph nodes (Bonney and Matzinger, 1997) suggesting that they may enter the maternal blood stream via the uterine vein, which drains into the maternal pulmonary arteries. The pulmonary circulation is therefore the first capillary bed to receive fetal cells. Many of them may be filtered out before they can pass to other organs, explaining their prevalence in the

lungs. Filtration is also supported by the finding that fetal cells in maternal lung express a diverse array of antigens that are typical of both mature and immature cell types (Fujiki et al., 2009). This is in contrast to more uniform populations of cells demonstrated in the bone marrow, kidney, thymus and brain (Fujiki et al., 2009). These results suggest that different organs contain different types of fetal cells, although the mechanism for site-specific homing or survival remains unknown.

While the bulk of research has been performed in mice, fetal cell trafficking is also known to occur in other eutherians, including rats (Wang et al., 2004), monkeys (Jimenez and Tarantal, 2003; Jimenez et al., 2005), pigs (Rudek and Kwiatkowska, 1983), and cows (Turin et al., 2007). Because of the widespread and consistent nature of fetomaternal trafficking between mammalian species, it is highly likely that the phenomenon plays an important role despite anatomic differences in the placentas of these species.

BIOLOGICAL FUNCTION

In the 1950s, the immunologist Peter Medawar was the first to recognize that something unique was happening during pregnancy (Medawar, 1953). He realized that while a female would mount an immune rejection response to a skin graft from the male partner, this did not occur in response to the fetus, despite its expression of foreign paternal antigens. Furthermore, during the presence of this “foreign transplant”, the woman remained immunocompetent, suggesting a more complex mechanism than global immune suppression during pregnancy (Chamley et al., 2011; Medawar, 1953; Taglauer et al., 2010). Since this discovery, multiple mechanisms have been proposed to facilitate this immunological tolerance: physical separation of maternal and fetal tissues (Chen et al., 2012), decreased major histocompatibility (MHC) protein expression

by fetal and placental tissues (Scherjon et al., 2011; Taglauer et al., 2010), the presence of T-regulatory cells that suppress the maternal immune response (Aluvihare et al., 2004; Zenclussen, 2005), increased levels of the Th2 cytokines IL-4, IL-10 and IL-13 (Chen et al., 2012; Thaxton and Sharma, 2010) and exposure to paternal antigens on circulating fetal and placental cells (Chamley et al., 2011; Taglauer et al., 2010).

In the 1960s, fetal cell trafficking was suspected to be an important factor in establishing maternal tolerance to paternal antigens in the fetus (Walknows.J et al., 1969). Starting early in pregnancy, chronic low dose exposure to fetal antigens was speculated to attenuate the ability of the maternal immune system to specifically respond. This finding is supported by more recent work showing altered levels of microchimerism depending on the extent of immunocompatibility between the mother and fetus (Adams Waldorf et al., 2010; Kallenbach et al., 2011a; Khosrotehrani et al., 2005). Additionally, macrophages and dendritic cells, when exposed to trophoblast debris, transition to an immunosuppressive phenotype (Abumaree et al., 2012; Salamone et al., 2012). Macrophages increase secretion of anti-inflammatory cytokines and reduced expression of co-stimulatory molecules such as CD40 and CD86 (Abumaree et al., 2012) while trophoblast-exposed dendritic cells increased the frequency of FoxP3+ T regulatory cells (Salamone et al., 2012).

Although trophoblasts likely make up a substantial proportion of fetal cells in the maternal organs and circulation, they can be detected before the placental circulation has developed. Fetal cells can be detected in the murine maternal lung, liver, spleen, bone marrow, pancreas, heart and kidney as early as gestational day six or seven (Khosrotehrani et al., 2005; Sunami et al., 2010). In humans they can be observed as early as week four (Huu et al., 2006) and they persist for decades postpartum (Bianchi et al., 1996; O'Donoghue et al., 2004; O'Donoghue et al., 2008). They are also capable of differentiating into multiple tissue types (Lee et al., 2010; O'Donoghue et al., 2004;

O'Donoghue et al., 2008). In contrast, trophoblasts are cleared from lungs by two weeks postpartum (Abumaree et al., 2012; Attwood and Park, 1961), and are terminally differentiated (Burton and Jones, 2009).

Of the solid organs, the maternal lungs contain the greatest quantity of fetal cells during pregnancy (Fujiki et al., 2008a; Kallenbach et al., 2011a; Khosrotehrani et al., 2005). The lung mucosal surface is a key site of interaction between the environment and the bloodstream. Multiple mechanisms have developed to protect the body from pathogens, including alveolar epithelial cells, dendritic cells and alveolar macrophages (Schaible et al., 2010). Resident dendritic cells are capable of inducing either an immune response or anergy (von Garnieir and Nicod, 2009). It is possible that cells of the immune system residing in the lung can also interact with fetal cells to induce tolerance during pregnancy.

Pregnancy complications that are associated with increased fetomaternal trafficking include fetal aneuploidy (Bianchi et al., 1997), idiopathic polyhydramnios (Zhong et al., 2000), and preeclampsia (Al-Mufti et al., 2000; Chua et al., 1991; Holzgreve et al., 1998; Lo et al., 1999). Preeclampsia is characterized by hypertension and proteinuria developing after 20 weeks' gestation. Although the exact etiology of preeclampsia is unknown, there is evidence to suggest a role for the maternal immune response. Exposure to paternal antigens in semen is protective while a prolonged interval between pregnancies or a change in partner increases the incidence of preeclampsia (Campbell et al., 1985; Koelman et al., 2000; Zhang and Patel, 2007). The pathophysiology involves the development of placental hypoperfusion due to failure of spiral artery remodeling and poor trophoblast invasion into the uterine myometrium during the first trimester.

It is possible that the increased fetal cell trafficking observed in preeclampsia is a result of the placental dysfunction and fetomaternal hemorrhage (Lee et al., 2010).

Alternatively it could be a compensatory reaction to this disease. The fetoplacental unit may be able to respond to maternal immune dysregulation and facilitate increased release of cells. This might not be the case, however, as levels of circulating trophoblasts do not correlate with disease severity (Johansen et al., 1999). More research is needed to fully appreciate the role of fetal and trophoblast trafficking during both normal and preeclamptic pregnancies.

Additional support for the immune tolerance hypothesis comes from observations of recurrent spontaneous abortion (RSA). RSA is defined as greater than two miscarriages with the same partner (Beaman et al., 2012). It has been postulated that insufficient fetal cell trafficking is partially to blame in some cases (Artlett, 2005). Pregnant women produce antibodies to mismatched fetal HLA antigens (Reed et al., 1991). Women who are treated with killed paternal white blood cells are able to successfully carry a pregnancy, suggesting an underlying immune etiology for RSA (Beer et al., 1985; Lubinski et al., 1993). It is possible that circulating fetal cells are able to bind and sequester anti-HLA antibodies and thus prevent transfer to and rejection of the fetus (Artlett, 2005; Reed et al., 1991).

Because most hypotheses regarding the biological function of fetal cell trafficking relate to pregnancy, microchimerism research has largely focused on the role of cell trafficking during pregnancy. Less attention has been paid to cell trafficking after birth, even in animal models. It is interesting to contemplate why these cells persist after parturition if their role were simply to facilitate maternal-fetal immunocompatibility. This raises the question or whether there is some evolutionary advantage to the longterm circulation of microchimeric fetal cells—if perhaps these cells remain in the mother to augment her response to injury and disease.

CLINICAL IMPLICATIONS OF FETAL CELL MICROCHIMERISM

The study of microchimerism is important because as a result of pregnancy, females acquire populations of foreign, viable cells that have unknown effects on their health. One postulated adverse consequence of long-term microchimerism is the induction of a form of "graft-versus-host reaction" leading to autoimmune disease. This is a potential explanation for why many autoimmune diseases are most prevalent in middle-aged women (Nelson, 1996). An alternative hypothesis is that fetal cells may home to sites of disease where they act as stem cells and participate in tissue repair (Khosrotehrani et al., 2004). A third hypothesis is that the fetal cells are merely passive bystanders that have no physiologic effect on maternal health (Johnson and Bianchi, 2004; Nelson, 2001).

It is also possible that fetal cells have different roles in different diseases, and could be harmful in some yet beneficial in other disorders (Fugazzola et al., 2011). The presence of fetal cells in the maternal organs may also impact solid organ transplantation when either the donor or the recipient is a parous female (Dutta and Burlingham, 2011). That female adult organs contain additional cell populations from their fetuses would seem to be a major biological difference between women and men, yet the mainstream medical community has not paid much attention to this fact (Bianchi and Fisk, 2007).

Isolation of circulating fetal cells from pregnant women has been actively investigated for use in non-invasive prenatal diagnosis (Bianchi, 2000). Although this did not come to fruition, it lead to the discovery of cell-free fetal nucleic acid in the maternal blood. Recent advances in high-throughput sequencing have permitted sequencing of the entire fetal genome using cell-free fetal DNA in the maternal blood (Lo et al., 2010). Non-invasive prenatal testing for fetal aneuploidy and smaller chromosomal

abnormalities is now possible (Bianchi et al., 2012; Chiu et al., 2011; Srinivasan et al., 2013). Although non-invasive prenatal diagnosis is a clinically important development, this thesis is focused on maternal health implications. The current status of non-invasive prenatal diagnosis has been extensively reviewed elsewhere (Bianchi, 2012; Chiu and Lo, 2013; Hui and Bianchi, 2013) and will not be further considered here.

TRANSPLANTATION BIOLOGY

During pregnancy, cellular trafficking is bidirectional. It is important to remember that everyone receives cells from their mothers during gestation when considering the role of microchimerism in transplantation tolerance and rejection. Substantial numbers of maternal cells cross the placenta and travel to the fetal lymph nodes where they induce production of fetal T-regulatory cells (T-regs). The anti-maternal fetal T-regs persist into adulthood (Michaelsson et al., 2006; Mold et al., 2008) and may result in lifelong tolerogenic effects (Dutta and Burlingham, 2011). Maternal microchimerism is an important factor to consider in transplantation biology because it occurs in both males and females. Parous females uniquely have cells from their mothers and their fetuses.

Organs transplanted from women who have been pregnant may contain fetal cells. These genetically distinct cells are not considered during tissue matching of the donor and recipient, and hence could potentially affect graft rejection. Gender differences are well known in transplantation medicine and evidence to support a role of pregnancy has been found in several studies. Transplant recipients with female donors, especially multiparous female donors, have a higher incidence of chronic graft versus host disease compared to recipients with male donors (Flowers et al., 1990; Kollman et al., 2001; Lissauer et al., 2007). Bone marrow transplants from male donors also engraft

significantly faster compared to those from females (Kollman et al., 2001) and 5-year survival is lower for patients with parous donors (Flowers et al., 1990).

Fetal cells presence in the maternal bone marrow has been documented decades following pregnancy, and it is accepted that these cells persist for the rest of the woman's life (O'Donoghue et al., 2004). The consequences for transplantation medicine may be two fold: fetal cells might prime the maternal immune system against inherited paternal antigens, or fetal T cells could initiate an anti-host reaction (Lee et al., 2010; Nelson, 2008; van Rood et al., 2002).

Fetal microchimerism can also benefit a patient. The use of hematopoietic transplants for the treatment of disease is chronically limited by the lack of appropriate histocompatible donors. As recipients, parous women may be able to accept transplants from donors mismatched for paternal antigens inherited by their fetuses, thus expanding the available pool of donors (van Rood et al., 2002). It would be of great clinical significance if recipient microchimerism permitted a greater degree of HLA mismatches without adverse effects (Ichinohe et al., 2005).

Bone marrow transplants are also used in cancer treatments to take advantage of a graft versus tumor reaction. The presence of fetal T lymphocytes in these transplants may be capable of increasing this effect. Bone marrow transplants from female donors are associated with a reduced risk of leukemia relapse in male recipients (Gratwohl et al., 2001; Randolph et al., 2004). In one case, a mother received a bone marrow transplant from her 32-year-old child after establishing significant persistent fetal microchimerism (Tokita et al., 2001). The patient's thymic carcinoma slowly disappeared and she remained in remission throughout the follow-up period. Although it has been reported that fetal microchimerism is more associated with sensitization than tolerance (Dutta and Burlingham, 2011), this case would suggest otherwise. Additional cases of

remission have not been reported. Whether this form of treatment can be generalized to other patients remains to be determined.

Autoimmune Disease

Many autoimmune diseases have greater prevalence in women with specific percentages varying by country (Ngo, Steyn and McCombe, 2014). In the United States, greater than 80% of cases of systemic lupus erythematosus, Sjogren's syndrome, Celiac disease, and Grave's disease occur in women. Similar gender bias is present, although less pronounced, in rheumatoid arthritis, multiple sclerosis and myasthenia gravis while inflammatory bowel disease is evenly split between the sexes. A few disorders, namely psoriatic arthritis and ankylosing spondylitis, are more common in males, except in China, where psoriatic arthritis is almost exclusively a disease of females.

There are many underlying factors that may explain why many autoimmune dieases display such a strong gender bias, including the effect of sex hormones, differences in immune reactivity, and organ vulnerability (Marder and Somers, 2014; Ngo, Steyn and McCombe, 2014). In addition, microchimerism has also been suggested to play a role (Nelson, 1996; Nelson, 2002; McNallan et al., 2007; Ngo, Steyn and McCombe, 2014).

The postulated role of fetal cells in the pathogenesis of autoimmune disease is one of the most well-studied areas in microchimerism (Nelson, 1996). Many reports show an increase in microchimeric cells in affected tissues or affected patients. Fetal cells (as identified by the presence of the Y-chromosome) have been shown to be present in healthy and diseased tissues of women with systemic sclerosis and absent in normal control tissues (Johnson et al., 2001; Sawaya et al., 2004). Chimeric cells are also found more frequently in skin biopsies of patients with localized scleroderma

compared to controls (McNallan et al., 2007). More fetal cells were found in the thyroids of affected mice in a model of autoimmune thyroiditis compared to controls (Imaizumi et al., 2002).

Fetal cells may initiate or exacerbate autoimmune disease in several ways. Fetal immune cells may be capable of causing graft versus host reactions (Adams Waldorf et al., 2010), similar to the underlying pathology characteristic of systemic sclerosis (Nelson, 2012). Alternatively, the specific HLA molecules on microchimeric fetal cells may be important. HLA susceptibility alleles were present on microchimeric cells in women with rheumatoid arthritis, implicating fetal cells in disease etiology (Rak et al., 2009; Yan et al., 2011). Furthermore, HLA class II compatibility between the mother and child was found more frequently in women affected with scleroderma compared to controls (Nelson et al., 1998). These studies suggest that microchimerism may contribute to the risk of developing an autoimmune disease.

Others, however, have reported opposite findings showing significant differences between patients and controls (Lambert and Reed, 2006). Fetal cells were not identified in salivary gland biopsies (Aractingi et al., 2002) or peripheral blood (Toda et al., 2001) of women with Sjogren's syndrome. No difference in male DNA presence was seen between controls and women with primary biliary cirrhosis (Tanaka et al., 1999).

The conflicting evidence suggests that the impact of fetal cells on maternal autoimmune disease may be dependent on multiple factors including the specific disease, the affected organ, years since delivery, and HLA compatibility between the woman and her offspring. The consequences of fetomaternal trafficking on autoimmune disease are complex and remain to be completely elucidated (Lambert and Reed, 2006).

CANCER

In addition to its effect on autoimmune diseases, many researchers are investigating the clinical significance of fetal cell microchimerism in cancer. Proposed hypotheses about the role of fetal cells in maternal cancer include participation in angiogenesis, immunosurveillance, development of tumor stroma and/or inflammatory infiltrate, and tissue repair (Kallenbach et al., 2011b; Khosrotehrani and Aractingi, 2009). The evidence is mixed, but most studies point to a protective rather than pathogenic function (Fugazzola et al., 2010).

The majority of work has focused on the relationship between fetal cell microchimerism and breast cancer. Parity is known to protect women against developing breast cancer, historically attributed to the influence of hormones (Gadi, 2009). While hormones likely do play a part, circulating fetal cells that express proteins resembling breast cancer antigens may prepare the maternal immune system and enhance immunosurveillance (Gadi, 2009). Alternatively, fetal antigen presenting cells could present maternal antigens to maternal immune cells and have the same effect (Gadi and Nelson, 2007; Gadi, 2009). It is also possible that fetal immune cells may be performing tumor surveillance (Ichinohe et al., 2004). Women with breast cancer appear less likely than controls to have fetal DNA in their peripheral blood (Gadi and Nelson, 2007; Gadi et al., 2008). One postulated explanation for this observation is that fetal cells inhibit tumor formation by a graft versus tumor mechanism, and that the absence of fetal cells allows tumorigenesis to proceed (Gadi and Nelson, 2007). On the other hand, it has been speculated that fetal cells are recruited to the tumor sites, thus decreasing their presence in the circulation (Dubernard et al., 2009).

Studies of other cancers have also showed potential influence of fetal cells. Fetal cells were increased in both thyroid (Cirello et al., 2008) and cervical (Cha et al., 2003)

tumors compared to normal tissues. In both human and murine melanomas, fetal cells were found to selectively congregate at the tumor site compared to normal skin and benign nevi (Huu et al., 2009). Fetal cells contributed to angiogenesis and expressed endothelial antigens, suggesting a potential mechanism for how fetal cells may facilitate metastasis and cancer progression (Huu et al., 2009; Khosrotehrani and Aractingi, 2009).

In summary, the relationship between fetal cells and maternal cancer is complex and remains poorly defined (Khosrotehrani and Aractingi, 2009). Identifying the phenotype of fetal cells present in tumors as well as normal tissue may help determine the role they play in maternal neoplasia (Gadi, 2009; Kallenbach et al., 2011b). With a better understanding of this phenomenon, it may one day be possible to either expand the therapeutic potential of fetal cells or mitigate the damage they cause (Lee et al., 2010).

OTHER

The role of fetal cells in human diseases other than cancer and autoimmunity has been poorly studied. There are many individual reports describing fetal cell or DNA presence in a variety of tissues and organs, but there is no consistent body of work focusing on one disease, or exploring underlying mechanisms of disease. Studies have documented the presence of male DNA or male cells in the brains of women with Alzheimer's disease (Chan et al., 2012), inflamed appendices in pregnant women (Santos et al., 2008), a liver biopsy from a woman with hepatitis C (Johnson et al., 2002) and diseased maternal thyroid (Srivatsa et al., 2001), heart (Bayes-Genis et al., 2005) and lungs (O'Donoghue et al., 2008).

Animal model experiments have focused on determining the extent of fetal cell differentiation in maternal organs. Fetal cells differentiate into cardiomyocytes in infarcted heart tissue (Kara et al., 2012), neurons in models of Parkinson's disease (Zeng et al., 2010) and excitotoxicity (Tan et al., 2005), hepatocytes following liver injury induced by carbon tetrachloride (Khosrotehrani et al., 2007) and endothelial cells in inflamed skin (Huu et al., 2007). Due to the diversity of diseases in which microchimeric fetal cells appear to play a role, it seems likely that at least some of the cells have stem-like properties.

Involvement of Fetal Cell Microchimerism in Tissue Repair

Although the precise relationship between microchimeric fetal cells and maternal disease is still unclear, recent literature suggests that fetal cells are more likely to have a role in healing rather than in etiology of disease.

Human Studies

Because of the limitations of human research as discussed above, fetal cell differentiation is not well studied in humans. Most human studies have focused on the presence of fetal cells that have completely integrated within diseased maternal structures, such as thyroid follicles (Srivatsa et al., 2001), livers (Stevens et al., 2004) and hearts (Bayes-Genis et al., 2005). The fetal cells in these organs were morphologically indistinguishable from the maternal tissue, and identifiable as fetal only by the presence of a Y chromosome.

Other human studies have shown that fetal cells can integrate within healthy tissues such as bone (O'Donoghue et al., 2004), lung (Koopmans et al., 2008; O'Donoghue et al., 2008), thymus (O'Donoghue et al., 2008), lymph nodes and skin

(Koopmans et al., 2008), although typically to a lesser degree than at disease sites (O'Donoghue et al., 2008). Together these findings suggest that fetal cells are capable of taking part in minor, as well as major, tissue repair.

MOUSE STUDIES

Murine models have allowed investigation of the role of fetal cells in a wide range of maternal tissue injuries. Microchimeric cells appear to respond to maternal inflammatory signals. For example, fetal cells were found to respond to liver and spleen injury induced by carbon tetrachloride, but not to partial hepatectomy (Khosrotehrani et al., 2007). In models of contact dermatitis and wound healing, fetal lymphocytes and endothelial cells preferentially trafficked to the injured skin and contributed to angiogenesis (Huu et al., 2007; Nassar et al., 2012). Fetal cell-derived blood vessels were contiguous with the maternal circulation, which could be a strong indicator of collaboration with native repair mechanisms.

Fetal cells have been shown to differentiate in tissues that have limited innate regeneration, including nervous and cardiac tissue. A small study showed fetal cells at the site of spinal cord injury (Zhong and Weiner, 2007). In other reports, fetal cells crossed the blood-brain barrier and integrated within the maternal brain (Tan et al., 2005; Zeng et al., 2010). The fetal cells had morphologies similar to neurons, showing axonal and dendritic projections that became more complex over time. In the heart fetal cells were shown to selectively home to infarcted maternal cardiac tissue where they differentiated into cardiomyocytes, endothelial cells and smooth muscle cells (Kara et al., 2012). Cultured fetal cells isolated from maternal heart formed vascular tubes and spontaneously-beating cardiomyocytes.

It has been speculated that fetal cells do not differentiate at injury sites, but instead fuse with or are engulfed by maternal cells. Several authors have addressed this. In one study, fetal cells in the kidney had a cytoplasmic GFP distribution, which is evidence against phagocytosis (Wang et al., 2004). Other studies have reported on the absence of binucleated cells (Kara et al., 2012). The strongest argument against fusion involved the transfer of eGFP hemizygous blastocysts to females expressing lacZ (which produces B-galactosidase). If fusion occurred, cells expressing both eGFP and lacZ would be observed. Confocal microscopy allowed visualization of entire cells, and this did not reveal co-expression of lacZ and eGFP. This led the authors to conclude that fusion did not occur (Zeng et al., 2010).

While it is increasingly apparent that fetal cells contribute to repair of maternal tissues following injury, it is unknown whether the cells convey a physiologic benefit for the mother. It is possible that the cells collaborate but do not significantly augment intrinsic repair mechanisms. Future experiments will be important to determine whether postpartum females recover more quickly or to a greater extent than nulliparous females.

FETAL CELL PHENOTYPE(S)

One of the biggest questions in this field is the type or types of cells that are microchimeric. It is important to understand the origin and identity of microchimeric fetal cells, as their phenotype and differentiation status may impact long-term maternal health (Johnson and Bianchi, 2004; Nelson, 2012). Evidence from studies in both humans and mice suggests that microchimeric fetal cells may be stem cells or have stem-like properties (Table 1). This includes differentiation in a wide variety of injured and normal tissues (Huu et al., 2006; Johnson and Bianchi, 2004; Koopmans et al., 2008). It was originally hypothesized that microchimeric fetal cells have uniform characteristics

somewhere between those of embryonic and adult stem cells (Guillot et al., 2006; Huu et al., 2006). Antibody studies have demonstrated that during pregnancy, fetal cells, especially within the maternal lungs and liver, are a diverse group, expressing a variety of surface markers typically found on both immature and mature cell types (Fujiki et al., 2009). These included CD34 and CXCR4/CD184, both of which are expressed by primitive hematopoietic stem cells, and endoglin/CD105 and PECAM1/CD31, both of which are characteristically found on endothelial cells. It is therefore likely that females acquire multiple stem cell types during pregnancy.

Differentiation and Proliferation of Fetal Cells

In order for fetal cells to contribute to maternal repair mechanisms, they must be able to home to, differentiate into and proliferate in maternal tissues (Johnson and Bianchi, 2004). Fetal cells are clearly able to differentiate into a variety of mature phenotypes and integrate into normal, healthy tissues (Koopmans et al., 2008). Fetal cells have also been detected in structural bone marrow and when cultured, differentiated into multiple tissue types including osteocytes (O'Donoghue et al., 2004). In all of these cases, the fetal cells were indistinguishable from the native maternal tissues, which was suggestive of differentiation.

It has also been shown that fetal cells are capable of proliferation in maternal tissues. Up to five percent of fetal cells in murine maternal spleen were mitotic at 10-16 days postpartum (Liegeois et al., 1981). In the murine maternal brain, the number of fetal cells increased postpartum, suggestive of either proliferation or chemotaxis from other organs (Tan et al., 2005; Zeng et al., 2010). The long-term presence of fetal cells in maternal organs implies that the fetal cells can proliferate (Dawe et al., 2007; Khosrotehrani and Bianchi, 2005).

Overall, the literature suggests that a sub-population of microchimeric fetal cells possess properties similar to stem cells, such as plasticity and proliferation. For these reasons, microchimeric fetal cells have been called “pregnancy-associated progenitor cells,” or PAPCs (Bianchi, 2004; Huu et al., 2006; Khosrotehrani and Bianchi, 2005; Zeng et al., 2010). At least some of the fetal cells are hematopoietic stem cells, while others appear to be of a mesenchymal or endothelial lineage (Dawe et al., 2007; Khosrotehrani and Bianchi, 2005; O'Donoghue et al., 2004; Parant et al., 2009).

HEMATOPOIETIC STEM CELLS

Hematopoietic stem cells (HSCs) are arguably the most well-characterized stem cell type. HSCs are capable of differentiating into all blood cell lineages (Grove et al., 2002) and have been used for the treatment of cancer, myelodysplastic syndromes, and hereditary immunodeficiency disorders (Tse et al., 2008). Bone marrow-derived stem cells can also contribute to the epithelium of the liver, lung, gastrointestinal tract and skin (Grove et al., 2002). Human HSCs are identified by the expression of specific surface markers, including CD34, CD45, CD133 and Thy-1/CD90. Murine HSCs also express CD34 and CD45 as well as c-kit/CD117 and Sca-1 (Tarnok et al., 2010). HSCs from both species are negative for lineage-specific markers (Tarnok et al., 2010; Wognum et al., 2003).

Fetal cells have many similarities to HSCs (Table 1). Multiple research groups have used classic HSC markers to characterize fetal cells in maternal blood and other organs. CD34+ cells of fetal origin have been identified in pregnant humans (Adams et al., 2003; Bianchi et al., 1996; Guetta et al., 2003; Parant et al., 2009) and mice (Fujiki et al., 2009; Kallenbach et al., 2011a), as well as postpartum females of both species (Bianchi et al., 1996; Khosrotehrani et al., 2008). Further evidence that some fetal cells

behave like HSCs comes from the successful culture of fetal hematopoietic colony-forming units from maternal blood postpartum (Osada et al., 2001). That fetal HSCs could form large colonies highlights their proliferative capability and suggests a continued source of fetal immune cells during a woman's life.

Mouse models allow further testing of the HSC-like capabilities of microchimeric fetal cells. Although fetal cells are rare in the maternal bone marrow, they appear to have some capacity to engraft in the bone marrow of irradiated recipients and produce cells of lymphoid lineage (Leduc et al., 2010). Fetal-derived functional B and T lymphocytes are seen in both wildtype and immunodeficient female mice (Khosrotehrani et al., 2008). Further research is required to determine whether fetal cells have true capacity for differentiation into all hematopoietic lineages, not just lymphoid cells.

Mesenchymal Stem Cells

Mesenchymal stem cells (MSCs) are stromal cells that adhere to plastic, are negative for hematopoietic lineage antigens, and have the potential for differentiation into adipocytes, chondrocytes and osteocytes in culture (Matthay et al., 2010). More recently MSCs have been shown to be capable of neuronal, epithelial and muscular differentiation in vitro (Brody et al., 2010; Kitada, 2012). MSCs possess the features of stromal cells that support growth and maintenance of a variety of cell types in tissues. Additionally, MSCs have decreased immunogenicity due to low expression of MHC class I proteins, and lack of MHC class II proteins and T-cell co-stimulatory molecules, such as CD80, CD86 and CD40. This allows administration of allogenic MSCs without generation of a significant host immune response (Matthay et al., 2010).

Unlike HSCs, there is variation in the constellation of cellular markers that define the MSC population. Various surface proteins have been identified to define MSCs,

although none are specific, thus constraining their usefulness (Summer and Fine, 2008). Human MSCs express CD105, CD73 and CD90/Thy-1, and lack expression of HLA-DR surface molecules and lineage markers such as CD34, CD45, integrin-alpha M/CD11b, and CD19 (Dominici et al., 2006; Tarnok et al., 2010). Other markers, including CD146 and CD56, have also been proposed (Tarnok et al., 2010). Murine MSC surface markers vary between different strains (Peister et al., 2004). MSCs from C57BL/6 mice express CD34, Sca-1 and VCAM1/CD106 while Balb/c MSCs only have low expression of CD34 and CD106. Other researchers have defined murine MSCs as expressing Sca-1, CD44 and CD106, and lacking CD45 and CD31 (Summer et al., 2007). Integrin-beta 1/CD29, CD73, and CD105 have also been used to identify MSCs in mice (Cheng et al., 2012). The lack of consensus in both species makes it difficult to clearly identify MSCs through flow cytometry. The only true test of whether cells are MSCs is in vitro differentiation into cartilage, bone and fat (Dominici et al., 2006; Summer et al., 2007).

Multiple researchers have suggested that at least some microchimeric fetal cells appear to be MSCs (Dawe et al., 2007; Huu et al., 2006; O'Donoghue et al., 2003). In mice, fetal cells expressing CD29, CD44, and CD105 have been detected in the maternal organs, including lung, spleen and bone marrow (Fujiki et al., 2009; Kallenbach et al., 2011a). However, each antibody was used individually, so it is unknown whether any of the cells were positive for multiple markers. Fetal cells expressing collagen type I were recruited to sites of kidney injury (Bou-Gharios et al., 2011). Since lymphoid and myeloid lineage cannot synthesize collagen type I, these cells were assumed to be of mesenchymal origin.

Fetal MSCs can be isolated from the peripheral blood of women following first trimester termination. The cells were shown to be capable of growth in tissue culture and demonstrated both osteocyte and adipocyte differentiation (O'Donoghue et al., 2003). Fetal cells can also be isolated from the bone marrow of postpartum females

(O'Donoghue et al., 2004). These cells can be cultured and induced to differentiate along with maternal MSCs. In both studies, the male (presumed fetal) cells expressed vimentin, a protein associated with mesenchymal tissues, and were CD29+, CD106+, CD45- and HLA-Class II-. MSCs from first trimester fetuses have growth advantages over their adult counterparts, including expression of pluripotency markers, faster growth, and maintenance of longer telomeres during cell culture passage (Guillot et al., 2007). Therefore, the presence of fetal MSCs in maternal organs would be of great clinical significance.

Endothelial Progenitor Cells

Endothelial progenitor cells (EPCs) are bone marrow-derived cells that contribute to vascular repair and homeostasis (Khakoo and Finkel, 2005). EPCs express surface markers of both hematopoietic and endothelial cell lineages, such as CD31, CD34, prominin/CD133, CD105, VEGFR-2 (KDR, Flk-1), and von Willibrand factor (vWF) (Khakoo and Finkel, 2005; Tarnok et al., 2010). These cells expand in culture and differentiate into mature, functional endothelial cells.

Murine fetal cells expressing CD31 have been identified in both healthy (Fujiki et al., 2009) and injured maternal tissues (Huu et al., 2007; Nassar et al., 2012). Fetal cells can participate in angiogenesis during maternal wound repair (Huu et al., 2007; Nassar et al., 2012) and melanoma (Huu et al., 2009). In both studies, fetal cell-derived blood vessels were contiguous with the maternal circulation and maternal lymphocytes could be detected within them.

An elegant experiment was designed to determine whether fetal cells are recruited en masse to these sites of injury or if they proliferate on site. In a murine model of melanoma, researchers hypothesized that if fetal cells proliferate in situ the cells in a

given area would be either almost all male or almost all female. If more mature cells were present and if cells were randomly recruited, the fetal cells would be a 50-50 mixture of male and female (Huu et al., 2009). Overall, 75% of the fetal cells contained a Y chromosome, and some vessels were made up of entirely male fetal cells. These results suggest derivation from a common endothelial progenitor cell that was attracted to the injury site.

Because EPCs express many markers of HSCs, simply looking for evidence of CD34 staining may result in the incorrect classification of fetal cells as hematopoietic. In one report, all of the CD34+ cells isolated from human placental intervillous space also expressed CD31 and vWF, which is suggestive of an endothelial origin (Parant et al., 2009). These findings highlight the complexity of determining fetal cell phenotype and the need for further investigation.

VARIABLES AFFECTING FETAL CELL MICROCHIMERISM

Part of the difficulty involved in determining fetal cell phenotype stems from the multiple ways in which cells can be classified. Additionally, there are many variables that may affect the fetal cells, including different types of fetal cells within each organ, the impact of fetomaternal histocompatibility, influence of prior or subsequent pregnancies and miscarriages, and the effect of time (Khosrotehrani and Bianchi, 2005). All of these factors need to be considered when investigating the biological relevance of fetal cell microchimerism.

Antibody studies suggest that each maternal organ may contain disparate groups of fetal cells (Fujiki et al., 2009; Kallenbach et al., 2011a). For example, in females mated to syngeneic males, 96.9% of fetal cells found in the bone marrow stained positive with an antibody against CD11b compared to only 28.8% of fetal cells in the

lung (Kallenbach et al., 2011a). Since the phenotype of fetal cells impacts upon how fetal cells help or harm during disease pathogenesis, this heterogeneity suggests that the organ in which a disease develops may dictate these properties.

In addition, the extent of immunological differences between the mother and her fetus may impact fetal cell type. Murine models examining fetal cell trafficking in allogeneic versus syngeneic matings have found differences in both the quantity (Kallenbach et al., 2011a; Khosrotehrani et al., 2005) and phenotype of fetal cells (Kallenbach et al., 2011a). For example, in the bone marrow of females in syngeneic matings, almost all of the GFP+ fetal cells also expressed CD11b. Only one-third of fetal cells in the maternal bone marrow in allogeneic matings stained positive for the same marker. Slight differences in fetal cell proliferation rates between syngeneic (3-5% of fetal cells) and allogeneic (4-7%) pregnancies have been observed (Liegeois et al., 1981).

Similar differences have been documented in humans, showing more microchimeric fetal cells in peripheral blood with greater immunocompatibility between mother and child (Adams Waldorf et al., 2010). The study of egg donor and surrogate pregnancies in humans allows further investigation of this area. One group verified the presence of persistent fetal cells in females who had delivered a male infant using a donor egg (Williams et al., 2009). Unfortunately no comparison was made to females who had utilized in vitro fertilization with their own eggs.

There are several ways that histocompatibility between the mother and her offspring may impact fetal cell microchimerism. MHC compatibility between the mother and her fetus may impact the maternal immune system's ability to regulate and clear fetal cells (Adams Waldorf et al., 2010). Moreover, fetal antigens may be presented to maternal T cells, and MHC similarities or differences are likely to affect the maternal immune response to non-self antigens.

It is also evident that cells acquired by the mother change throughout the course of the pregnancy. For example, CD4+ and CD8+ fetal cells are found in a higher percentage of pregnant women in the third trimester compared to earlier in the pregnancy (Adams Waldorf et al., 2010). Because fetal cell trafficking starts early in gestation, uncompleted pregnancies also contribute to a woman's chimerism. Following elective terminations, a significant quantity of nucleated fetal cells were found in the maternal blood (Bianchi et al., 2001). Work in mice has shown increased fetal cell trafficking after miscarriages induced by lipopolysaccharide (Johnson et al., 2010). Therefore, in determining the role of fetal cells in maternal disease, the length of the pregnancy, whether it ended due to elective termination, miscarriage, or premature birth, must be taken into account.

Another variable includes any invasive procedures that occur during pregnancy. Conflicting reports have shown both increased and no significant change after various diagnostic or clinical procedures. In one study chorionic villus sampling resulted in elevated fetal erythroblasts in maternal blood (Al-Mufti et al., 2003) while showing no significant change in another (Meleti et al., 2012). In utero surgical repair of myelomeningocele resulted in increased maternal-to-fetal but not fetal-to-maternal microchimerism (Saadai et al., 2012). In contrast, fetal DNA was elevated in women following laser ablation for twin-twin transfusion syndrome (Wataganara et al., 2005). The reasons behind these differences may stem from the relative invasiveness of the intervention as well as whether the Y chromosome or non-shared HLA molecules were quantified. It is also possible that fetal cell type is impacted while overall trafficking is not.

Fetal cells in the mother may be further affected by additional pregnancies or other sources of chimerism. A mouse study showed an increase in detectable fetal cells in multiparous females (Khosrotehrani et al., 2005) while a human study showed no significant change (Gammill et al., 2010). The specific MHC markers on the cells, the

duration between pregnancies, the specific types of cells present in the mother, and other factors may influence how the microchimeric cells interact with each other.

The fetal cell population present in the maternal organs may also change during the postpartum period. Some cells may be cleared more rapidly after parturition. For instance, fetal granulocytes are cleared from the maternal blood by one week postpartum while fetal lymphocytes remain much longer (Schroder et al., 1974). Additionally, certain cells may have a greater capacity for proliferation than others, and may become proportionally more abundant over time. Finally, as with the mother's own cells, fetal cells may be subject to the aging process, thus changing their properties (Nelson, 2012). Thus the timing of disease development may also influence the role fetal cells play.

All of these potential differences and modifications may alter how microchimeric fetal cells impact maternal health. Further research is needed to clarify exactly what types of cells are crossing from the fetus and/or placenta, and how that population changes throughout the pregnancy and the postpartum period. Once phenotype is known, function can be inferred and the long-term role of fetal cells in maternal health can be ascertained.

KNOWLEDGE GAPS THIS THESIS ADDRESSES

It is apparent from this literature review that more data on the phenotype of fetal cells is necessary to shed light on their biological function and the potential health consequences of microchimerism. Once fetal cells are well characterized, further research could focus on developing clinical applications to harness their helpful features, or abate their harmful properties. Information on postpartum trafficking patterns is also essential for understanding the role of microchimerism in maternal disease etiology or

repair. This thesis concentrated on four main knowledge gaps: (1) Limited data on fetal cell phenotype(s); (2) Unknown effects of fetomaternal histocompatibility on phenotype; (3) Uncertain physiologic impact on maternal health; and (4) Limited knowledge of postpartum fetal cell kinetics.

Limited Data on Fetal Cell Phenotype(s)

Because fetal cells are relatively rare within maternal organs, their characterization presents a significant challenge. We sought to overcome this obstacle by combining flow cytometry with comprehensive gene expression microarray analysis of fetal cells isolated from the murine maternal lung during late pregnancy. Global gene expression microarrays are exceptionally powerful for unbiased data generation. Our discovery-driven approach avoids the limitations of prior studies in which a handful of markers or genes were selected for review. Furthermore, we used systematic pathways analysis to determine potential fetal cell function.

Unknown Effects of Fetomaternal Histocompatibility on Phenotype

Most animal studies have used syngeneic matings in the study of fetal microchimerism. This model does not precisely address the important immunologic differences present in human pregnancies. While others have reported on how histocompatibility impacts microchimerism, no comprehensive studies have been performed. Our use of gene expression microarrays allowed us to compare fetal cells in syngeneic versus allogeneic pregnancies, and identify differentially expressed genes and biological pathways.

Uncertain Physiologic Impact on Maternal Health

Although it is increasingly evident that fetal cells contribute to maternal tissue repair following injury, it is currently not known whether the cells convey a physiologic benefit for the mother. In fact, functional tests are not typically performed prior to or following maternal injury (Kara et al., 2012; Seppanen et al., 2012). It is possible that the cells collaborate with, but do not significantly enhance, natural repair mechanisms. We hypothesized that pregnant or postpartum females would recover more quickly or to a greater extent than nulliparous females. We used two disease models, contact hypersensitivity and unilateral pneumonectomy, to test this hypothesis.

Limited Knowledge on Postpartum Fetal Cell Kinetics

In mouse models, most injury experiments have been performed during pregnancy. In a clinical setting, however, most injuries or diseases occur postpartum. Therefore, experiments using animal models should be designed to address questions in the time period following delivery. Despite the importance of postpartum studies, surprisingly little is known about the kinetics of fetal cell trafficking in murine maternal organs following parturition. We conducted an extensive study of the postpartum natural history of fetal cells. Because the lung contains the highest concentration of fetal cells during pregnancy, we selected this organ for further examination. In addition, we also studied bone marrow because of its use for transplants and microchimerism has significant clinical implications in this organ. The results inform the design of future experiments and may have implications for women's health.

SUMMARY

In summary, fetal cells exist in mammals and persist long term in small numbers. A given organ may contain a variety of fetal cell phenotypes. Microchimeric fetal cells have some qualities of stem cells, including differentiation and proliferation. There are technical challenges associated with fetal cell characterization due to their limited availability. Fetal cell participation in maternal health and disease is evident but the role of these cells is not completely understood. The research presented here contributes to the understanding of microchimerism by providing new data on the kinetics, phenotype and putative biological functions of fetal cells in the maternal organs. We developed a new technology to circumvent some of the technical challenges associated with this field. Additionally we report on pilot studies designed to address whether fetal cells have a physiologic impact on maternal health.

Table 1: Similarities of Microchimeric Fetal Cells to Stem Cells

Evidence from studies in both humans and mice suggests that microchimeric fetal cells may be stem cells or have stem-like properties. HSC = Hematopoietic stem cells; MSC = mesenchymal stem cells; EPC = Endothelial stem cells

	HSC	MSC	EPC
HUMAN STUDIES	CD34+ fetal cells detected in pregnant and postpartum women (Bianchi et al., 1996; Guetta et al., 2003)	Male cells identified as MSCs by morphology and expression of vimentin, CD29 and CD44 (O'Donoghue et al., 2004; O'Donoghue et al., 2003)	Fetal cells expressing vWF, CD34 and CD31 in the placental intervillous space (Parant et al., 2009)
	Fetal hematopoietic colony-forming units cultured from maternal blood postpartum (Osada et al., 2001)	Male cells in maternal bone marrow and blood capable of osteogenic and adipogenic differentiation (O'Donoghue et al., 2004; O'Donoghue et al., 2003)	
	Male cells in CD34-enriched apheresis products from non-pregnant female bone marrow donors (Adams et al., 2003)	Vimentin+ cells in breast carcinoma (Dubernard et al., 2008)	
	Enrichment of fetal cells in circulating CD34+ adherent cells (Mikhail et al., 2008)		
MURINE STUDIES	CD45+ fetal cells within the maternal blood vessels (Huu et al., 2007; Nassar et al., 2012)	Fetal cells expressing CD29 (integrin b1), CD44, and CD105 (endoglin) in the maternal organs (Fujiki et al., 2009; Kallenbach et al., 2011a)	CD31+ fetal cells in healthy maternal tissues (Fujiki et al., 2009)
	CD34+ fetal cells in the maternal organs (Fujiki et al., 2009)	Fetal cells expressing collagen type I home to maternal kidney after injury (Bou-Gharios et al., 2011)	CD31+ fetal cells present in areas of inflammation (Huu et al., 2007; Nassar et al., 2012)
	Fetal lymphoid progenitors differentiate into functional T and B lymphocytes during and following pregnancy (Khosrotehrani et al., 2008)		Fetal cells participate in angiogenesis in melanoma and wound healing (Huu et al., 2007; Huu et al., 2009; Nassar et al., 2012)
	Fetal-derived lineage-negative c-kit+ stem cells detected in the bone marrow of postpartum mice (Dutta et al., 2010)		Fetal cells differentiated into endothelial cells and formed vascular structures in vitro (Kara et al., 2012)
	Fetal cells with hematopoietic capacity can be transferred to irradiated recipients (Leduc et al., 2010)		

CHAPTER ONE: OPTIMIZATION OF NUGEN ONE-DIRECT AMPLIFICATION SYSTEM FOR FOR USE WITH MICROCHIMERIC FETAL CELLS

INTRODUCTION

Identification of the cell types in the fetal microchimeric population will permit a better understanding of the possible mechanisms by which they affect maternal health. Because fetal cells are relatively rare within maternal organs, their characterization presents a significant challenge. A relatively new kit from NuGEN Technologies, Inc. (San Carlos, California) the WT-Ovation One-Direct Amplification System (subsequently referred to here simply as the One Direct Kit), can amplify cDNA from small amounts of RNA. The manufacturer reports that the kit can amplify cDNA from as few as five and up to 20 cells. However, NuGEN recommends performing cell-specific titration experiments to assess the ideal number of cells per assay. To optimize the One Direct Kit for use with microchimeric fetal cells, varying quantities of input cells were tested. RNA quantity and microarray hybridization percentages were used to determine the most effective quantity of input cells.

METHODS

MICE

The Institutional Animal Care and Use Committee of the Tufts University School of Medicine Division of Laboratory Animal Medicine approved all protocols. All institutional and standard guidelines regarding the ethical use of experimental animals were followed. Male mice homozygous for the enhanced green fluorescent protein

(*Egfp*) transgene (C57BL6/J-Tg(CAG-EGFP)C14-Y01-FM131Osb [stock number 267, Riken BioResource Center, Japan, originally provided by Dr. Masaru Okabe (Okabe et al., 1997), bred in-house]) were mated to 10-12 week-old wild type C57BL/6J females (stock no. 664, Jackson Labs, Bar Harbor, Maine). From the homozygous male all pups inherit one copy of the *Egfp* transgene. *Egfp* expression was used as a marker for all fetal cells independent of fetal gender.

For Samples With 11 or Fewer Input Cells

Pregnant females were euthanized 18-19 days after mating due to prior evidence that fetal cell trafficking peaks immediately before delivery (Fujiki et al., 2008a). The thoracic cavity was opened and the pulmonary vasculature was perfused with ice-cold Dulbecco phosphate buffered saline (DPBS). The lungs were harvested. A single cell suspension was separately created from each lung pair using a GentleMACS dissociator (Miltenyi Biotech, Auburn, California) following the manufacturer's protocol. Briefly, lungs were incubated in HEPES Buffer (10mM HEPES, 150mM NaCl, 5mM KCl, 1mM $MgCl_2$, 1.8mM $CaCl_2$ in DPBS, brought to pH 7.4 with NaOH) with 1.5mg/mL collagenase D and 80U/mL DNase I at 37°C and physically dissociated. Samples were filtered using 100μm and 70μm nylon cell strainers. Cell suspensions were spun at 300xg and resuspended in DMEM supplemented with 10% fetal bovine serum, penicillin/streptomycin, HEPES and L-glutamine. Cells were cultured at 37°C and 5% CO_2 in 6-well plates. After 24 hours the media was removed, the cells were washed once with DPBS, and fresh media was replaced for an additional 24 hours. The cultures were then trypsinized to remove adherent cells and processed for FACS analysis.

For Samples With 20 or Higher Input Cells

Single cell suspensions were created from each lung pair as described above. However the samples were not cultured, and were immediately processed for FACS analysis.

Fluorescence-Activated Cell Sorting

Single cell suspensions were spun at 300xg and resuspended in flow cytometry buffer (DPBS with 2% bovine serum albumin [BSA] and 0.1% sodium azide) and 1.5µg/ml propidium iodide (PI) to exclude dead cells. On a MoFlo high-speed flow cytometer (DAKO, Fort Collins, Colorado), a 488nm laser was used to excite the fluorophores. As the GFP is sufficiently bright, no antibodies were used to identify fetal cells (Fujiki et al., 2008a; Fujiki et al., 2008b; Johnson et al., 2012). Green fluorescence was collected with a 530/40 filter, and PI with a 670/40 filter. Fetal liver from euthanized pups was used as a GFP+ control. C57BL/6J virgin female lungs were used as a negative control and the GFP gate was drawn to exclude all cells in the virgin female lungs (Figure 1). GFP+, PI- cells from each set of lungs were sorted directly into the lysis buffer provided with the WT-Ovation One-Direct Amplification system (NuGEN Technologies, Inc., San Carlos, California) at a dilution of 10-40 cells/µl. Two pairs of samples were combined but all other samples were from individual mice. Fetal cell lysates from each female were pipetted repeatedly to mix them in the buffer. They were then stored at -80°C following sorting.

One-Step Quantitative Reverse Transcriptase Polymerase Chain Reaction

To show whether the cell lysates are compatible with qRT-PCR and to assess RNA quality, we performed qRT-PCR on total cell lysates for *Egfp* (forward primer: 5′-ACTACAACAGCCACAACGTCTATATCA-3′, reverse primer: 5′-GGCGGATCTTGAAGTTCACC-3′, and TaqMan probe: 5′-FAM-CCGACAAGCAGAAGAACGGCATCA-TAMRA-3′) and ß-actin (*Actb*; forward primer 5'-AGGTCATCACTATTGGCAACGA-3'; reverse primer 5'-CAACGTCACACTTCATGATGGA-3'; probe 5'-FAM-AGCCTTCCTTCTTGGGTATGGAATCCTGT-TAMRA-3'). All samples were run in singlicate due to limited volume. Reactions were run on an ABI 7900 sequence detector with the TaqMan One-Step RT-PCR Master Mix reagents kit (Applied Biosystems, Foster City, California).

Amplification of Fetal Nucleic Acid and Microarray Hybridization

cDNA was amplified from each lysate using the One Direct Kit according to the manufacturer's protocol. Although cell number input varied, the total volume of lysate added to the reaction remained fixed at 2µl. The quantity of cDNA was measured using a Nanodrop 2000 (ThermoScientific, Wilmington, Delaware) and the quality of cDNA was assessed using a Bioanalyzer 2100 (Agilent, Santa Clara, California).

3.3µg cDNA were fragmented and biotinylated using the Encore Biotin Module (NuGEN Technologies, Inc., San Carlos, California) and hybridized to mouse 430 2.0 arrays (Affymetrix, Santa Clara, California). The arrays were hybridized in an Affymetrix oven at 45°C and 60rpm for 18-40 hours. Arrays were washed using a GeneChip Fluidics Station 450, stained with streptavidin–phycoerythrin, scanned with the

GeneArray Scanner, and analyzed using the GeneChip Microarray Suite 5.0 (Affymetrix). An Affymetrix MAS5 background correction and analysis was performed to evaluate percent hybridization.

RESULTS/DISCUSSION

We demonstrated that cell lysates created with the One Direct kit are compatible with qRT-PCR (Figure 2). Because RNA in these lysates can be assessed using qRT-PCR, we were able to evaluate the quality of RNA in the fetal cell lysates before amplification (which costs approximately $170 per reaction). We verified the presence of *Egfp* transcripts in the samples to confirm collection of $GFP^{+/-}$ fetal cells. As expected, *Egfp* amplified at a later cycle in homozygous GFP samples compared to heterozygous (fetal) samples. One fetal cell sample did not amplify *Egfp* before 40 cycles. However, this sample had lower levels of *ActB* (beta-actin) compared to other samples (Ct=34.9 vs. 29.7-31.1 in the others). Since *Egfp* consistently amplified after *ActB*, it is likely that *Egfp* would have amplified around 41-42 cycles.

A maximum of 5µg cDNA can be hybridized to Affymetrix gene expression microarrays. At least 20 cells were needed as input material to reliably obtain this concentration of cDNA, but as few as 10 cells could be used (Figure 3). Significant differences in cDNA yield were not seen between 20, 40, and 80 cells.

Being able to use a greater number of cells in each reaction also improved our microarray hybridization efficiency ($p = 0.002$; Figure 4). Since the quantity of cDNA applied to each array was normalized, this was not initially anticipated. However, since more cells were used, and since fetal cell types are known to be diverse (Fujiki et al., 2009), it is likely that the variety of transcripts was increased. The increased hybridization percentages therefore probably reflect a broader collection of transcripts

being introduced to the arrays. For our microarray experiments described in Chapters Two and Three, we chose to use up to 80 cells since this would allow analysis of multiple fetal cell types.

Figure 1: Flow Cytometry Gates for the Isolation of Fetal Cells from Maternal Lung

GFP+, PI- cells were collected using the triangular gate shown in the lower right-hand corner. This gate also eliminates the autofluorescence seen in the lungs.

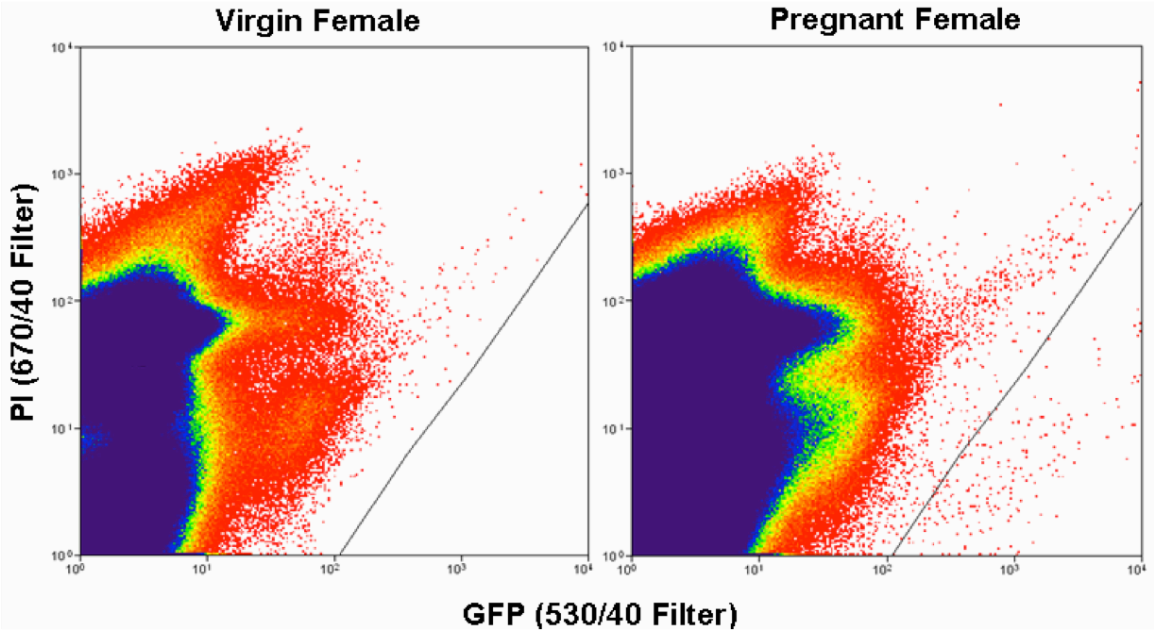

Figure 2: Quantitative Reverse Transcriptase PCR for *Egfp* and *Actb* in Fetal Cell Lysates

qRT-PCR of cell lysates shows amplification of *Egfp* and *Actb* in fetal cell lysates, permitting quantitative and qualitative evaluation of RNA prior to amplification of cDNA.

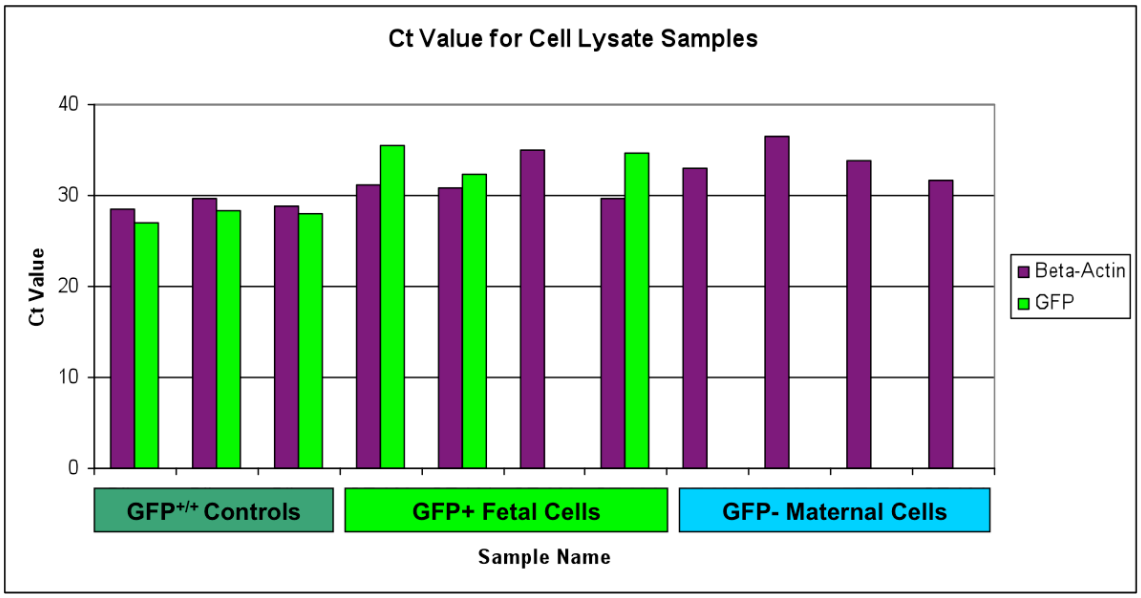

Figure 3: Increasing Cell Number in the One Direct Kit Improves cDNA Yield

After amplification cDNA concentration was measured on a Nanodrop 2000. The number of cells refers to how many cells were added to the One Direct Amplification kit. A concentration of 200µg/µl (dotted line) is equivalent to 5µg cDNA in the 25µl maximum volume allowed for the Encore Biotin Module.

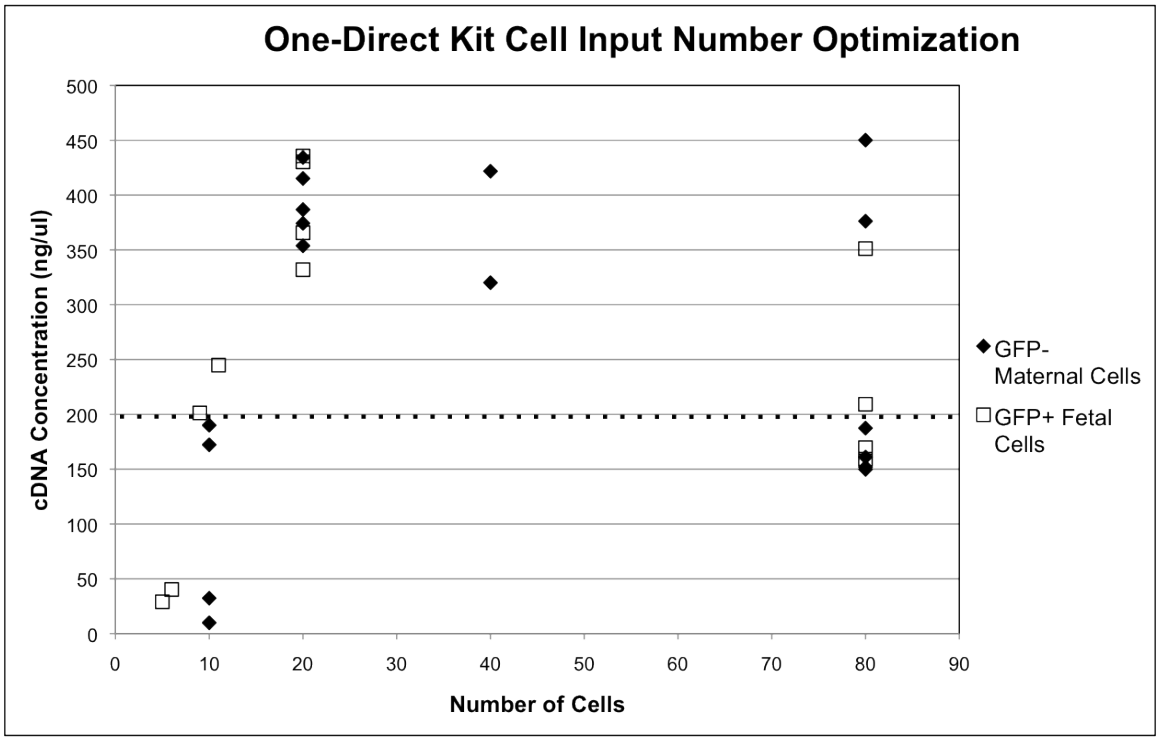

Figure 4: Increasing Cell Number in the One Direct Kit Improves Array Hybridization Percentage

After amplification of cDNA from the number of cells indicated, 3.3µg of amplified cDNA were fragmented, biotinylated and hybridized to Affymetrix arrays. Percent hybridization is defined as the percent of probes tagged as present. One-tailed T test p= 0.002.

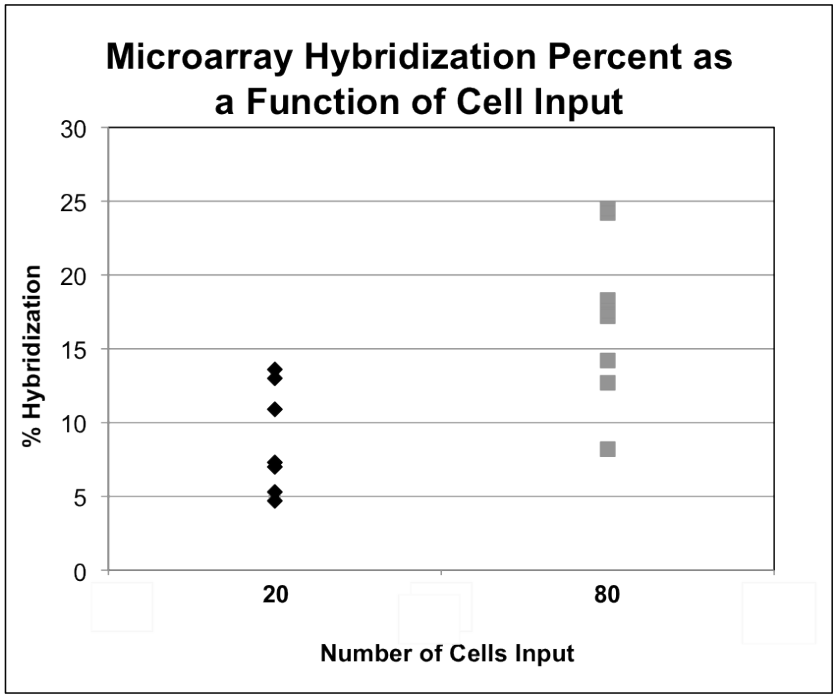

CHAPTER TWO: GENE EXPRESSION STUDY OF FETAL CELLS IN THE MATERNAL LUNG DURING SYNGENEIC PREGNANCY

INTRODUCTION

It is important to understand the origin and identity of microchimeric fetal cells, as their phenotype and differentiation status may impact long-term maternal health. For example, fetal cells are found at tumor sites in postpartum women (Kallenbach et al., 2011b) but it is not known whether they are helpful or harmful in this context. If the fetal cells show characteristics of hematopoietic and/or immune cells, they may have a role in tumor surveillance and destruction. Alternatively, fetal cells with endothelial cell properties could contribute to tumor angiogenesis and progression (Fugazzola et al., 2011).

Fetal cells have been found in a differentiated state in many different organs and tissues. Currently it is unknown whether (1) committed cells enter the maternal circulation and transdifferentiate, (2) a variety of committed cells cross the placenta *en masse*, (3) multipotent stem-progenitor cells differentiate to multiple cell types, or (4) a variety of unipotent stem-progenitor cells differentiate along their commitment lineages (Lee et al., 2010).

Because fetal cells are relatively rare within maternal organs, their characterization presents a significant challenge. In this study, we sought to overcome this obstacle by combining flow cytometry with comprehensive gene expression microarray analysis of fetal cells isolated from the murine maternal lung during late pregnancy.

METHODS

MICE

Male mice homozygous for the *Egfp* transgene were mated to 10-12 week-old wildtype C57BL/6J females in syngeneic matings. *Egfp* expression was used as a marker for all fetal cells independent of gender. Mice were housed in standard laboratory conditions and all institutional and standard ethical guidelines were followed.

FLOW SORTING OF FETAL CELLS FROM MATERNAL LUNG

Female mice were euthanized 18 days after mating. Gestational ages of the pups studied were 14-17.5 days as determined by Theiler staging (Theiler, 1989). The thoracic cavity was opened and the pulmonary vasculature was perfused with ice-cold DPBS. The lungs were harvested. A single cell suspension was separately created from each lung pair using a GentleMACS dissociator as described earlier in this thesis. Cell suspensions were spun at 300xg and resuspended in flow cytometry buffer and 1.5µg/ml PI to exclude dead cells. GFP+, PI- cells from each set of lungs were sorted (Figure 1) directly into the lysis buffer provided with the WT-Ovation One-Direct Amplification system at a dilution of 10-40 cells/µl. Cell lysates from each female were pipetted repeatedly to mix and stored at -80°C following sorting.

FETAL NUCLEIC ACID AMPLIFICATION

To assess RNA quality and verify the presence of *Egfp*, one-step qRT-PCR was performed on the total cell lysate for *Egfp* and *Actb* as described above. cDNA was converted and amplified from the RNA in the cell lysates using the WT-Ovation One Direct Amplification system following the manufacturer's protocol. Following amplification

the quantity of cDNA was measured using a Nanodrop 2000 and the quality of cDNA was assessed using a Bioanalyzer 2100.

Gene Expression Microarrays

3.3µg cDNA were fragmented and biotinylated using the Encore Biotin Module (NuGEN Technologies, Inc.) and hybridized to Affymetrix Mouse 430 2.0 arrays as described above. The arrays were normalized in the computer language R using quantile-normalization, with ideal mismatch background correction and Tukey biweight summarization. Following normalization a list was made of probes with a present call (Affymetrix, 2001) on at least six of seven arrays. This was called the "fetal cell core transcriptome." Raw and normalized data are available in NCBI's Gene Expression Omnibus (www.ncbi.nlm.nih.gov/geo) under GEO series accession number GSE10246.

Analysis of the Fetal Cell Core Transcriptome

The list of fetal cell core transcriptome probes was uploaded to NetAffx, a web-based analytic tool maintained by Affymetrix. NetAffx was used to translate the fetal cell core transcriptome probes into the corresponding genes (www.affymetrix.com/analysis/index.affx). This allows use of the published literature and other resources for analysis, as well as elimination of genes represented in the dataset by multiple probes.

Ingenuity Pathway Analysis

Functional information was obtained from the web-based software tool Ingenuity Pathway Analysis (IPA; build version 192063; content version 14400082). The fetal cell core transcriptome was used to identify enriched pathways. The categories "Top Canonical Pathways" and "Top Upstream Regulators" were primarily used in this

analysis. IPA uses the right-tailed Fisher exact test to calculate a p-value, which represents the likelihood that a non-relevant biological function is reported as significant. We also applied the Benjamini-Hochberg correction for multiple testing where appropriate.

Tissue Specificity

To gain information about fetal cell function, tissue-specific probes from the fetal cell core transcriptome were identified using the Novartis Research Foundation Gene Expression Database (http://biogps.org) (Hui et al., 2012; Wu et al., 2009). This publicly available atlas of protein-encoding transcripts uses previously published gene expression data (Lattin et al., 2008). The database includes information from 71 tissues obtained from healthy C57BL/6 mice, 9 cell types stimulated in vitro, and 11 cell lines. All were analyzed using Affymetrix Mouse Genome 430 2.0 arrays. For the study here, BioGPS version 2.0.4.9037 was used. For each of the probes within the fetal cell core transcriptome, we defined tissue-specificity as expression in one tissue over 30 multiples of the median (MoM), and no unrelated tissue with an expression value greater than one third of the maximum expression value (Hui et al., 2012). With the exception of placenta, the tissues used in the BioGPS database were not fetal; hence, the reported expression levels reflect those of adult tissue.

To partially address the gene expression differences between adult and fetal tissues, the Eurexpress Transcriptome Atlas Database (http://www.eurexpress.org) (Diez-Roux et al., 2011) was also used. The Eurexpress Atlas is a free web-based collection of gene expression patterns measured by in situ hybridization in mouse fetuses at gestational day e14.5. It does not include placenta or other extraembryonic tissues. Gene names were individually searched and annotations provided by the atlas were used to determine embryonic expression.

Principal Component Analysis

Principal component analysis (PCA) is an orthogonal transformation of potentially correlated variables into an equal number of non-correlated variables. This approach allows representation and visualization of the dominant patterns in large datasets (Massy, 1965). PCA was performed on two datasets downloaded from GEO: Thorrez et al. (GEO accession number GSE9954) (Thorrez et al., 2008) and Lattin et al. (GEO accession number GSE10246) (Lattin et al., 2008). We chose these datasets because both used C57BL/6 mice and Affymetrix Mouse Genome 430 2.0 arrays (as we did in our study). Two independent datasets were used to reduce the influence of the characteristics of an individual dataset. The GEO datasets, together with data collected from GFP+ fetal cells, were normalized in R using quantile-normalization with ideal mismatch background correction and Tukey biweight summarization. Principal components 1 vs. 2, 2 vs. 3, and 3 vs. 4 were plotted.

Genes of Interest

We used Ingenuity Pathway Analysis, NCBI Gene, UniProt Knowledgebase and the primary literature to further discover genes in the fetal cell core transcriptome that were associated with the tissue types suggested by the BioGPS database and PCAs.

RESULTS

FLOW SORTING OF FETAL CELLS IN MATERNAL LUNG AND FETAL NUCLEIC ACID AMPLIFICATION

From each set of maternal lungs, 66-420 GFP+, PI- fetal cells were flow-sorted (Figure 1). qRT-PCR was performed on four of the cell lysate samples and confirmed presence of the GFP transcript, indicating that fetal cells had been collected and that there was good quality mRNA present. One of the four samples had lower mRNA

concentration as measured by *Actb* qRT-PCR amplification, and *Egfp* did not amplify in that sample. After amplification the cDNA concentration for all samples ranged from 159.2-351.1ng/µl.

Analysis of the Fetal Cell Core Transcriptome

Eight hundred eighty-three (883) probes had a present call on at least six of the seven arrays. As determined through NetAffx, the probes represented 594 genes, 71 predicted genes or loci, and 45 unmapped probes. About one-third of the 594 genes are considered housekeeping genes (eg. heat shock proteins, mitochondrial respiration proteins such as cytochrome C oxidase, glycolysis enzymes such as citrate synthase, and ribosomal proteins).

Ingenuity Pathway Analysis

Of the 883 probes in the fetal cell core transcriptome, 647 probes were available for pathway analysis, indicating the IPA database had sufficient information on the gene product to place it in one or more pathways. The top five canonical pathways identified in the core analysis (BH-corrected p-value) were EIF2 signaling ($p=2.51x10^{-45}$), regulation of eIF4 and p70S6K signaling ($p=3.98x10^{-12}$), mTOR signaling ($p=5.01x10^{-7}$), remodeling of epithelial adherens junctions (p=0.0059) and epithelial adherens junction signaling (p=0.0065). The top five upstream regulators (p-value) were IGF1R ($p=4.2x10^{-10}$), INSR ($p=1.22x10^{-7}$), FAAH ($p=2.46x10^{-7}$), ADORA2A ($p=4.49x10^{-7}$), and FOS ($p=7.72x10^{-6}$). Complete results and specific genes in each pathway are presented in Table 3 and Table 4.

Tissue Specificity

Using the BioGPS database and the fetal cell core transcriptome, 52 probes, corresponding to 49 genes, met the criteria for establishing tissue specificity (Table 5).

These 49 genes derive from several organs and organ systems (Figure 5). Lungs, nervous tissue, testes and placenta were represented most often. Using the Eurexpress Transcriptome Database, the following fetal tissues were most highly represented by the 49 genes: nervous system, lung, kidney, intestines, bone, thymus and mesenchyme (Table 2). None of the placenta-specific genes were expressed in the embryos.

Principal Component Analysis

The data from the fetal cell microarrays had several key differences with the reference datasets. For example, the fetal cell arrays had higher scale factors and lower percent calls, indicating an overall poorer quality of the starting material. These differences dominated the first two principal components of the data set, which separated the fetal cell data from the GEO datasets in both cases (Figure 6A and Figure 7A).

In a PCA that compared our data to the Lattin data set, graphing PC3 vs PC4 (Figure 6B) allowed tissue type relationships to be determined. The data points closest to the GFP+ fetal cells were placenta, cells and tissues of immune origin (bone marrow, mast cells, peripheral macrophages, and lymph nodes), pancreas, and osteoblasts.

PCA comparing our data to the Thorrez data revealed slightly different results. PC3 vs PC4 (Figure 7B) showed the closest relationship of the GFP+ fetal cells to placenta, with additional similarity to lung, ovary, eye, embryonic stem cells, and adrenal gland. Because both versions of the PCA showed similarities to placenta, in addition to the presence of placenta-specific genes as identified using the BioGPS expression atlas, it is likely that many of the fetal cells originated from the placenta (Figure 8).

Genes of Interest

Seventy-nine genes of interest were identified (Table 5) that fell into four main categories with some overlap: Reproduction (33 genes), Immune (32 genes), Endothelial (13 genes), and Mesenchymal (12 genes). The large number of reproductive- and

immune-specific genes suggests a role for fetal cell trafficking in development of immune tolerance during pregnancy.

DISCUSSION

FUNCTIONAL INFORMATION ABOUT FETAL CELLS CAN BE OBTAINED FROM GENE EXPRESSION

Here we report that low numbers of fetal cells can be flow-sorted from the maternal lung and that reproducible gene expression information can be obtained from them. We performed a discovery-driven analysis to deduce the cell type(s) of origin as well as the putative function of the fetal cells. Our multidimensional analysis suggests that fetal cells in the maternal lung are primarily trophoblasts, cells of the immune system, and mesenchymal stem cells, and that these cells may be involved in the development of immune tolerance during pregnancy.

FETAL CELLS APPEAR TO BE PROLIFERATING

It has been previously shown that 3-5% of fetal cells undergo mitosis (Liegeois et al., 1981). Our gene expression results support these findings. IPA functional analysis implies active growth and protein synthesis. The top two canonical pathways represented in the fetal cell core transcriptome, EIF2 Signaling and Regulation of eIF4 and p70S6K signaling, are both involved in initiation of translation. p70S6K is a serine/threonine kinase in the PI3K pathway that phosphorylates the 40S ribosomal subunit protein S6, inducing protein synthesis and progression of the cell cycle (Chung et al., 1994). To precisely investigate active proliferation, a marker of DNA replication such as bromodeoxyuridine (BrdU) could be supplied to pregnant dams, and fetal cells could be assessed for BrdU staining.

Fetal Cells in the Maternal Lung Show Similarity to Placental Trophoblasts

Our analyses, particularly the PCA, suggest that at least some of the fetal cells in the murine maternal lung are placental in origin. Expression of placenta-specific genes such as *Peg10*, *Ctsq*, *Psg28*, *Plac9*, and several placental prolactin genes supports this conclusion. Additional evidence is the presence of other genes and pathways known to be necessary for placental development such as *Notch2* and IGF1R. *Notch2* plays a role in trophoblast invasion (Hunkapiller et al., 2011) while placental levels of IGF1R are known to influence fetal growth (Baker et al., 1993; Iniguez et al., 2010).

Trophoblasts, the main cell type of the placenta, circulate in humans and become trapped in the pulmonary microcirculation, but have not been previously described in other mammals (Askelund and Chamley, 2011). This finding is unexpected and novel in the mouse, yet it is supported by a recent report of placental cells trafficking to infarcted heart tissue in pregnant female mice. The fetal cells differentiated into cardiomyocytes and also expressed *Cdx2*, an important early regulator of trophoblast differentiation (Kara et al., 2012; Strumpf et al., 2005). *Cdx2* was not within our fetal cell core transcriptome, suggesting that fetal cells in the maternal lung may be at a later differentiation state than those seen in the infarcted heart.

It is also possible that a subset of these cells may be placental endothelial cells, as suggested by the expression of endothelial-specific genes. For example, *Tek* is a receptor tyrosine kinase expressed almost exclusively by endothelial cells. It appears to be critical for vascular patterning (Sung et al., 2011) and is highly expressed by the term mouse placenta (Dumont et al., 1995) with reduced levels in preeclamptic pregnancies (Sung et al., 2011). Additional evidence comes from the presence of *Thsd7a*, known to

affect endothelial migration and vascular patterning (Wang et al., 2010); *Cd36*, a surface receptor for thrombospondin (Dye et al., 2001); and *Epas1,* a regulator of endothelial cell transcription in response to hypoxia (Jarvenpaa et al., 2007). All of these genes are expressed in the placenta. The specific type of placental cells present in the murine lung during pregnancy warrants further investigation.

Fetal Cells May Have a Role in Development of Maternal Immune Tolerance to the Fetus

During pregnancy, exposure to the paternal antigens on circulating fetal and placental cells is thought to help facilitate development of immunological tolerance (Chamley et al., 2011; Taglauer et al., 2010). In humans, trophoblast deportation is hypothesized to be important for induction of immune tolerance to the fetus (Chamley et al., 2011) and is elevated in preeclampsia (Chamley et al., 2011; Johansen et al., 1999). Other evidence comes from previous work in our laboratory showing that allogeneic matings have more fetal cell trafficking (Kallenbach et al., 2011a), suggesting that fetal cell transfer during pregnancy is affected by genetic differences between the mother and fetus.

Several of our analyses presented here support for the hypothesis that fetomaternal trafficking plays an important role in immune tolerance development. Fetal cells in the maternal lung express genes involved in modulation of the immune system, including *Aicda*, *Zap70*, *Cd24a*, *Psg28*, *Scgb1a1* (also known as uteroglobin), and *Foxp1* (Table 5). Principal component analysis showed similarity to many immune system cells and tissues (bone marrow, mast cells, peripheral macrophages, and lymph nodes; Figure 6 and Figure 7).

IPA functional analysis showed presence of several pathways involved in immunoregulation. For example, the mTOR pathway plays a role in differentiation of T-regulatory cells, IL-10 production, and longevity and proliferation of memory CD8+ T cells (Araki et al., 2011). Immunologic and inflammatory responses also appeared on the list of top biological functions identified by IPA (p-values range from $8.34x10^{-6}$ to 0.04), suggestive of a broad resemblance to immune cells.

Moreover, trophoblasts and other fetal cells are concentrated in the lung, a key site of interaction between the environment and bloodstream. Resident pulmonary dendritic cells can induce immune response or anergy (von Garnieir and Nicod, 2009). It is therefore possible that fetal cells influence immune cells residing in the lung. The impact of fetal cell microchimerism on the maternal immune system is an intriguing area for future research.

Analysis Reveals Similarity to Mesenchymal Tissues

In addition to placenta and immune cells, the PCA, BioGPS and Eurexpress Atlas results showed that fetal cells have similar transcriptional profiles as cells of the nervous system, lung, adipose, bone, pancreas, and mesenchyme. Combined with the expression of genes and pathways (such as *Vim*, *Ctnnb1*, *Notch2*, *Smad1*, *Bmpr2,* and *ß-catenin*; Table 5) known to be involved in epithelial-mesenchymal transition, our results suggest that some of the fetal cells are mesenchymal stem cells (MSCs).

MSCs have demonstrated immunomodulary properties. They are able to alter the functions of dendritic cells, B and T lymphocytes and neutrophils (Matthay et al., 2010). Administration of MSCs results in increased levels of IL-10 and IL-13 (Matthay et al., 2010), cytokines known to be upregulated during pregnancy (Rieger et al., 2002; Thaxton and Sharma, 2010; Wegmann et al., 1993). MSCs additionally have low levels

of MHC class I and II proteins, making them well-tolerated by the host (Chamberlain et al., 2007; Matthay et al., 2010). This provides additional support for our hypothesis that cell trafficking during pregnancy plays a role in immune tolerance.

We have previously suggested that fetal cells in the maternal organs may be MSCs (Pritchard et al., 2011). Earlier work in our laboratory demonstrated fetal cell expression of surface markers characteristic of MSCs (Fujiki et al., 2009; Kallenbach et al., 2011a). Another group demonstrated the presence of fetal MSCs in the bones and bone marrow of postpartum women (O'Donoghue et al., 2004). These isolated fetal cells were able to differentiate in vitro into adipocytes and osteocytes. Furthermore, microchimeric fetal cells are known to differentiate in vivo in response to injury in both mice and humans, contributing to repair of injury in multiple maternal organs, demonstrating pluripotency (Lee et al., 2010; Pritchard et al., 2011).

Umbilical cord blood (Lv et al., 2012), placental tissues (Parolini et al., 2010) and maternal blood during pregnancy (O'Donoghue et al., 2003) contain mesenchymal stem cells that have significant plasticity and low immunogenicity. The possibility that the MSCs and placental cells are the same population cannot be excluded (Parolini et al., 2010). Future work could incorporate cell surface markers and flow cytometry to sort subpopulations of cells, followed by comparative transcriptomic analysis to determine if these cells derive from the same original population.

CONCLUSIONS

Here we report a comprehensive gene expression analysis of fetal cells within the murine maternal lung during pregnancy. We show that these cells are a mixed population, as previously suggested by cell surface marker experiments in our laboratory. The major contributors to the microchimeric population are trophoblasts,

mesenchymal stem cells and cells of the immune system. We propose that trophoblast trafficking occurs in mice, which may allow development of a model to investigate the role of trophoblast deportation in the etiology of preeclampsia. Our results have additional implications for the development of immune tolerance during pregnancy, providing a model system for future research. Finally, the persistence of fetal or placental MSCs may impact long-term maternal postpartum health.

Note: The results of this study were published in *Biology of Reproduction* in August 2012.

Figure 5: Source Organ of Fetal Cell Tissue-Specific Genes

Analysis of the fetal cell core transcriptome using the BioGPS Gene Expression database revealed expression of 49 tissue-specific genes from several different organs. The numbers represent the number of tissue-specific genes for each organ.

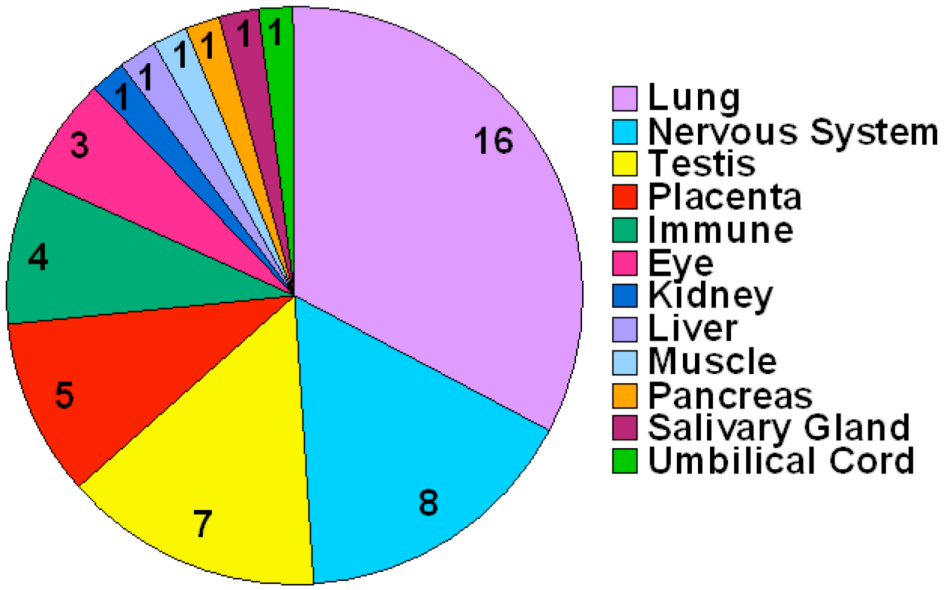

Figure 6: PCA Comparison of Fetal Cells to Lattin Data

Fetal cell data compared to Lattin et al. (2008) data. **(A)** Principal components 1vs2. **(B)** Principal components 3vs4. Fetal cell data is circled in green.

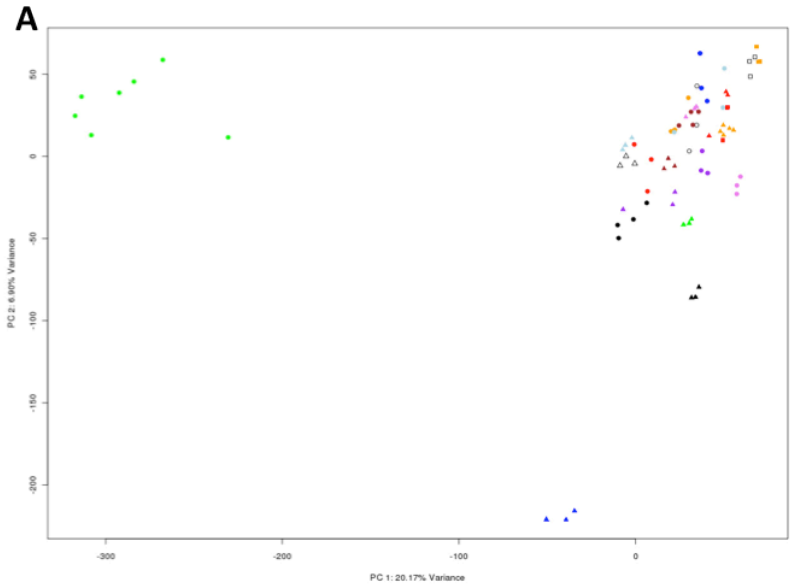

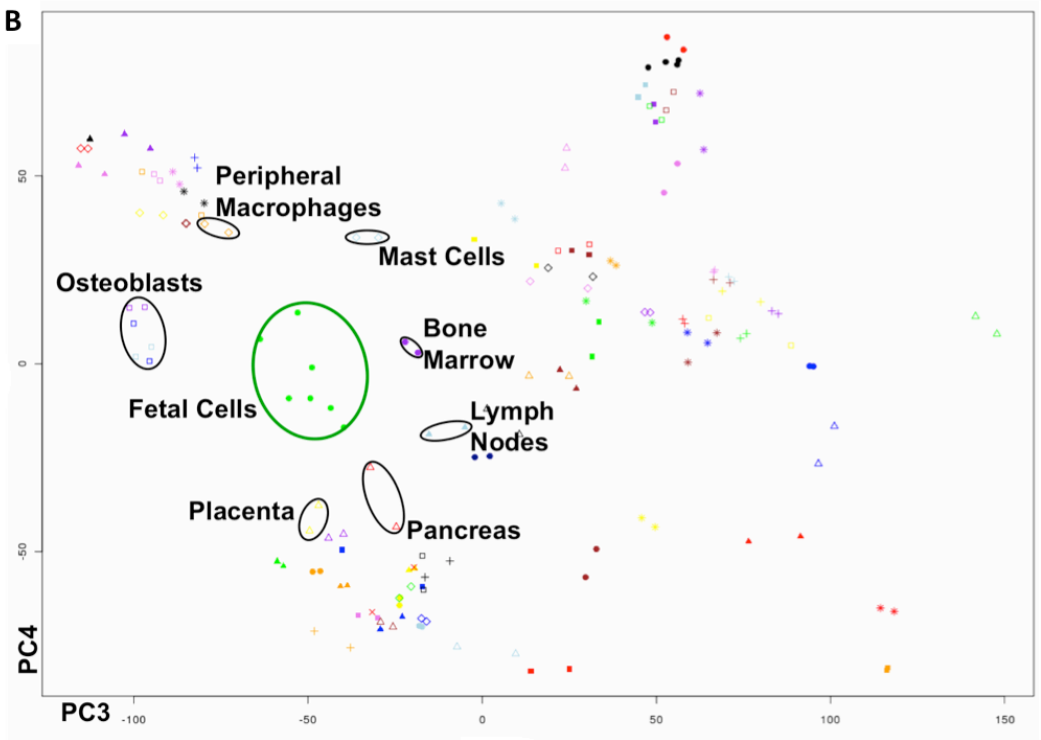

Key

- GFP+ mouse
- Adipose brown
- Adipose white
- Adrenal gland
- Amygdala
- B-Cells
- Bladder
- Bone
- Bone marrow
- Cerebellum
- Cerebral cortex
- Ciliary bodies
- Common myeloid progenitor
- Cornea
- Dendritic cells lymphoid (CD8a+)
- Dendritic cells myeloid (CD8a-)
- Dendritic plasmacytoid (B220+)
- Dorsal root ganglia
- Dorsal striatum
- Embryonic stem line Bruce4 p13
- Embryonic stem line V26_2 p16
- Epidermis
- Eyecup
- Follicular B-cells
- Granulo mono progenitor
- Granulocytes mac1+ gr1+
- Heart
- Hippocampus
- Hypothalamus
- Large intestine
- Small intestine
- Iris
- Kidney
- Lacrimal gland
- Lens
- Liver
- Lung
- Lymph nodes
- Macrophage bone marrow
- Macrophage bone marrow 24hr LPS
- Macrophage bone marrow 2hr LPS
- Macrophage bone marrow 6hr LPS
- Macrophage peri LPS thio 0hr
- Macrophage peri LPS thio 1hr
- Macrophage peri LPS thio 7hr
- Mammary gland lactating
- Mammary gland non-lactating
- Mast cells
- Mast cells IgE
- Mast cells IgE+antigen 1hr
- Mast cells IgE+antigen 6hr
- Mega-erythrocyte progenitor
- Microglia
- NK cells
- Nucleus accumbens
- Olfactory bulb
- Osteoblast day 14
- Osteoblast day 21
- Osteoblast day 5
- Osteoclasts
- Ovary
- Pancreas
- Pituitary
- Placenta
- Prostate
- Retina
- Retinal pigment epithelium
- Salivary gland
- Skeletal muscle
- Spinal cord
- Spleen
- Stem cells HSC
- Stomach
- T-cells (CD4+)
- T-cells (CD8+)
- T-cells (foxP3+)
- Testis
- Thymocyte DP CD4+ CD8+
- Thymocyte SP CD4+
- Thymocyte SP CD8+
- Umbilical cord
- Uterus

Figure 7: PCA Comparison of Fetal Cells to Thorrez Data

Fetal cell data compared to Thorrez et al. (2008) data. **(A)** Principal components 1vs2. **(B)** Principal components 3vs4. Fetal cell data is circled in green.

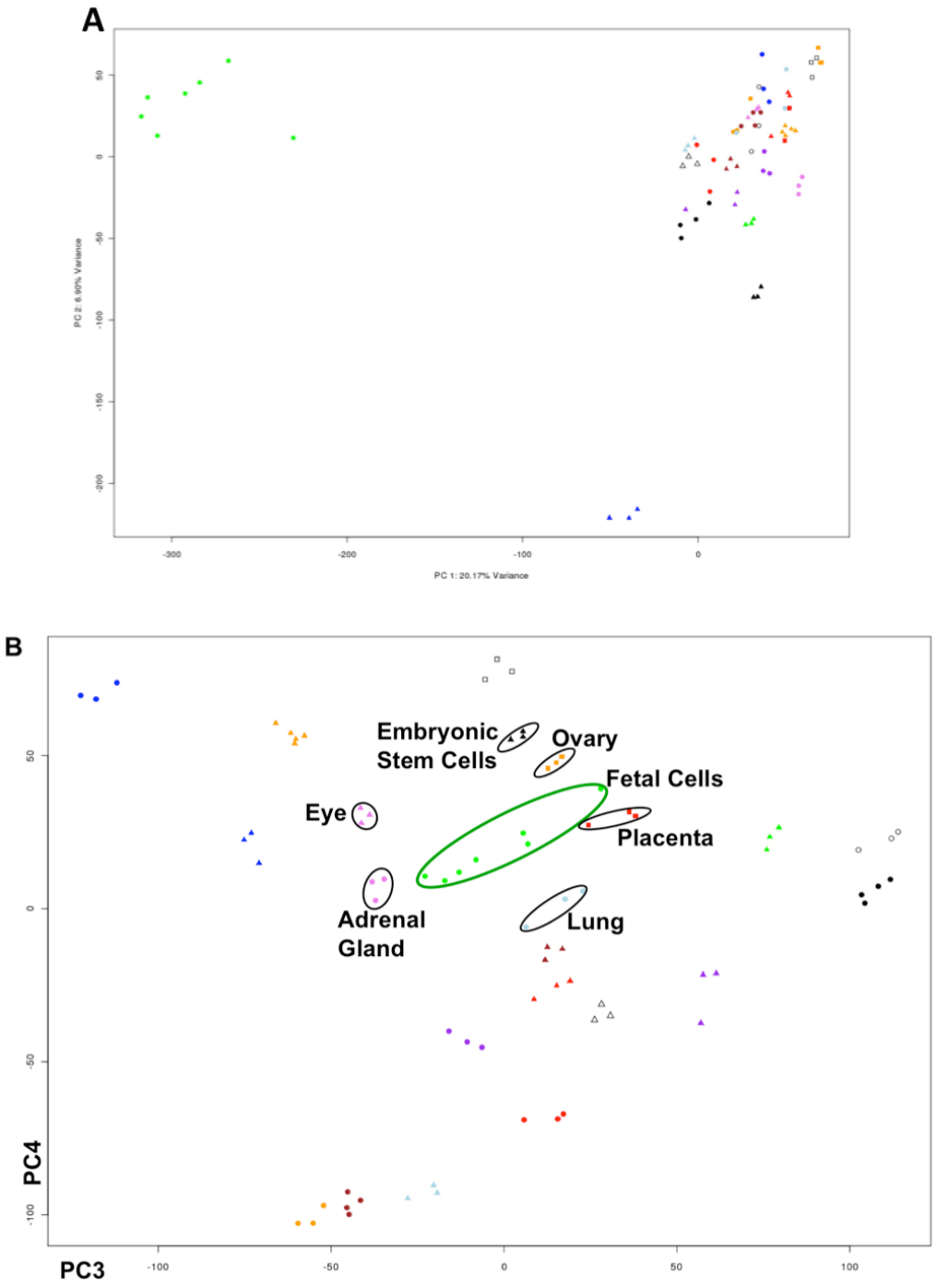

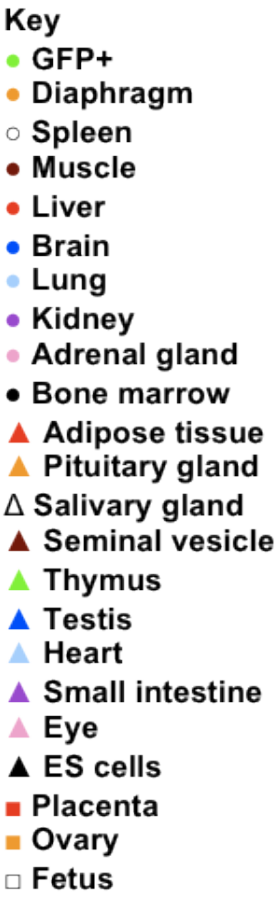
Key
GFP+
Diaphragm
Spleen
Muscle
Liver
Brain
Lung
Kidney
Adrenal gland
Bone marrow
Adipose tissue
Pituitary gland
Salivary gland
Seminal vesicle
Thymus
Testis
Heart
Small intestine
Eye
ES cells
Placenta
Ovary
Fetus

Figure 8: Overlap of Analyses

Venn diagram showing overlap between the PCA and BioGPS analyses. Each circle contains the overlap between our data and the external datasets analyzed. All three circles converge on placenta.

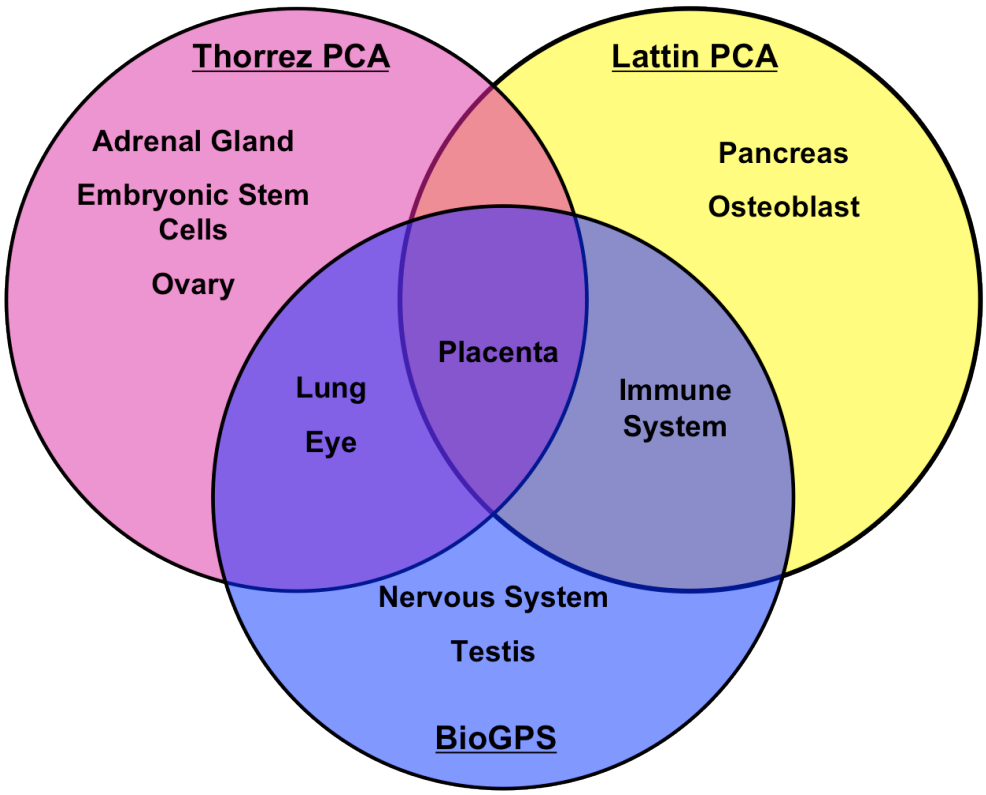

Table 2: Organ-Specific Probes

A detailed list of the genes and the organs, tissues and cell types in which they are expressed, as identified by BioGPS analysis. The Eurexpress embryo atlas annotations for each gene are also listed.

Organ/ System	Specific Tissue	Probe(s)	Gene Name	EurExpress (e14.5)
Lung	Lung	1416854_at	Slc34a2	Not annotated
	Lung	1418639_at	Sftpc	Lung
	Lung	1418788_at	Tek	Mesenchyme, kidney, lung, heart
	Lung	1419905_s_at	Hpgd	lip, thymus, choroid plexus, olfactory epithelium
	Lung	1422334_a_at; 1429626_at	Sftpa1	Not detected
	Lung	1425814_a_at	Calcrl	Not detected
	Lung	1435436_at	Epas1	Vertebral axis muscles, kidney, adrenal gland, limb
	Lung	1435823_x_at	Egfl7	Highly expressed broad distribution
	Lung	1436367_at	Ptprb	Heart valve, mesenchyme
	Lung	1439368_a_at; 1439369_x_at	Slc9a3r2	No regional signal
	Lung	1440225_at	Gpr116	No regional signal
	Lung	1440685_at	Unknown	Unknown
	Lung	1448529_at	Thbd	Bone, epithelium, skeletal muscle, urethra, lung, trachea, meninges
	Lung	1451359_at	Lpcat1	Not found
	Lung	1456428_at	Cxcl15	Not annotated: looks like no regional signal
	Lung	1456873_at	Clic5	Kidney, midgut, thymus, lungs
Nervous	Cerebellum	1424958_at	Car8	Stomach, brain, gut, brain, thyroid, salivary gland, pancreas, kidney, lung, clavicle
	Dorsal Striatum; Nucleus Accumbens	1425132_at	Neto1	Not Annotated
	Dorsal Root Ganglia; Retina	1429667_at	Pou4f1	Nervous tissue (brain, neural retina)
	Dorsal Striatum; Nucleus Accumbens; Olfactory Bulb; Amygdala	1440901_at	Dgkb	Several areas of the brain, Anterior wall of gut
	Dorsal Root Ganglia; Nucleus	1450435_at	L1cam	Brain, spinal cord, tongue, stomach, kidney, lung,

Organ/ System	Specific Tissue	Probe(s)	Gene Name	EurExpress (e14.5)
	Accumbens			
	Olfactory Bulb; Nucleus Accumbens; Cerebellum; Dorsal Striatum; Amygdala	1452728_at	Kirrel3	Probably ubiquitous
	Neuro2a	1456721_at	Thsd7a	Not found
	Dorsal Root Ganglia; Spinal Cord; Prefrontal Cerebral Cortex; Hypothalamus; Olfactory Bulb; Amygdala; Cerebellum; Cerebral Cortex; Hippocampus; Nucleus Accumbens	1460181_at	Stmn3	Nervous system, stomach, intestines
Testes	Testes	1415955_x_at	Prm1	No regional signal
	Testes	1419422_at	Pkd2l2	Not found
	Testes	1430644_at	Wbscr25	
	Testes	1439465_x_at	Agbl5	Not found
	Testes	1444303_at	LOC100503986	Not found
	Testes	1447799_x_at	1700001P01Rik	No regional signal
	Testes	1456693_at	LOC100504413	Not found
Placenta	Placenta	1415835_at	Prl3b1	Not found
	Placenta	1422289_a_at	Ctsq	Not found
	Placenta	1425881_at	Psg28	Not detected
	Placenta	1426730_a_at; 1452165_at	Prl2b1	Not found
	Placenta	1427550_at	Peg10	Not available
Immune	Macrophage	1420089_at	Nfkbia	Thymus, bone, nose
	Baf3	1424703_at	Hemk1	Not detected
	CD4+ SP Thymocytes; CD8+ SP Thymocytes	1430448_at	6720418B01Rik	Not found
	CD4+CD8+ DP Thymocytes	1439947_at	Cyp11a1	Adrenal gland, Testes
Eye	Eyecup	1439920_at	unknown	
	Eyecup; Ciliary Bodies; Iris	1447410_at	unknown	
	Cornea	1456348_x_at	Paqr5	Not annotated; eye maybe
Kidney	mIMCD-3	1460305_at	Itga3	Salivary gland, teeth, thyroid, lung, brain, ear, eye
Liver	Liver	1449337_at	Tdo2	No regional signal
Muscle	Skeletal Muscle; Bladder	1431335_a_at	Wfdc1	No regional signal
Pancreas	Min6 cells	1430642_at	2900001G08Rik	Not found

Organ/ System	Specific Tissue	Probe(s)	Gene Name	EurExpress (e14.5)
Salivary Gland	Salivary Gland	1457140_s_at	Rassf10	Not found
Umbilical Cord	Umbilical Cord	1438588_at	Plagl1	Cranium, Mesenchyme, Ear, Eye, Brain

Table 3: Canonical Pathways

Complete list of the statistically significant canonical pathways as identified by Ingenuity Pathway Analysis. Shaded boxes show non-significant BH-corrected p-values. B-H p-value column shows the Benjamini-Hochberg corrected p-value as applied by the IPA software.

Ingenuity Canonical Pathways	p-value	B-H p-value	Molecules
EIF2 Signaling	6.3E-43	2.0E-40	RPL11, RPL22, RPL27A, EIF1, EIF4A2, RPS23, RPS11, RPS7, RPS3A, EIF4G2, EIF5, PABPC1, RPL27, RPL23A, EIF3E, Rpl38, RPLP0, RPS29, RPS4X, FAU, RPL35A, RPS25, RPL41, RPL13A, RPSA, EIF2S3, PPP1CB, RPS6, RPS8, RPL26, RPL14, RPS21, EIF2B2, RPL37A, RPL7, RPL6, RPL18A, RPS16, RPS9, RPL35, RPLP2, RPL18, RPL4, RPL7A, RPL34, RPS2, RPL30, RPL23, RPL5, RPL28, RPS26, EIF4A1, EIF2AK2, RPS14
Regulation of eIF4 and p70S6K Signaling	3.1E-14	5.0E-12	EIF2S3, EIF1, RPS6, RPS8, EIF4A2, RPS21, RPS23, EIF2B2, RPS11, RPS7, RPS3A, EIF4G2, RPS16, RPS9, PABPC1, RPS2, EIF3E, ITGA3, RPS29, FAU, RPS4X, RPS26, EIF4A1, RPS25, RPSA, RPS14
mTOR Signaling	1.8E-09	2.0E-07	RPS2, RAC1, RPS6, RPS8, EIF4A2, RPS21, EIF3E, RPS23, RPS11, RPS7, RPS29, FAU, RPS4X, RPS3A, EIF4G2, RPS26, RHOA, RPS16, RPS9, EIF4A1, RPS25, RPS14, RPSA
Sertoli Cell-Sertoli Cell Junction Signaling	4.1E-06	3.3E-04	SPTBN1, DLG1, TJP1, AXIN1, ACTB, TUBB2A, RAC1, TUBA4A, ITGA3, BCAR1, ACTG1, TUBA1B, MAP3K12, TUBA1A, TJP3, CLDN14, CTNNB1, PRKAR1A
Protein Kinase A Signaling	6.0E-06	3.8E-04	TCF4, Calm1, PPP1CB, H3F3C, NFKBIA, HLA-B, ATF4, CTNNB1, APEX1, AKAP5, YWHAE, YWHAB, CHP, YWHAZ, PLCG1, MYL9, GNAI2, ANAPC4, GNAI3, AKAP13, AKAP2/PALM2-AKAP2, MYL12B, RHOA, PPP1R12A, PRKAR1A
Germ Cell-Sertoli Cell Junction Signaling	1.5E-05	8.1E-04	TJP1, AXIN1, ACTB, TUBB2A, RAC1, TUBA4A, IQGAP1, ITGA3, GSN, BCAR1, ACTG1, TUBA1B, MAP3K12, TUBA1A, RHOA, CTNNB1
Protein Ubiquitination Pathway	3.5E-05	0.0016	B2M, UBE2R2, DNAJC19, Ubb, HSPD1, HSPA5, DNAJA1, LOC728622/SKP1, NEDD4, FZR1, HSPA8, ANAPC4, HSP90B1, DNAJC8, DNAJC1, HLA-B, HSP90AA1, SMURF2, UBC, UBE2D3, HLA-C
Polyamine Regulation in Colon Cancer	4.6E-05	0.0018	TCF4, AZIN1, OAZ1, OAZ2, CTNNB1, ODC1
Signaling by Rho Family GTPases	6.1E-05	0.0022	ACTB, SEPT7, RAC1, SEPT4, VIM, IQGAP1, ITGA3, ACTG1, MYL9, GNAI2, MAP3K12, GNAI3, STMN1, PIP5K1A, CDH5, MYL12B, RHOA, NCF2, PPP1R12A
Virus Entry via Endocytic Pathways	7.2E-05	0.0023	B2M, AP2M1, ACTB, CAV1, RAC1, HLA-B, PLCG1, ITGA3, ACTG1, DNM2, HLA-C
Leukocyte Extravasation Signaling	0.0001	0.0033	MMP16, ACTB, RAC1, PLCG1, RAPGEF3, CRK, DLC1, BCAR1, ACTG1, GNAI2, GNAI3, CDH5, RHOA, NCF2, CLDN14, CTNNB1
Gap Junction Signaling	0.0002	0.0062	ACTB, TUBB2A, CSNK1D, TUBA4A, CSNK1A1, PLCG1, ACTG1, TUBA1B, GNAI2, GNAI3, TUBA1A, CAV1, CTNNB1, PRKAR1A

Ingenuity Canonical Pathways	p-value	B-H p-value	Molecules
Caveolar-mediated Endocytosis Signaling	0.0003	0.0074	B2M, ACTB, CAV1, HLA-B, ITGA3, ACTG1, DNM2, HLA-C, COPB2
Mitochondrial Dysfunction	0.0003	0.0074	NDUFA4, FIS1, UCP2, COX6A1, COX6C, NDUFB7, CAT, UQCRB, COX7A2L, NDUFA2, PINK1, COX6A2
Hypoxia Signaling in the Cardiovascular System	0.0005	0.010	HSP90B1, NFKBIA, UBE2R2, CSNK1D, HIF1AN, HSP90AA1, ATF4, UBE2D3
RhoA Signaling	0.0005	0.010	MYL9, PIP5K1A, MYL12B, ACTB, RHOA, SEPT7, SEPT4, PPP1R12A, PPP1CB, DLC1, ACTG1
Phospholipase C Signaling	0.0005	0.010	PEBP1, Calm1, CHP, RAC1, PPP1CB, PLCG1, RAPGEF3, ITGA3, TGM2, MYL9, AHNAK, MYL12B, RHOA, ZAP70, ATF4, PPP1R12A, MARCKS
Actin Cytoskeleton Signaling	0.0007	0.012	TMSB10/TMSB4X, ACTB, RAC1, PPP1CB, CRK, ITGA3, GSN, IQGAP1, BCAR1, ACTG1, MYL9, PIP5K1A, MYL12B, RHOA, PPP1R12A, MYH9
Regulation of Actin-based Motility by Rho	0.0008	0.012	MYL9, PIP5K1A, MYL12B, ACTB, RHOA, RAC1, PPP1R12A, PPP1CB, GSN
PI3K/AKT Signaling	0.0008	0.012	HSP90B1, NFKBIA, YWHAE, YWHAB, YWHAZ, HLA-B, HSP90AA1,I TGA3, CTNNB1, CCND1, MCL1
Integrin Signaling	0.0009	0.013	TSPAN7, ACTB, RAC1, PPP1CB, PLCG1, CRK, ITGA3, BCAR1, ACTG1, MYL9,ARF1, MYL12B, RHOA, CAV1, PPP1R12A
Oxidative Phosphorylation	0.0010	0.014	Atp5h, NDUFA4, ATP6V1D, COX6A1, COX6C, NDUFB7, UQCRB, COX7A2L, NDUFA1, NDUFA2, COX6A2
Aldosterone Signaling in Epithelial Cells	0.0010	0.014	DNAJC19, PLCG1, HSPD1, DNAJA1, HSPA5, NEDD4, HSPA8, PIP5K1A, HSP90B1, DUSP1, DNAJC8, DNAJC1, HSP90AA1
FAK Signaling	0.0014	0.019	HMMR, ACTB, RAC1, PLCG1, CRK, ITGA3, TNS1, BCAR1, ACTG1
ERK/MAPK Signaling	0.0016	0.020	YWHAB, YWHAZ, RAC1, PLCG1, PPP1CB, RAPGEF3, CRK, ITGA3, BCAR1, H3F3C, DUSP1, PPP1R12A, ATF4, PRKAR1A
Breast Cancer Regulation by Stathmin1	0.0019	0.023	Calm1, TUBB2A, RAC1, TUBA4A, PPP1CB, TUBA1B, GNAI2, GNAI3, STMN1, TUBA1A, RHOA, PPP1R12A, UHMK1, PRKAR1A
RhoGDI Signaling	0.0022	0.026	ACTB, RAC1, ITGA3, DLC1, ACTG1, GNAI2, MYL9, GNAI3, PIP5K1A, CDH5, MYL12B, RHOA, PPP1R12A
NRF2-mediated Oxidative Stress Response	0.0028	0.032	SOD1, PRDX1, ACTB, DNAJC19, DNAJA1, ACTG1, AKR1A1, DNAJC8, CAT, DNAJC1, ATF4, TXN, FTH1
Dopamine-DARPP32 Feedback in cAMP Signaling	0.0038	0.041	GNAI2, GNAI3, Calm1, CHP, CSNK1D, CSNK1A1, PLCG1, PPP1R12A, ATF4, PPP1CB, PRKAR1A, KCNJ11
Chemokine Signaling	0.0051	0.054	GNAI2, GNAI3, Calm1, RHOA, PLCG1, PPP1R12A, PPP1CB
Cellular Effects of Sildenafil (Viagra)	0.0052	0.054	MYL9, Calm1, MYL12B, ACTB, MYH9, PLCG1, PPP1R12A, PPP1CB, ACTG1, PRKAR1A
Tight Junction Signaling	0.0060	0.059	MYL9, TJP1, TJP3, ACTB, RHOA, RAC1, MYH9, CLDN14, CTNNB1, ACTG1, PRKAR1A
Ephrin Receptor Signaling	0.0062	0.059	GNAI2, GNAI3, EFNB2, SDCBP, AXIN1, RHOA, ACP1, RAC1, ATF4, CRK, ITGA3, BCAR1
Axonal Guidance Signaling	0.0068	0.063	DPYSL2, CHP, TUBB2A, RAC1, TUBA4A, L1CAM, CRK, ITGA3, BCAR1, TUBA1B, GNAI2, MYL9, GNAI3, EFNB2, SDCBP, TUBA1A, MYL12B, RHOA, ADAM23, NRP1, PRKAR1A

Ingenuity Canonical Pathways	p-value	B-H p-value	Molecules
14-3-3-mediated Signaling	0.0081	0.072	TUBA1A, YWHAE, YWHAB, TUBB2A, YWHAZ, TUBA4A, PLCG1, VIM, TUBA1B
Glycolysis/Gluconeogenesis	0.0087	0.074	ADH5, PGK1, ALDH2, HK1, AKR1A1, ALDOA, Gapdh
Clathrin-mediated Endocytosis Signaling	0.0089	0.074	HSPA8, AP2M1, ACTB, CHP, RAC1, SH3GLB1, Ubb, DNM1L, UBC, AAK1, ACTG1, DNM2
Mitotic Roles of Polo-Like Kinase	0.0089	0.074	SLK, ANAPC4, HSP90B1, PTTG1, HSP90AA1, FZR1
Antigen Presentation Pathway	0.0098	0.078	B2M, CALR, HLA-B, HLA-C
Prostate Cancer Signaling	0.0100	0.079	HSP90B1, NFKBIA, HSP90AA1, ATF4, CTNNB1, CCND1, SIN3A
ERK5 Signaling	0.0105	0.081	IL6ST, YWHAE, YWHAB, YWHAZ, ATF4, WNK1
Regulation of IL-2 Expression in Activated and Anergic T Lymphocytes	0.0107	0.081	Calm1, NFKBIA, BCL10, ZAP70, CHP, RAC1, PLCG1
Citrate Cycle	0.0110	0.081	CS, IDH3A, MDH1, ACLY
p70S6K Signaling	0.0117	0.085	GNAI2, GNAI3, YWHAE, YWHAB, EEF2, YWHAZ, PLCG1, RPS6, BCAP31
Calcium Signaling	0.0129	0.089	MYL9, AKAP5, CALR, TPM1, Calm1, ATP2B1, CHP, MYH9, TPM3, ATF4, PRKAR1A
Methane Metabolism	0.0129	0.089	ADH5, PRDX1, CAT
VEGF Signaling	0.0148	0.100	EIF2S3, YWHAE, ACTB, EIF1, PLCG1, EIF2B2, ACTG1
Molecular Mechanisms of Cancer	0.0158	0.103	TCF4, AXIN1, TAB2, RAC1, BMPR2, RAPGEF3, CRK, CCND1, SIN3A, GNAI2, GNAI3, NFKBIA, CCND2, RHOA, CFLAR, CTNNB1, SMAD1, PRKAR1A
Cdc42 Signaling	0.0158	0.103	B2M, MYL9, MYL12B, HLA-B, PPP1R12A, PPP1CB, ITGA3, IQGAP1, HLA-C
G Beta Gamma Signaling	0.0170	0.106	GNAI2, GNAI3, CAV1, PLCG1, CAV2, DNM2, PRKAR1A
Inositol Phosphate Metabolism	0.0174	0.106	GNAI2, GNAI3, PIP5K1A, PIM1, CSNK1D, GRK6, MTM1, CSNK1A1, PLCG1, EIF2AK2
Neuregulin Signaling	0.0178	0.106	HSP90B1, PLCG1, HSP90AA1, RPS6, CRK, ERRFI1, ITGA3
Glyoxylate and Dicarboxylate Metabolism	0.0178	0.106	CS, HOGA1, MDH1
ILK Signaling	0.0186	0.108	MYL9, TMSB10/TMSB4X, ACTB, RHOA, MYH9, PPP1R12A, VIM, ATF4, CTNNB1, CCND1, ACTG1
Neuroprotective Role of THOP1 in Alzheimer's Disease	0.0214	0.123	YWHAE, HLA-B, HLA-C, PRKAR1A
Fcγ Receptor-mediated Phagocytosis in Macrophages and Monocytes	0.0224	0.125	PIP5K1A, ACTB, RAC1, DGKB, PLCG1, CRK, ACTG1
cAMP-mediated signaling	0.0229	0.125	GNAI2, AKAP5, AKAP13, AKAP2/PALM2-AKAP2, GPER, Calm1, DUSP1, ATF4, RAPGEF3, APEX1, PKIG, PRKAR1A
PDGF Signaling	0.0229	0.125	ABL2, ACP1, CAV1, PLCG1, CRK, EIF2AK2
Role of NFAT in Regulation of the Immune Response	0.0263	0.141	GNAI2, AKAP5, GNAI3, Calm1, NFKBIA, ZAP70, CHP, CSNK1D, CSNK1A1, PLCG1
Mechanisms of Viral Exit from Host Cells	0.0282	0.149	ACTB, SH3GLB1, ACTG1, NEDD4

Ingenuity Canonical Pathways	p-value	B-H p-value	Molecules
Paxillin Signaling	0.0288	0.150	ARF1, ACTB, RAC1, CRK, ITGA3, BCAR1, ACTG1
GNRH Signaling	0.0316	0.163	GNAI2, MAP3K12, GNAI3, EGR1, RAC1, ATF4, DNM2, PRKAR1A
Role of Osteoblasts, Osteoclasts and Chondrocytes in Rheumatoid Arthritis	0.0372	0.186	TCF4, Calm1, NFKBIA, AXIN1, TAB2, CHP, CSNK1A1, BMPR2, ITGA3, GSN, CTNNB1, SMAD1
Insulin Receptor Signaling	0.0380	0.187	HLA-B, PPP1R12A, PPP1CB, CRK, ACLY, EIF2B2, PRKAR1A, GRB10
fMLP Signaling in Neutrophils	0.0389	0.188	GNAI2, GNAI3, Calm1, NFKBIA, NCF2, CHP, RAC1
Cell Cycle: G2/M DNA Damage Checkpoint Regulation	0.0398	0.189	YWHAE, YWHAB, YWHAZ, LOC728622/SKP1
Synaptic Long Term Potentiation	0.0407	0.191	Calm1, CHP, PPP1R12A, ATF4, PPP1CB, RAPGEF3, PRKAR1A
CXCR4 Signaling	0.0417	0.195	GNAI2, MYL9, GNAI3, MYL12B, EGR1, RHOA, RAC1, CRK, BCAR1
Role of Wnt/GSK-3β Signaling in the Pathogenesis of Influenza	0.0457	0.207	TCF4, AXIN1, CSNK1D, CSNK1A1, CTNNB1
RANK Signaling in Osteoclasts	0.0468	0.207	MAP3K12, Calm1, NFKBIA, TAB2, CHP, GSN
Glucocorticoid Receptor Signaling	0.0479	0.207	CHP, RAC1, SMARCD2, HSPA5, NR3C1, HSPA8, HSP90B1, SCGB1A1, NFKBIA, DUSP1, PTGES3, HSP90AA1, CREBZF
PI3K Signaling in B Lymphocytes	0.0479	0.207	CD81, Calm1, NFKBIA, BCL10, CHP, RAC1, PLCG1, ATF4
Cardiac β-adrenergic Signaling	0.0479	0.207	AKAP5, AKAP13, AKAP2/PALM2-AKAP2, PPP1R12A, PPP1CB, APEX1, PKIG, PRKAR1A
α-Adrenergic Signaling	0.0490	0.209	GNAI2, GNAI3, Calm1, HLA-B, PLCG1, PRKAR1A

Table 4: Upstream Regulators

Complete list of the statistically significant transcription factor pathways as identified by Ingenuity Pathway Analysis.

Upstream Regulator	p-value of overlap	Target molecules in dataset
IGF1R	4.21E-10	ACP1,ALDOA,Atp5h,CD36,COX5B,COX6A2,CYCS,FTH1,IVNS1ABP,LASP1,NDUFA1,NDUFA4,PRKAR1A,RAB1A,RPL10A,RPL35A,RPL37A,RPL7,RPL9,RPS21,RPS24,RPS26,SDC4,TXN
INSR	1.22E-07	ALDH2,Atp5h,Calm1 (includes others),CCND2,CD36,COX5B,COX6A2,CS,CYCS,DCTN4,FOXN3,GANAB,Gapdh/LOC100042025,HSPD1,IDH3A,IQGAP1,Lyz1/Lyz2,NDUFA1,NDUFA4,PAX6,Rpl5,RPL7A,RPS16,UCP2,YBX1
FAAH	2.46E-07	Atp5h,RPL17,Rpl5,RPL7,RPS18,RPS2,RPS3A,RPS6,SEPT4
ADORA2A	4.49E-07	ATP2B1,ATP8A1,Cd24a,CD81,DUSP1,EEF2,EIF1,Gapdh/LOC100042025,HNRNPK,Ifitm3,PRKAR1A,RAB6A,SPARC,SPTBN1,TJP1,TUBB2A
FOS	7.72E-06	A130040M12Rik,AQP3,CADM1,CAT,CCND1,DDX3X,DLG1,HBB,HMMR,KLF6,MACF1,MYH9,ODC1,PTTG1,QKI,RAPGEF3,RBBP4,SCD,STK3,STMN1,Tpm1,UTRN,VIM,YWHAZ
APOE	1.09E-05	ACTB,BGN,CALR,CAT,CCND2,CD36,CTNNB1,CTSL2,EGR1,GPX3,HMMR,HSPD1,ITGA3,MGP,NCF2,NPNT,SDC4,SMAD1,SOD1
PTEN	2.93E-05	ACAA1,CA8,CCND1,CTNNB1,CTSL2,EFNB2,EPAS1,MCL1,Nedd4,PIM1,RPS6,SCD,SDC4,SFTPA1,SFTPC,SMAD1
ANK2	5.27E-05	KCNJ11,L1CAM,SPTBN1
NFE2L2	1.64E-04	ACTG1,AKR1A1,ALDOA,Arf1,Calm1 (includes others),CAT,CCRN4L,EIF3E,EIF4G2,FTH1,HSP90AA1,HSP90B1,INMT,L1CAM,MORF4L2,PRDX1,RPL18,RPLP0,RPS16,SERINC3,SOD1,SRXN1,TMED2,Tpm1,TXN
TP53	1.88E-04	ACLY,ACTB,ADH5,APEX1,BTG1,CAT,CAV1,CCND2,CLIC4,COL4A1,COX5B,CSNK1D,CTNNB1,DBI,DUSP1,FAM120A,Gapdh/LOC100042025,GPX3,GSN,HSP90AA1,HSPD1,IFI35,LASP1,Lyz1/Lyz2,MCM3,MYH9,ND5,NRP1,PAFAH1B2,RBBP4,SOD1,STMN1,TDO2,TGM2,TJP1,Tpm1,UBC,VIM
DAB2	2.05E-04	AXIN1,CCND1,CTNNB1
PPP3R1	2.06E-04	CLIC5,Lyz1/Lyz2,SCD,SFTPA1,SFTPC,SLC34A2
E2F1	2.37E-04	Calm1 (includes others),CALR,CAV1,CCND1,DUSP1,EGR1,FGFR2,INMT,NCL,NRP1,RBBP4
CAV1	3.02E-04	CAV1,CAV2,CCND1,CTNNB1,HSPA8,NPM1,RPL17,RPS13,Rps9,TJP1
YY1	3.46E-04	API5,ATF4,CBX3,COX5B,EEF1B2,EIF4G2,LUC7L2,MAT2A,PLAGL1,PNRC2,PTBP3,RBBP4,SRSF1,TCF4,TGM2,Tpm1,YWHAE
RHOJ	4.18E-04	ACTG1,CAV1,CNBP,GSN,MYH9
CD44	4.23E-04	ACTB,BGN,CALR,CCND2,HMMR,ITGA3,NPNT,SDC4,SMAD1
DYSF	4.25E-04	ACTG1,B2M,CORO1C,CTSL2,ERRFI1,GNAI3,HLA-C,IDH3A,Lyz1/Lyz2,PROS1
CYP1A1	4.88E-04	AP2M1,CBX3,CCND1,CHP1,DYNLRB1,MYO10,NDUFA1,ODC1,PTP4A1,QKI,RBBP4
GATA6	7.65E-04	CYP11A1,SCGB1A1,SFTPA1,SFTPC
PRKAG3	8.53E-04	CD36,METTL7A,NAP1L1,PAM,RPL13A,RPL22,Rpl5,Snhg8
SOD1	9.67E-04	APEX1,CCND1,SOD1

Upstream Regulator	p-value of overlap	Target molecules in dataset
miR-16-5p (and other miRNAs w/seed AGCAGCA)	9.67E-04	CCND1,CCND2,UCP2
IKBKAP	9.67E-04	CTNNB1,RHOA,TEK
PPARG	0.0012	ACAA1,ATP6V1D,Bex1,CAT,CAV1,CD36,Ces1d,CTNNB1,GABARAPL2,KLF6,LAPTM4A,Prl2c2 (includes others),SCD,SDPR,SOD1,TCF4,VIM,YWHAE
NRF1	0.0014	COX5B,COX6A1,COX6C,FTH1,VDAC1
ERAP1	0.0014	HLA-B,HLA-C
JARID2	0.0014	CCND1,CCND2
ARNT	0.0015	CCND2,CD81,MACF1,MYL6,OAZ1,TUBA4A,VIM
Creb	0.0016	ABL2,CFLAR,DDX6,DUSP1,FOXN3,LASP1,MCM3,PGK1,SOD1
SLC13A1	0.0017	ACLY,ACTG1,COPB2,G0S2,GPAM,HSPA5,HSPA8,INMT,RPL41,SCD
FMR1	0.0020	ALDOA,ATPIF1,CTNNB1,EEF2,Gapdh/LOC100042025,RPSA
Igm	0.0025	CCND2,CFLAR,EGR1,PIM1
SMTNL1	0.0026	PPP1R12A,Prl2c2 (includes others),Prl3b1
AMPK	0.0026	CTNNB1,EGR1,UCP2
BMPER	0.0026	CDH5,EFNB2,MGP
NR3C1	0.0029	ACTB,B2M,CAT,CYP11A1,DBI,DDX5,DUSP1,EGR1,SERINC3,SFTPA1,SFTPC,TXN,YWHAE
VEGFA	0.0032	CDH5,CST3,CTSL2,TEK
PPARGC1A	0.0033	CAT,CD36,COX5B,CS,CYCS,IDH3A,SCD,SOD1,UCP2
MECP2	0.0035	ACTB,DPYSL2,HSPA5,Meg3,YWHAB,YWHAZ
USF1	0.0040	DUSP1,GPAM,PRKAR1A,UCP2
MED30	0.0040	COX5B,COX6A2,CS,NDUFB7
SERPINF1	0.0041	CDH5,TJP1
IQGAP2	0.0041	CCND1,IQGAP1
MAX	0.0049	CCND2,NCL,ODC1,RBBP4
FLI1	0.0049	HSPA8,NPM1,RPL18,TEK
GPX1	0.0049	CAT,GPX3,SOD1,TXN
CTGF	0.0051	CCND1,CTNNB1,HSD17B7,SDPR,Tpm1,WNK1
CLCN5	0.0052	SLC34A2,SOD1,TXN
SOD2	0.0052	CAT,ODC1,YWHAZ
MNT	0.0052	CCND2,NCL,ODC1
PARK2	0.0052	CCND1,COX5B,PRDX1
XBP1	0.0056	AICDA,CAT,HSPA5,SOD1,TXN
NKX3-1	0.0064	CA8,CTNNB1,CTSL2,PIM1,SDC4,SMAD1
KLF5	0.0069	CCND1,CTNNB1,UCP2
FOLR1	0.0076	CAT,CELF2,DTD1,GAS5,GPAM,HNRPDL,Lyz1/Lyz2,NAP1L1,RPS24
TCR	0.0079	CFLAR,EGR1,HSP90B1,HSPA5,LAMP1,MCL1
mir-15	0.0080	CCND1,CCND2
PDE3A	0.0080	CCND1,DUSP1
SIX3	0.0080	CCND1,PAX6
ABCC8	0.0080	CAT,SOD1
AJUBA	0.0080	BCAR1,CRK
MST1R	0.0080	CCND1,CTNNB1
HIPK2	0.0083	CCND2,EGR1,HBB,POU4F1,RAC1
FAS	0.0088	BGN,CFLAR,COL4A1,EGR1,MGP,NFKBIA
LIPE	0.0089	EGR1,G0S2,Gapdh/LOC100042025,GRB10,H3f3a/H3f3b,INMT,PAM,SCD,SDC4,ST8SIA4
CLDN6	0.0099	ATF4,CLDN14,HSPA5,KLF4

Upstream Regulator	p-value of overlap	Target molecules in dataset
NR4A2	0.0099	ABL2,CFLAR,DDX6,SOD1
MTORC1	0.0114	ATF4,KLF4,SCD
INSIG2	0.0114	ACLY,GPAM,SCD
NFYA	0.0114	CAT,FGFR2,PGK1
IL5	0.0116	AICDA,ALDOA,BNIP3L,CCND2,GPAM,HMMR,HSP90B1,HSPA5,LMO7,PIM1,VIM
CNTF	0.0130	IL6ST,VIM
CCND1	0.0130	CCND1,CCND2
miR-17-5p (and other miRNAs w/seed AAAGUGC)	0.0130	CCND1,CCND2
miR-92a-3p (and other miRNAs w/seed AUUGCAC)	0.0130	CCND1,CCND2
CCND3	0.0130	CCND1,CCND2
Hmgn3	0.0130	KCNJ11,PAX6
CCND2	0.0130	CCND1,CCND2
MTA1	0.0130	CTNNB1,HBB
CAPNS1	0.0130	CCND1,CCND2
ATF2	0.0133	ACTB,CCND1,CTNNB1,DUSP1
CREBBP	0.0136	CCND1,CCND2,CDH5,MCM3,RHOA,SFTPA1,SIN3A
ELOVL5	0.0141	GPAM,PLTP,SCD
CREM	0.0154	EGR1,ERRFI1,MARCKS,MCL1,NPC2,PGK1,PRM1,Tpm1
PAX7	0.0158	Cd24a,DEPTOR,Hmgn1,MARCKS,NPNT,PLAGL1,RNF128
TCOF1	0.0170	AZIN1,BNIP3L,CNBP,HNRPDL,IQGAP1,PPIL4,STMN3
GLIS2	0.0171	MGP,SPARC,VIM
NR4A3	0.0171	CCND1,CCND2,UCP2
CYP1A2	0.0180	CBX3,CCND1,QKI,RBBP4,SFTPA1
FGFR1	0.0180	CCND1,CCND2,DNAJC1,Eef1a1,RPS6
MAPK14	0.0181	CALR,CAT,CCND1,HBB,SOD1,TGM2
IHH	0.0191	CCND1,CTNNB1
FHL2	0.0191	BCAR1,CYP11A1
AFP	0.0191	EGR1,PTP4A1
PIWIL2	0.0191	CCND1,LATS2
EPOR	0.0191	HBB,PIM1
SLC19A1	0.0191	Ly6a (includes others),SKP1/SKP1P2
ID2	0.0191	AICDA,CTNNB1
Alpha catenin	0.0214	BGN,CTSL2,IL6ST,Lyz1/Lyz2,NFKBIA,Prl2c2 (includes others),TGM2,VIM,ZEB2
TEAD4	0.0242	FGFR2,NOTCH2,SMAD1
THBS4	0.0242	ATF4,CALR,HSPA5
HOXC6	0.0248	ERRFI1,FGFR2,SEPT7,SH3D19
NLRC5	0.0261	B2M,HLA-C
IL7R	0.0261	MCL1,PIM1
GATA2	0.0261	CCND1,Prl2c2 (includes others)
EIF4E	0.0261	MCL1,NFKBIA
DDX58	0.0277	AHNAK,EIF2AK2,IFI35,RPS7
BCR (complex)	0.0308	CCND2,CFLAR,EGR1,MCL1
PSEN1	0.0321	ACTB,CCND1,CTNNB1,DUSP1,FAM32A,Gapdh/LOC100042025,GAS5,L1CAM,UBC
ESRRA	0.0326	ALDOA,COX5B,COX6A2,COX7A2L,IDH3A,NDUFA2

Upstream Regulator	p-value of overlap	Target molecules in dataset
PPARGC1B	0.0326	CS,CYCS,SCD
MAPK11	0.0339	CALR,CAV1
Mup1 (includes others)	0.0339	CYCS,SCD
let-7a-5p (and other miRNAs w/seed GAGGUAG)	0.0339	CCND1,CCND2
ALOX15	0.0339	CD36,CTNNB1
IL2	0.0340	CFLAR,HSP90B1,HSPA5,Ly6a (includes others)
P38 MAPK	0.0360	CCND1,CCND2,DUSP1,EGR1,Nedd4
ACOX1	0.0367	ACAA1,CAT,CD36,CTSL2,HSPA5,KLF6,RPL12,Rpl36,RPS24,UCP 2
NR2E1	0.0373	CCND1,MAP3K12,POU4F1
CCR1	0.0373	ATF4,CTSL2,SPARC
PTPN1	0.0374	CFLAR,DUSP1,NFKBIA,PLAGL1
voltage-gated calcium channel	0.0375	CCND2
Rac	0.0375	CCND1
Pdgf (complex)	0.0375	COL4A1
Smad	0.0375	MCL1
SUV39H2	0.0375	SFTPA1
FBXO31	0.0375	CCND1
FXN	0.0375	ACLY
FOXD2	0.0375	PRKAR1A
CCM2	0.0375	RHOA
Raet1a	0.0375	HLA-C
Raet1b	0.0375	HLA-C
GPC3	0.0375	CCND1
TRA2B	0.0375	PPP1R12A
ARHGAP26	0.0375	RHOA
RXFP2	0.0375	CTNNB1
SFTPB	0.0375	SFTPC
TNKS	0.0375	AXIN1
CTNND1	0.0375	CTNNB1
AMD1	0.0375	TMSB10/TMSB4X
JUP	0.0375	CTNNB1
HNRPDL	0.0375	COX5B
mir-101	0.0375	DUSP1
mir-216	0.0375	YBX1
H60a	0.0375	HLA-C
SYNCRIP	0.0375	RHOA
ALAS2	0.0375	HBB
Raet1d/Raet1e	0.0375	HLA-C
HIPK3	0.0375	CYP11A1
SSPN	0.0375	UTRN
MYH10	0.0375	MYH9
AVP	0.0375	HSPA5
ANGPT2	0.0375	TEK
IGBP1	0.0375	RAC1
PRKAR2A	0.0375	PRKAR1A
TRAF7	0.0375	CFLAR
TP53INP1	0.0375	SPARC

Upstream Regulator	p-value of overlap	Target molecules in dataset
FBXO4	0.0375	CCND1
CTSK	0.0375	CTSL2
MAGI2	0.0375	RHOA
TAPBP	0.0375	HLA-C
BTG2	0.0375	CCND1
ULBP1	0.0375	HLA-C
CAV2	0.0375	CAV1
DAXX	0.0375	CYP11A1
ATF5	0.0375	MCL1
ADCY3	0.0375	NRP1
MYB	0.0424	HSPA8,IQGAP1,PAX6
SIN3A	0.0424	CCND2,ING1,NCL
VHL	0.0425	EPAS1,RPS6
MAPK3	0.0425	CTNNB1,MCL1
GPER	0.0425	CCND1,HSPA5
PRKAR1A	0.0425	CCND1,VIM
SNAI1	0.0425	CCND1,CCND2
PPARA	0.0429	ACAA1,ALDH2,APEX1,AQP3,CAT,CCND1,CD36,CS,DBI,G0S2,GPAM,H2AFZ,Hmgn1,Ifitm3,NFKBIA,PLTP,SCD,UCP2
CEBPA	0.0458	ACLY,CCND2,CYP11A1,EFNB2,G0S2,NRP1,SCD,SFTPA1,SFTPC
CEBPB	0.0466	CCND2,CYP11A1,DDX5,DHX9,EFNB2,HNRNPA3,HSP90AA1,INMT,MCM3,NRP1,SCD,SERP1
AGER	0.0477	COL4A1,EGR1,TJP1
NR1H3	0.0480	GPAM,NFKBIA,PLTP,RPS14,SCD

Table 5: Genes of Interest

The number of genes in each category is shown in parentheses next to the overall category. Alternate gene names are listed in parentheses next to the official gene designation. If a probe hybridizes to mRNA from more than one gene, both are listed separated by a forward slash.

Reproduction (33)

Male Reproductive System (10)
- *Cyp11a1*
- *Ddx17*
- *Ddx3x*
- *Ddx5*
- *Pip5k1a*
- *Prm1*
- *Ptma*
- *Spin1*
- *Tuba4a*
- *Tsks*

General Pregnancy (8)
- *Cyp11a1*
- *Deptor* (*Depdc6*)
- *Gpr30*
- *Plscr3*
- *Psg28*
- *Scgb1a1* (Uteroglobin)
- *Serbp1*
- *Tdo2*

Female Reproductive System (6)
- *Cyp11a1*
- *Gpr30*
- *Kpna7*
- *Pkd2l2*
- *Ptges3*
- *Tmsb10*

Placenta (13)
- *Clic5*
- *Ctsq*
- *Cyp11a1*
- *Grb10*
- *Notch2*
- *Peg10*
- *Plac9*
- *Prl2b1*
- *Prl2c2/Prl2c3/Prl2c4*
- *Prl3b1*
- *Smurf2*
- *Thsd7a*
- *Tmed2*

Endothelial (13)

Blood Vessels (10)
- *Cdh5* (*VE-cad*)
- *Egfl7*
- *Klf4*
- *Lbh*
- *Mtus1*
- *Nrp1*
- *Rhoa*
- *Sepp1*
- *Tek*
- *Thbd*

Hematopoietic Cells (3)
- *Hbb-b1/Hbb-b2*
- *Ly6a* (*Sca-1*)
- *Ybx1*

Immune (32)

Innate Immunity (16)

- *Ahnak*
- *B2m*
- *H2-K1*
- *H2-Q7*
- *Hpgd*
- *Hspd1*
- *Il6st*
- *Irf2bp2*
- *Klf4*
- *Lyz1*
- *Lyz2*
- *Ncf2*
- *Nfkbia*
- *Nr3c1*
- *Tab2*
- *Tm9sf3*

Acquired Immunity (13)

- *Aicda*
- *Bcap31*
- *Cd24a* (*Hsa*)
- *Dusp1*
- *Foxp1*
- *Gas5*
- *Igha/Igh-VJ558*
- *Pim1*
- *Pou4f1*
- *Pptc7*
- *Rnf128*
- *Zap70*
- *Zxdc*

General (3)

- *Abhdl6a* (*Bat5*)
- *Ppil4*
- *Smad1*

Mesenchymal (12)

Expressed in Mesenchyme (2)

- *Ahnak*
- *Epas1*

Epithelial-Mesenchymal Transition (10)

- *Axin1*
- *Bmpr2*
- *Cav1*
- *Csnk1a1*
- *Ctnnb1*
- *Klf4*
- *Lbh*
- *Notch2*
- *Smad1*
- *Vim*

CHAPTER THREE: GENE EXPRESSION STUDY OF FETAL CELLS IN THE MATERNAL LUNG DURING ALLOGENEIC PREGNANCY

INTRODUCTION

Murine models examining fetal cell trafficking in allogeneic versus syngeneic matings have found differences in both the quantity (Kallenbach et al., 2011a; Khosrotehrani et al., 2005) and phenotype (Kallenbach et al., 2011a) of fetal cells. Slight differences in fetal cell proliferation rates between fetal cells from syngeneic (3-5%) and allogeneic (4-7%) pregnancies have been observed (Liegeois et al., 1981). Similar alterations have been documented in humans, showing more microchimeric fetal cells in peripheral blood with greater fetomaternal immunocompatibility (Adams Waldorf et al., 2010). MHC matches between the mother and her offspring may also affect the postpartum impact of fetal cells on maternal health. HLA class II compatibility between the mother and child was found more frequently in women affected by scleroderma compared to controls (Nelson et al., 1998).

In our gene expression study of fetal cells in the maternal lung in syngeneic matings, we concluded that immune cells were one of the main constituents of the fetal cell population (Chapter Two). We hypothesized that these cells may be responsible for facilitating fetomaternal immune tolerance and may be different in an allogeneic pregnancy. Furthermore, an allogeneic mating model is a closer reflection of human reproduction. We thus performed gene expression analysis of fetal cells in the maternal lung during allogeneic pregnancies.

METHODS

MICE

Wildtype FVB/NJ mice (stock no. 1800, Jackson Labs) were mated to $GFP^{+/+}$ males as described above (page 33). Six female mice were euthanized 19 days after mating. Gestational ages of the pups studied were 14.5-17.5 days as determined by Theiler staging (Theiler, 1989). The maternal lungs were harvested and a single cell suspension was prepared as discussed previously (page 34). GFP+, PI- cells from each set of lungs (Figure 1) were sorted directly into the One Direct Kit lysis buffer (NuGEN Technologies, Inc.) at a dilution of 40 cells/µl. Cell lysates from each female were pipetted repeatedly to mix and stored at -80°C until amplification.

cDNA AMPLIFICATION AND ARRAY HYBRIDIZATION

cDNA was converted and amplified from the RNA in the cell lysates using the WT-Ovation One Direct Amplification system following the manufacturer's protocol with the exception of using up to 80 cells as input material. The quantity of cDNA was measured using a Nanodrop 2000 (ThermoScientific) and the quality of cDNA was assessed using a Bioanalyzer 2100 (Agilent).

3.3 µg of cDNA were fragmented and biotinylated using the Encore Biotin Module (NuGEN Technologies, Inc.) and hybridized to mouse 430 2.0 arrays (Affymetrix) as described earlier (page 36). The arrays were normalized in R using quantile-normalization, with ideal mismatch background correction and Tukey biweight summarization. Following normalization a list was made of probes with a present call on all six arrays. This was called the "allogeneic fetal cell core transcriptome."

Analysis of the Fetal Cell Core Transcriptome

The list of fetal cell core transcriptome probes was uploaded to NetAffx to translate the fetal cell core transcriptome probes into the corresponding genes. Ingenuity Pathway Analysis (build version 192063; content version 14400082) was used to identify pathways enriched in the allogeneic core transcriptome. The categories “Top Canonical Pathways” and “Top Upstream Regulators” were primarily used in this analysis. Tissue-specific probes from the fetal cell core transcriptome were identified using the Novartis Research Foundation Gene Expression Database as described above (page 46). To partially address the gene expression differences between adult and fetal tissues, the Eurexpress Transcriptome Atlas Database (http://www.eurexpress.org) (Diez-Roux et al., 2011) was also used. Gene names were individually searched and annotations provided by the atlas were used to determine embryonic expression. Principal component analysis (PCA) was utilized to compare the fetal cell transcriptome to two publicly available datasets downloaded from the Gene Expression Omnibus as described earlier (page 47). The GEO datasets, together with data collected from GFP+ fetal cells, were normalized in R using quantile-normalization with ideal mismatch background correction and Tukey biweight summarization. Principal components one through four were plotted. Finally, genes of interest were identified using IPA, NCBI Gene, UniProt Knowledgebase and the primary literature.

Results

Flow Sorting of Fetal Cells in Maternal Lung and Fetal Nucleic Acid Amplification

From each set of maternal lungs, 300-609 GFP+, PI- fetal cells were flow-sorted (Figure 1). After amplification the cDNA concentration ranged from 132-254ng/µl.

ANALYSIS OF THE FETAL CELL CORE TRANSCRIPTOME

One thousand one hundred thirty-nine (1139) probes had a present call on all six arrays. As determined through NetAffx, the probes represented 806 genes, 231 predicted genes or loci, and 123 unmapped probes. As with the fetal cells in syngeneic matings (Chapter Two) about one-third of the 806 genes are considered housekeeping genes (eg. heat shock proteins, mitochondrial respiration proteins such as cytochrome C oxidase, and ribosomal proteins).

Ingenuity Pathway Analysis

Of the 1,139 probes in the allogeneic fetal cell core transcriptome, 991 probes were available for pathway analysis. The top five canonical pathways identified in the core analysis (B-H corrected p-value) were EIF2 signaling ($p=3.16x10^{-41}$), regulation of eIF4 and p70S6K signaling ($p=1.58x10^{-7}$), remodeling of epithelial adherens junctions ($p=3.89x10^{-7}$), mTOR signaling ($p=4.57x10^{-5}$), and epithelial adherens junction signaling ($p=2.34x10^{-4}$). The top five upstream regulators (p-value) were IGF1R ($p=3.70x10^{-8}$), INSR ($p=3.83x10^{-8}$), NFE2L2 ($p=5.36x10^{-8}$), ADORA2A ($p=3.39x10^{-6}$), and PSEN2 ($p=6.55x10^{-6}$). Complete results and specific genes in each canonical pathway and upstream regulator are presented in Table 7 and Table 8, respectively.

IPA was used to find genes common to both the syngeneic and the allogeneic fetal cell core transcriptomes. Three hundred sixty-four (364) genes were identified, although the genes were sometimes represented by different probes. Pathways analysis suggests that the shared genes are primarily involved with gene expression, protein synthesis, cellular movement and cell death and survival.

Tissue Specificity

Using the BioGPS database and the fetal cell core transcriptome, 111 probes, corresponding to 109 genes, met the criteria for establishing tissue specificity (Table 6). These 109 genes derive from several organs and organ systems (Figure 9). Nervous system, immune system, testis, eye and placenta were represented most often. Using the Eurexpress Transcriptome Database, the following fetal tissues were most highly represented by the 109 genes: nervous system, muscle, epithelium, adrenal glands, and thymus (Table 6). Two genes, *Tfpi* and *Nrk* were identified as tissue specific by the BioGPS database but Eurexpress annotation showed expression in day 14.5 embryos. *Nrk* had strong expression in muscle, mesenchyme and the submandibular gland. *Tfpi* was weakly expressed in the meninges. The rest of the placenta-specific genes were not expressed in the embryos.

Principal Component Analysis

As with the syngeneic analyses presented in Chapter Two, baseline differences dominated the first and second principal components, which separated the fetal cell data from the GEO datasets in both cases (Figure 10A and Figure 11A). In a PCA that compared our data to the Lattin et al. data set, graphing component three (PC3) vs PC4 (Figure 10) allowed tissue type relationships to be determined. The data points closest to the GFP+ fetal cells were placenta, testis, macrophages, embryonic stem cells, pancreas, and osteoblasts. A PCA comparing our data to the Thorrez et al. data revealed slightly different results. PC3 vs PC4 (Figure 11) showed the closest relationships of the GFP+ fetal cells to be with the placenta, testis, lung, ovary, eye, and adrenal gland. Both versions of the PCA and the BioGPS Expression Atlas suggest similarities to placenta and testis (Figure 12).

Genes of Interest

A partial list of genes of interest is presented in Table 9. However, at this time a full in-depth analysis of all 806 genes has not been completed.

DISCUSSION

SIMILARITIES TO SYNGENEIC GENE EXPRESSION RESULTS

As expected, fetal cells found in the maternal lungs during syngeneic and allogeneic matings have a high degree of similarity. The top five canonical pathways and upstream regulators identified by IPA were the same in both analyses. When comparing the two core transcriptomes, slightly more than half of the probes in the syngeneic fetal cell core transcriptome are also present in the allogeneic core transcriptome. As expected, the common probes were involved in shared functions such as EIF2 and mTOR signaling.

PCA and BioGPS analyses of the two fetal cell gene expression datasets also identified comparable organs such as the placenta, immune cells, osteoblasts, pancreas, ovary, nervous system and lung (Table 10). These results suggest that in both types of pregnancy, the same general types of cells are passing from fetus to mother: trophoblasts, mesenchymal stem cells, and cells of the immune system.

DIVERGENCE FROM SYNGENEIC GENE EXPRESSION RESULTS

More fetal cells were detected in the maternal lungs during allogeneic matings (mean: per 10 million total events) compared to syngeneic matings (mean: per 10 million total events; p=.005). We have previously reported a similar finding (Kallenbach et al., 2011a). Together these results suggest that allogeneic matings may permit collection of a greater number of fetal cells for in vitro testing and other analysis.

Six hundred twenty-seven (627) genes and predicted sequences were unique to the allogeneic transcriptome. Cell-to-cell signaling, cellular movement, and cellular function and maintenance were the most enriched molecular and cellular functions according to IPA. Broadly, similar results were obtained from the unique syngeneic transcriptome genes. It is therefore likely that many of the genes unique to allogeneic matings are involved in cellular homeostasis and do not represent fundamental functional differences.

Although similar tissues were identified by PCA and BioGPS analysis, there was increased similarity between the gene expression profiles of allogeneic mating fetal cells to that of testicular tissue. We believe this is a reflection of increased immaturity of the fetal cells. The testes are one of only a few sources of stem cells in the adult mouse (Morrison and Spradling, 2008). Sperm are produced starting at puberty and continuing throughout life at a high rate, thus requiring support from a robust stem cell population (Griswold and Oatley, 2013).

The presence of a large number of testis-specific probes according to the BioGPS database may be due to the prevalence of unique transcripts in that tissue by comparison to other tissues. In an extensive analysis of housekeeping and tissue-specific transcripts, the testes were found to have 484 specific transcripts, compared to an average of 43 for other tissues (Dezso et al., 2008). The testis transcripts were mostly related to meiosis, supporting our hypothesis that fetal cell similarity is a reflection of stem cell resemblance.

Further support for stem cell properties of microchimeric fetal cells is expression of *Cxcr4*. *Cxcr4* encodes the receptor for CXCL12, a signaling molecule vital for maintenance of HSCs (Sugiyama et al., 2006). *Cxcr4* was not expressed in the syngeneic dataset although previous antibody studies have shown that a small proportion of fetal cells in syngeneic matings do (Fujiki et al., 2009). It would be

interesting to analyze CXCR4+ fetal cells in allogeneic matings as our data suggest their presence would be increased.

A substitute hypothesis is that affinity to the testis is purely a reflection of functional similarities between testis, placenta and ovary. All three tissue types synthesize steroid hormones (Albrecht and Pepe, 1990), a commonality that also may explain the presence of adrenal gland on PCA (Figure 6, Figure 7, Figure 10, and Figure 11). The placenta and testis both synthesize oxytocin (Gimpl and Fahrenholz, 2001). This small peptide hormone is involved in labor and milk secretion in women, and regulation of seminiferous tubule contractility and steroidogenesis in men. Future experiments are warranted to more fully understand the relationship between fetal cells and the testis.

Another distinction between the results presented here and those in Chapter Two lies with the specific immune tissues emphasized by the analyses. Fetal cells in syngeneic pregnancies showed similarity to bone marrow, lymph nodes, peripheral macrophages, and mast cells, while in allogeneic pregnancies the fetal cells were closest to macrophages only. The presence of macrophages might suggest phagocytosis of fetal cell debris by maternal macrophages. Indeed, evaluation of GFP+ fetal cells in the maternal lung by fluorescent microscopy showed some cells with highly fragmented GFP signal (Johnson et al., 2012). Alternatively, fetal macrophages could be present in the maternal lungs, as GFP+ cells with cellular projections similar to pseudopodia were also observed in the same study (Johnson et al., 2012). This interpretation is further supported by known fetal cell expression of CD11b, (Fujiki et al., 2009) a macrophage surface antigen (Mazzone and Ricevuti, 1995), and the presence of Y chromosome sequences in the CD14+ macrophage/monocyte cellular subset in postpartum women (Evans et al., 1999; Nelson, 2012). Further research is needed to

confirm whether functional fetal macrophages are truly passing into the mother during pregnancy or whether these results are a reflection of phagocytosis of fetal cell debris.

It is not currently known what aspects of fetomaternal allogeneicity cause the observed fetal cell trafficking changes. Conventional hypotheses state that major histocompatibility complex (MHC) differences are responsible. However, it may also be some other characteristic of the maternal background strain (Seppanen et al., 2013). To distinguish between these two possibilities, two strains of mice that differ only in the composition of their MHC loci and are otherwise isogenic could be used. For example, one can purchase C57BL/6J mice expressing the Balb/C MHC haplotype, and vice versa. Matings using these transgenic mice compared to their associated wildtype strains would permit focused experiments to determine the role of fetomaternal MHC differences in cell trafficking during and following pregnancy.

CONCLUSIONS

Although similarities exist, we show key differences in the fetal cell populations in the maternal lung during syngeneic and allogeneic matings. In allogeneic matings, the fetal cells appear to have a more primitive phenotype compared to those in syngeneic pregnancy. The use of allogeneic matings for the study of fetal cell microchimerism is a closer reflection of human reproduction and should be the primary model in future experiments.

Figure 9: Source Organ of Fetal Cell Tissue-Specific Genes in Allogeneic Pregnancies

Analysis of the fetal cell core transcriptome using the BioGPS Gene Expression database revealed expression of 109 tissue-specific genes from several different organs. The numbers in parentheses represent the number of tissue-specific genes for each organ.

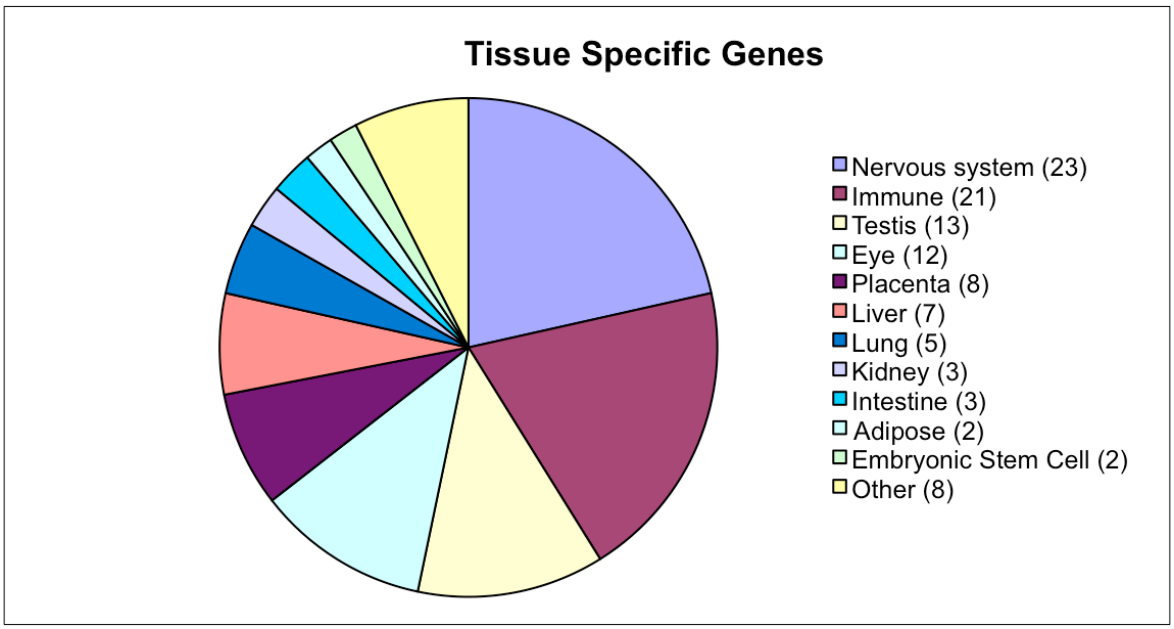

Figure 10: PCA Comparison of Fetal Cells in the Maternal Lung to Lattin et al. Dataset

Fetal cell data, circled in green, compared to Lattin et al. (Lattin et al., 2008) data. **(A)** Principal components 1vs2. **(B)** Principal components 3vs4.

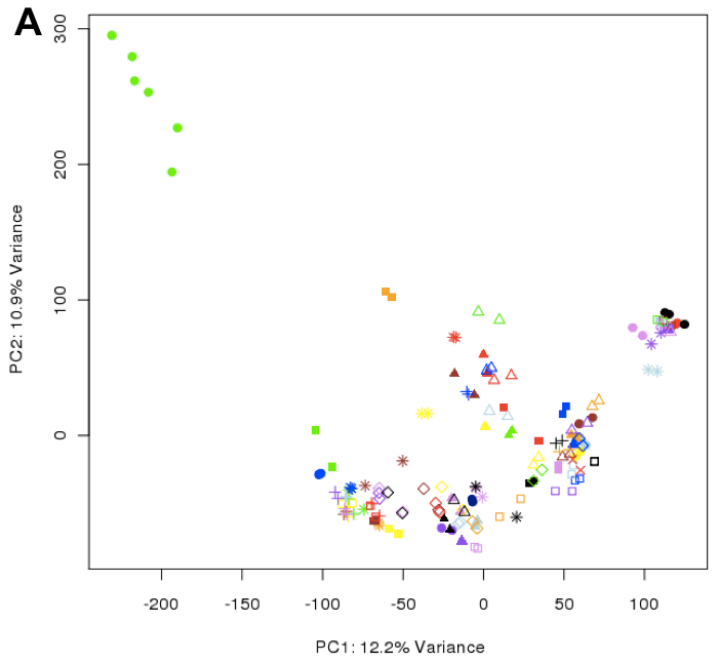

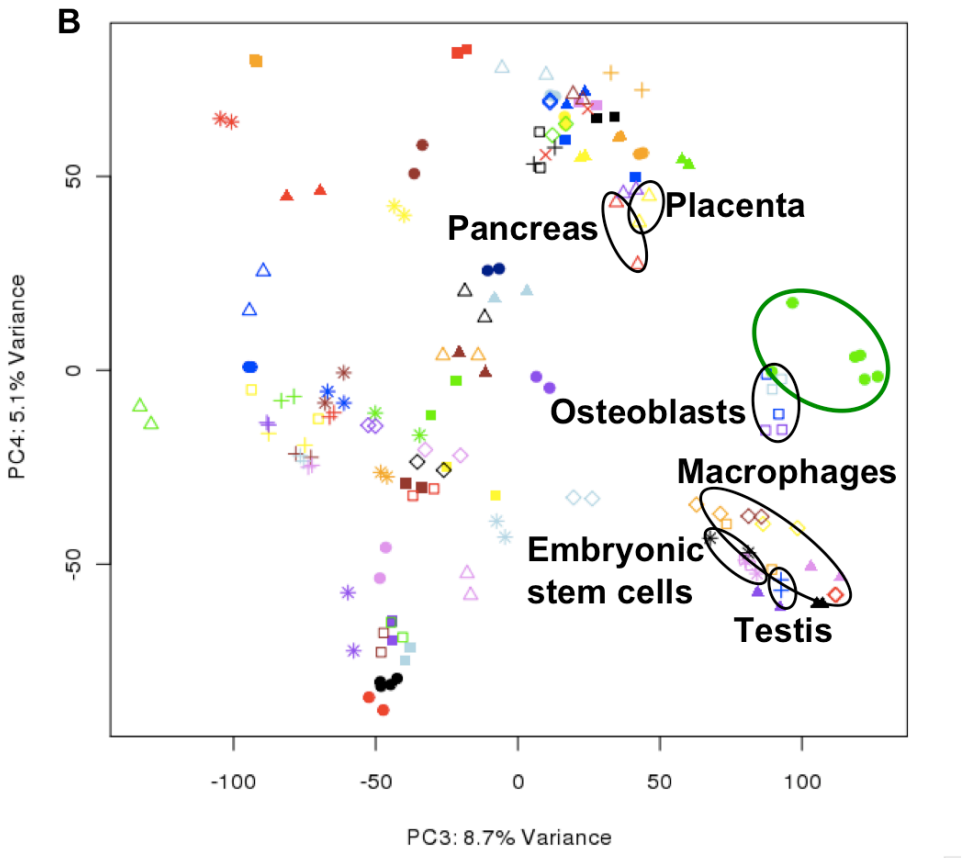
B
Pancreas
Placenta
Osteoblasts
Macrophages
Embryonic
stem cells
Testis
PC4: 5.1% Variance
PC3: 8.7% Variance
50
0
-50
-100
-50
0
50
100

Key

- GFP+ mouse
- Adipose brown
- Adipose white
- Adrenal gland
- Amygdala
- B-Cells
- Bladder
- Bone
- Bone marrow
- Cerebellum
- Cerebral cortex
- Ciliary bodies
- Common myeloid progenitor
- Cornea
- Dendritic cells lymphoid (CD8a+)
- Dendritic cells myeloid (CD8a-)
- Dendritic plasmacytoid (B220+)
- Dorsal root ganglia
- Dorsal striatum
- Embryonic stem line Bruce4 p13
- Embryonic stem line V26_2 p16
- Epidermis
- Eyecup
- Follicular B-cells
- Granulo mono progenitor
- Granulocytes mac1+ gr1+
- Heart
- Hippocampus
- Hypothalamus
- Large intestine
- Small intestine
- Iris
- Kidney
- Lacrimal gland
- Lens
- Liver
- Lung
- Lymph nodes
- Macrophage bone marrow
- Macrophage bone marrow 24hr LPS
- Macrophage bone marrow 2hr LPS
- Macrophage bone marrow 6hr LPS
- Macrophage peri LPS thio 0hr
- Macrophage peri LPS thio 1hr
- Macrophage peri LPS thio 7hr
- Mammary gland lactating
- Mammary gland non-lactating
- Mast cells
- Mast cells IgE
- Mast cells IgE+antigen 1hr
- Mast cells IgE+antigen 6hr
- Mega-erythrocyte progenitor
- Microglia
- NK cells
- Nucleus accumbens
- Olfactory bulb
- Osteoblast day 14
- Osteoblast day 21
- Osteoblast day 5
- Osteoclasts
- Ovary
- Pancreas
- Pituitary
- Placenta
- Prostate
- Retina
- Retinal pigment epithelium
- Salivary gland
- Skeletal muscle
- Spinal cord
- Spleen
- Stem cells HSC
- Stomach
- T-cells (CD4+)
- T-cells (CD8+)
- T-cells (foxP3+)
- Testis
- Thymocyte DP CD4+ CD8+
- Thymocyte SP CD4+
- Thymocyte SP CD8+
- Umbilical cord
- Uterus

Figure 11: PCA Comparison of Fetal Cells in the Maternal Lung to Thorrez et al. Dataset

Fetal cell data, circled in green, compared to Thorrez et al. (Thorrez et al., 2008) data. **(A)** Principal components 1vs2. **(B)** Principal components 3vs4.

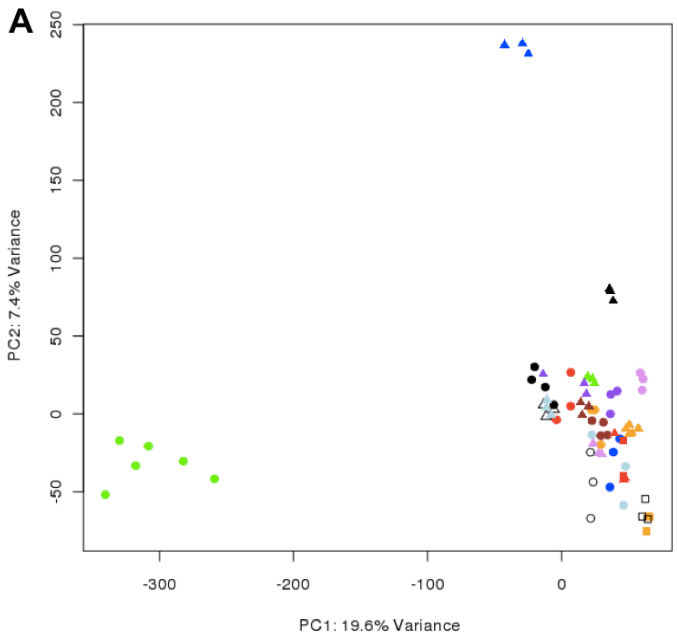

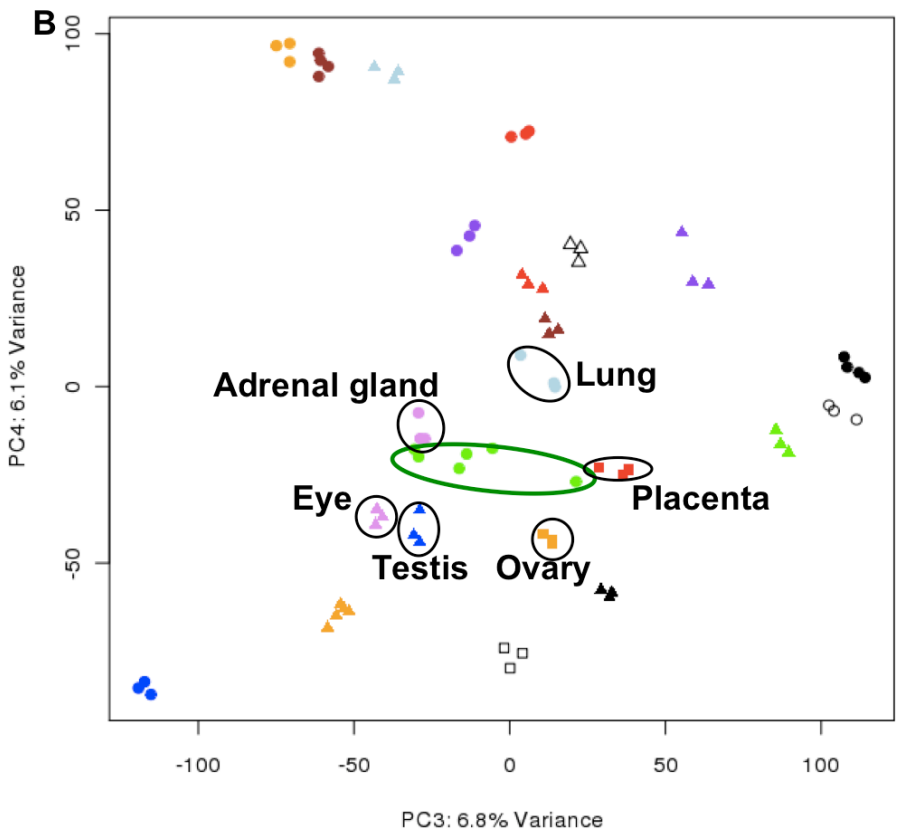

Key
- GFP+
- Diaphragm
- Spleen
- Muscle
- Liver
- Brain
- Lung
- Kidney
- Adrenal gland
- Bone marrow
- Adipose tissue
- Pituitary gland
- Salivary gland
- Seminal vesicle
- Thymus
- Testis
- Heart
- Small intestine
- Eye
- ES cells
- Placenta
- Ovary
- Fetus

Figure 12: Overlap of Analyses for Fetal Cells in the Maternal Lung During Allogeneic Matings

Venn diagram showing overlap between the PCA and BioGPS analyses. Each circle contains the overlap between the results found from our data and from the external datasets analyzed. All three circles converge on placenta and testis.

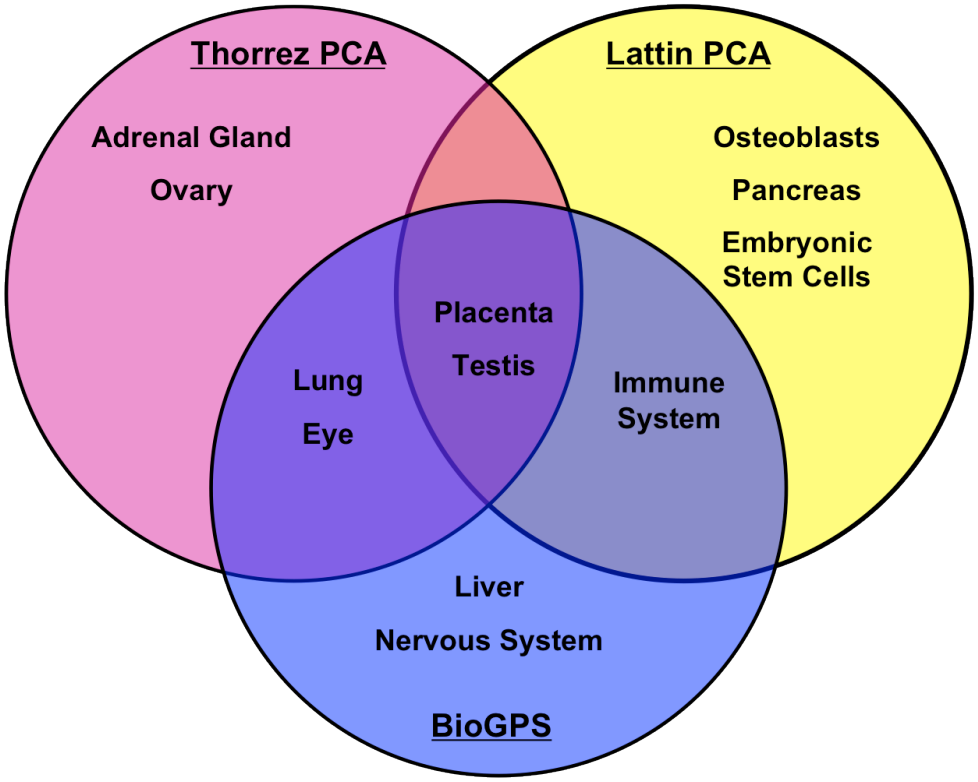

Table 6: Organ-Specific Probes Expressed by Fetal Cells in Allogeneic Matings

A detailed list of the genes and the organs, tissues and cell types in which they are expressed, as identified by BioGPS analysis. The Eurexpress embryo atlas annotations for each gene are also listed.

Organ/ System	Tissue	Probe(s)	Gene Symbol	EurExpress
Nervous system	neuro2a	1452452_at	---	---
	olfactory bulb	1458052_at	---	---
	dorsal root ganglia	1421660_at	Scn9a	Not Annotated
	neuro2a	1453589_a_at	2610005L07Rik, 6820431F20Rik, LOC100861653	Record Not Found
	neuro2a	1427346_at	RBM15/Ott, Luzp4	Not Detected
	cerebral cortex; prefrontal cerebral cortex; amygdala; hypothalamus; spinal cord; dorsal root ganglia; nucleus accumbens; olfactory bulb	1416753_at	Prkar1b	Muscle, brain, nervous system
	cerebral cortex; olfactory bulb; cerebral cortex prefrontal; hippocampus; amygdala; nucleus accumbens	1421990_at	Syt1	Intestines, brain, spinal cord, retina, pituitary
	spinal cord; hippocampus; dorsal striatum	1429798_s_at	Cmtm5	Record Not Found
	cerebellum; cerebral cortex; hypothalamus	1434742_s_at	Aifm3	Record Not Found
	cerebral cortex; prefrontal cerebral cortex; amygdala; hippocampus; nucleus accumbens; hypothalamus spinal cord	1435336_at	Celsr2	Brain, spinal cord, whiskers
	cerebral cortex; prefrontal cerebral cortex; amygdala; hippocampus	1435687_at	Sv2b	Nervous system, stomach, thymus, kidney, epidermis, retina
	cerebellum; cerebral cortex; prefrontal cerebral cortex; hippocampus; dorsal striatum; amygdala	1437640_at	6430704M03Rik	Record Not Found

Organ/ System	Tissue	Probe(s)	Gene Symbol	EurExpress
	dorsal striatum; nucleus accumbens; olfactory bulb; amygdala	1440901_at	Dgkb	Brain mantle layer, anterior abdominal wall
	nucleus accumbens; dorsal striatum	1442166_at	Cpne5	Not Annotated
	cerebellum; olfactory bulb; cerebral cortex; prefrontal cerebral cortex	1443824_s_at	Car7	No Regional Signal
	dorsal root ganglia; nucleus accumbens	1450435_at	L1cam	Nervous system, intestines
	olfactory bulb; dorsal root ganglia; nucleus accumbens	1455271_at	Gm13889	Record Not Found
	cerebellum; amygdala; hypothalamus; cerebral cortex; prefrontal cerebral cortex; nucleus accumbens	1456570_at	Epb4.1l4b	Brain mantle layer, trigeminal nerve ganglia, whiskers
	amygdala; hypothalamus; retina; cerebral cortex prefrontal; spinal cord; cerebral cortex; dorsal striatum; nucleus accumbens; hippocampus; olfactory bulb; retinal pigment epithelium; dorsal root ganglia	1457305_at	Btrc	Brain, spinal cord, dorsal root ganglia, cranial nerve ganglia
	cerebellum; retina; olfactory bulb; amygdala; nucleus accumbens; dorsal striatum	1459126_at	---	---
	spinal cord; cerebellum	1459197_at	Cntn1	Brain, kidneys, cranial nerve ganglia, retina, jaw
	dorsal root ganglia; spinal cord; cerebral cortex prefrontal; hypothalamus; olfactory bulb; amygdala; cerebellum; cerebral cortex; hippocampus; nucleus accumbens	1460181_at	Stmn3	Bone, cartilage, nervous system

Organ/ System	Tissue	Probe(s)	Gene Symbol	EurExpress
	dorsal root ganglia; cerebral cortex; prefrontal cerebral cortex; hippocampus; spinal cord; hypothalamus; cerebellum; amygdala	1460286_at	Sept6	Not Detected
Immune System	thymocyte DP	1436154_at	---	---
	dendritic cells myeloid CD8a-	1425215_at	Ffar2	Pancreas
	thymocyte DP	1456919_at	A930013B10Rik	Not Annotated
	Baf3	1424703_at	Hemk1	Not Detected
	Baf3	1454171_x_at	9530053H05Rik	Record Not Found
	macrophage bone marrow 24h LPS	1428733_at	Gngt2	Thymus
	NK cells	1450495_a_at	Klrk1	Not Detected
	mast cells	1420894_at	Tgfbr1	Olfactory epithelium, vomeronasal organ
	macrophages; microglia	1417523_at	Plek	Not Annotated
	macrophages	1418099_at	Tnfrsf1b	Not Detected
	macrophages	1418280_at	Klf6	Brain mantle layer, brain marginal layer
	macrophages	1420089_at	Nfkbia	Thymus, jaw, teeth, naris
	macrophages; osteoclasts	1420361_at	Slc11a1	Not Detected
	macrophages	1424287_at	Prkx	Not Annotated
	osteoclasts; macrophages; microglia	1429775_a_at	Gpr137b/Gpr137b-ps	Record Not Found
	macrophages	1437226_x_at	Marcksl1	Not Annotated
	thymocyte DP; thymocyte SP CD4+	1439315_at	Satb1	Brain marginal layer, epidermis, sympathetic ganglia, thymus
	mast cells	1449864_at	Il4	No Regional Signal
	microglia; macrophages	1451161_a_at	Emr1	Not Detected
	macrophages	1451755_a_at	Apobec1	No Regional Signal
	macrophages	1452519_a_at	Zfp36	Not Annotated
Testis	testis	1455274_at	---	---
	testis	1460582_x_at	---	---
	testis	1418878_at	Acrv1	Not Detected
	testis	1453440_at	4921539E11Rik	Record Not Found
	testis	1444782_at	4930417H01Rik	Record Not Found
	testis	1453506_at	Fam154a	Record Not Found
	testis	1417594_at	Gkap1	Not Annotated
	testis	1456693_at	Gm20213	Record Not Found
	testis	1436831_at	Iqub	Record Not Found
	testis	1432122_at	Lrriq3	Record Not Found
	testis	1429572_at	Nsun7	Olfactory epithelium, choroid plexus, male reproductive system

Organ/ System	Tissue	Probe(s)	Gene Symbol	EurExpress
	testis	1419422_at	Pkd2l2	Record Not Found
	testis	1455784_at	Sec1	Record Not Found
Eye	eyecup	1439920_at	---	---
	retina	1458418_at	---	---
	cornea	1456348_x_at	Paqr5	No Regional Signal
	retinal pigment epithelium	1460601_at	Myrip	Record Not Found
	iris	1440803_x_at	Tacr3	Adrenal gland, testes
	lens	1447881_x_at	Usp15	Thymus, brain, spinal cord, submandibular gland, teeth
	eyecup; iris; ciliary bodies	1422170_at	Slc5a3	Choroid plexus, brain ventricular layer, axial muscle, rectum
	ciliary bodies; iris	1439688_at	Fbln1	Mesenchyme, stomach, midgut, bladder, meninges
	retinal pigment epithelium; lens	1440870_at	Prdm16	No Regional Signal
	ciliary bodies; eyecup; retinal pigment epithelium	1446172_at	---	---
	eyecup; ciliary bodies; iris	1447410_at	---	---
	lens; ciliary bodies; iris	1448669_at	Dkk3	Record Not Found
Placenta	placenta	1416413_at	Ctsj	Record Not Found
	placenta	1422289_a_at	Ctsq	Record Not Found
	placenta	1436399_s_at	Nrk	Diaphragm, skeletal muscle, mesenchyme, submandibular gland, tongue
	placenta	1427550_at	Peg10	Not Annotated
	placenta	1426730_a_at, 1452165_at	Prl2b1	Record Not Found
	placenta	1415835_at	Prl3b1	Record Not Found
	placenta	1425881_at	Psg28	Not Detected
	placenta	1451790_a_at, 1451791_at	Tfpi	Meninges
Liver	liver	1420722_at	Elovl3	Not Detected
	liver	1427214_at	Agmat	Record Not Found
	liver	1450624_at	Bhmt	Liver
	liver	1438937_x_at	Ang	Pancreas
	liver	1419974_at	Scp2, Gm19491	No Regional Signal
	liver	1449337_at	Tdo2	No Regional Signal
	liver	1428676_at	Tmprss6	Not Annotated
Lung	lung	1425814_a_at	Calcrl	Not Detected
	lung	1433670_at	Emp2	Thymus, teeth, gut epithelium, muscle, lung, larynx, trachea, whiskers, bladder, urethra
	lung	1435436_at	Epas1	Vertebral axis muscle system, limbs, kidneys, adrenal gland

Organ/ System	Tissue	Probe(s)	Gene Symbol	EurExpress
	lung	1436367_at	Ptprb	Heart valve, mesenchyme
	lung	1439369_x_at	Slc9a3r2	No Regional Signal
Intestine	intestine small	1418550_x_at	Defa-rs1	Record Not Found
	stomach	1449902_at	Lce1c, Lce1f, Lce1g, Lce1k	Record Not Found
	intestine large; stomach	1420328_at	Rep15	Record Not Found
Kidney	kidney	1422898_s_at	Slc22a12	Brain marginal layer, cranial nerve ganglia, dorsal root ganglia
	kidney	1416966_at	Slc22a8	Meninges, brain mantle layer
	kidney	1421912_at	Slc23a1	Adrenal gland, choroid plexus
Adipose	adipose brown	1422973_a_at	Thrsp	No Regional Signal
	adipose white	1429935_at	Lcn12	Not Annotated
Bone	osteoblast	1416803_at	Fkbp7	Cartilage, teeth, chondrocranium
	osteoblast	1425574_at	Epha3	Lip, tongue, teeth, vomeronasal organ, mesenchyme, skeletal muscle, brain mantle layer, brain ventricular layer
Embryonic Stem Cell	embryonic stem line V26 2	1449344_s_at	2210409E12Rik	Record Not Found
	embryonic stem line V26 2; embryonic stem line Bruce4	1422058_at	Nodal	No Regional Signal
Epidermis	epidermis	1427352_at	Krt79	Record Not Found
Heart	heart	1451203_at	Mb	Heart
Hematopoietic Stem Cell	stem cells HSC	1442812_at	Gm10482	Record Not Found
Muscle	skeletal muscle	1430241_at	Fbxl17	Midbrain ventricular layer, ventral grey horn
Ovary	ovary	1431294_at	Speer7-ps1, Speer8-ps1	Record Not Found
Pancreas	min6 cells	1455765_a_at	Abcc8	Record Not Found
Prostate	prostate	1420063_at	---	---
Salivary Gland	salivary gland	1421788_x_at	Egfbp2	Record Not Found

Table 7: Canonical Pathways Enriched in Fetal Cells from Allogeneic Matings

Complete list of the statistically significant canonical pathways as identified by Ingenuity Pathway Analysis. Shaded boxes show non-significant BH-corrected p-values. B-H p-value column shows the Benjamini-Hochberg corrected p-value as applied by the IPA software.

Ingenuity Canonical Pathways	p value	B-H p-value	Molecules
EIF2 Signaling	7.94328E-44	3.16E-41	RPL11,RPL22,RPS4Y1,RPL27A,EIF1,RPS23,RPS24,RPS3A,RPL7A,EIF4G2,EIF5,RPL19,MRAS,RPL12,RPL3,RPL27,RPL37,RPLP0,RPL15,RPS29,FAU,RPL39,RPL10,RPS15,RPS25,RPS15A,RPL41,RPL13A,RPSA,EIF2S3,RPL31,RPS18,PPP1CB,RPS6,RPS8,RPS13,RPL26,RPL14,RPS21,RPL37A,RPL10A,RPL7,RPS27,RPL6,RPL18A,RPS16,RPLP2,RPS3,RPL18,RPL29,RPL13,RPL4,RPL17,RPS2,RPL30,RPL21,RPL23,RPL35A,RPL9,RPS12,RPS10,RPS26,RPL28,UBA52,RPL36A,RPL32,EIF2AK2,RPL38,EIF3L,RPS14
Regulation of eIF4 and p70S6K Signaling	7.58578E-10	1.58E-07	EIF2S3,RPS4Y1,EIF1,RPS18,RPS13,RPS8,RPS6,RPS21,RPS23,RPS27,RPS24,RPS3A,EIF4G2,RPS16,MRAS,RPS3,ITGA4,RPS2,RPS12,RPS29,FAU,RPS10,RPS26,RPS15,RPS15A,RPS25,EIF3L,RPS14,RPSA
Remodeling of Epithelial Adherens Junctions	2.81838E-09	3.89E-07	ACTR2,ARPC1B,TUBB4B,ACTB,MAPRE1,TUBB2A,RAB7A,TUBA4A,CTNNA1,IQGAP1,ACTG1,TUBA1B,CLIP1,ARF6,TUBA1A,ACTR3,DNM1L,CTNNB1,DNM2
mTOR Signaling	4.46684E-07	4.57E-05	RPS4Y1,RPS18,FKBP1A,RPS13,RPS8,RPS6,RPS21,RPS23,RPS27,RPS24,RPS3A,EIF4G2,RHOB,RPS16,MRAS,RPS3,RPS2,RPS12,RPS29,FAU,RPS10,RPS26,RHOA,RPS15,RPS25,RPS15A,EIF3L,RPS14,RPSA
Epithelial Adherens Junction Signaling	2.81838E-06	2.34E-04	RAP1B,ACTR2,TGFBR1,MYL6,ARPC1B,TUBB4B,ACTB,TUBB2A,TUBA4A,CTNNA1,IQGAP1,CDC42,ACTG1,PTPRM,TUBA1B,CLIP1,NOTCH2,ACTR3,TUBA1A,RHOA,MRAS,MYH9,CLINT1,CTNNB1
Signaling by Rho Family GTPases	2.39883E-05	0.0017	MYL6,ARPC1B,WASF3,GNB2L1,CDC42,IQGAP1,CLIP1,GNB1,ACTR3,RHOB,CYBB,MRAS,ITGA4,ACTR2,CFL1,ACTB,VIM,ACTG1,GNG5,GNAI2,MAP3K12,FOS,MYL12A,MYL12B,RHOA,GNAO1,PPP1R12A,SEPT6,SEPT2,MSN
Regulation of Actin-based Motility by Rho	6.60693E-05	0.0039	ACTR2,PFN1,ARPC1B,CFL1,MYL6,ACTB,PPP1CB,CDC42,GSN,MYL12A,ACTR3,RHOB,MYL12B,RHOA,PPP1R12A
Ephrin B Signaling	7.58578E-05	0.0039	CFL1,CXCR4,GNB2L1,CDC42,GNG5,HNRNPK,GNAI2,GNB1,EFNB2,RHOA,ACP1,GNAO1,MRAS,CTNNB1
Protein Kinase A Signaling	1.74E-04	0.0079	RAP1B,AKAP12,TGFBR1,Calm1 (includes others),MYL6,GNB2L1,H3f3a/H3f3b,PPP1CB,PTPN12,DUSP2,PTPRC,YWHAQ,BRAF,GNB1,NFKBIA,PPP3R1,CREB1,PRKAR1B,ATF4,CTNNB1,APEX1,ADCY9,PPP1R14C,YWHAB,CHP1,YWHAZ,PTPN18,PTPRM,PTP4A1,GNG5,GNAI2,MYL12A,DUSP1,MYL12B,PTPRB,RHOA,ACP1,ANAPC5,PPP1R12A
Hypoxia Signaling in the Cardiovascular System	2.09E-04	0.0087	HSP90B1,UBE2H,NFKBIA,HSP90AB1,UBE2R2,CREB1,UBE2D2,CSNK1D,HSP90AA1,ATF4,UBE2D3,ARNT

Ingenuity Canonical Pathways	p value	B-H p-value	Molecules
RhoA Signaling	3.89E-04	0.0148	ACTR2,PFN1,NRP2,ARPC1B,CFL1,MYL6,ACTB,PPP1CB,ACTG1,MYL12A,ACTR3,MYL12B,RHOA,PPP1R12A,SEPT6,SEPT2,MSN
Lipid Antigen Presentation by CD1	4.47E-04	0.0148	B2M,CALR,ARF6,PSAP,CANX
Cdc42 Signaling	4.68E-04	0.0148	B2M,ACTR2,MYL6,CFL1,ARPC1B,PPP1CB,IQGAP1,CDC42,CLIP1,FOS,MYL12A,ACTR3,HLA-C,MYL12B,HLA-DOB,PPP1R12A,CDC42SE1,ITGA4
Ephrin Receptor Signaling	5.13E-04	0.0151	RAP1B,ACTR2,CFL1,ARPC1B,CXCR4,GNB2L1,EPHA3,NCK1,CDC42,GNG5,GNB1,GNAI2,EFNB2,ACTR3,SDCBP,RHOA,GNAO1,CREB1,ACP1,MRAS,ATF4,ITGA4
Sertoli Cell-Sertoli Cell Junction Signaling	9.77E-04	0.0263	SPTBN1,DLG1,GUCY1A3,TJP1,TUBB4B,ACTB,TUBB2A,TUBA4A,CTNNA1,CSDA,CDC42,TUBA1B,ACTG1,MAP3K12,TUBA1A,PRKAR1B,MRAS,CLDN14,CLINT1,CTNNB1,ITGA4
RhoGDI Signaling	0.0011	0.0263	ACTR2,MYL6,CFL1,ARPC1B,ACTB,GNB2L1,CDC42,ACTG1,GNG5,GNB1,GNAI2,MYL12A,ACTR3,RHOB,MYL12B,RHOA,GNAO1,MRAS,PPP1R12A,ITGA4,MSN
Integrin Signaling	0.0011	0.0263	RAP1B,ACTR2,TSPAN7,ARPC1B,ACTB,PPP1CB,Arf1,NCK1,CDC42,ACTG1,BRAF,ARF6,MYL12A,ACTR3,RHOB,MYL12B,ARF4,RHOA,MRAS,ITGAV,PPP1R12A,NEDD9,ITGA4
Germ Cell-Sertoli Cell Junction Signaling	0.0014	0.0324	TGFBR1,TJP1,TUBB4B,ACTB,TUBB2A,TUBA4A,CTNNA1,IQGAP1,CDC42,GSN,ACTG1,TUBA1B,MAP3K12,TUBA1A,RHOB,RHOA,MRAS,CLINT1,CTNNB1
Actin Nucleation by ARP-WASP Complex	0.0015	0.0324	ACTR2,ACTR3,ARPC1B,RHOB,RHOA,MRAS,PPP1R12A,NCK1,CDC42,ITGA4
Polyamine Regulation in Colon Cancer	0.0015	0.0324	AZIN1,SAT1,OAZ1,OAZ2,CTNNB1,ODC1
Phospholipase C Signaling	0.0031	0.0617	ADCY9,RAP1B,PEBP1,Calm1 (includes others),MYL6,CHP1,GNB2L1,PPP1CB,RAPGEF3,GNG5,GNB1,TGM2,MYL12A,AHNAK,RHOB,MYL12B,RHOA,PPP3R1,CREB1,MRAS,ATF4,PPP1R12A,MARCKS,ITGA4
fMLP Signaling in Neutrophils	0.0033	0.0617	ACTR2,Calm1 (includes others),ARPC1B,GNB2L1,CHP1,CDC42,GNG5,GNAI2,GNB1,ACTR3,NFKBIA,PPP3R1,CYBB,MRAS
Cleavage and Polyadenylation of Pre-mRNA	0.0045	0.0794	CPSF6,WDR33,PABPN1,CSTF2
ERK/MAPK Signaling	0.0059	0.0977	RAP1B,PPP1R14C,YWHAB,YWHAZ,PPP1CB,H3f3a/H3f3b,ETS2,RAPGEF3,MKNK2,DUSP2,BRAF,YWHAQ,FOS,DUSP1,CREB1,PRKAR1B,MRAS,PPP1R12A,ATF4,ITGA4
Protein Ubiquitination Pathway	0.0059	0.0977	B2M,UBE2H,HSPA1A/HSPA1B,UBE2D2,Ubb,FBXW7,HSPA5,DNAJA1,HSP90B1,HSP90AB1,DNAJC1,USP15,UBE2R2,HSPD1,UBE3A,FZR1,XIAP,HSPA8,HLA-C,ANAPC5,HSP90AA1,BTRC,SMURF2,UBC,UBE2D3
Tight Junction Signaling	0.0066	0.1059	TGFBR1,MYL6,TJP1,ACTB,CTNNA1,CSDA,CDC42,ACTG1,CPSF6,FOS,RHOA,PRKAR1B,MYH9,CSTF2,CLDN14,TNFRSF1B,CTNNB1
IL-1 Signaling	0.0072	0.1064	GNAI2,ADCY9,GNB1,FOS,NFKBIA,GNAO1,GNB2L1,TAB2,MRAS,PRKAR1B,GNG5,IRAK2

Ingenuity Canonical Pathways	p value	B-H p-value	Molecules
Relaxin Signaling	0.0074	0.1064	RAP1B,ADCY9,GUCY1A3,GNB2L1,GNG5,BRAF,GNAI2,GNB1,FOS,NFKBIA,CREB1,GNAO1,PRKAR1B,MRAS,APEX1
Caveolar-mediated Endocytosis Signaling	0.0074	0.1064	B2M,ARCN1,HLA-C,ACTB,ITGAV,COPG2,ACTG1,DNM2,ITGA4,COPG1
Axonal Guidance Signaling	0.0078	0.1064	RAP1B,DPYSL2,PFN1,ARPC1B,MYL6,GNB2L1,UNC5B,NCK1,CDC42,GNB1,EFNB2,ACTR3,PPP3R1,MRAS,PRKAR1B,ADAM23,ITGA4,ACTR2,CFL1,NRP2,CXCR4,TUBB4B,CHP1,TUBB2A,TUBA4A,L1CAM,EPHA3,TUBA1B,GNG5,GNAI2,MYL12A,NTRK2,SDCBP,TUBA1A,MYL12B,RHOA,GNAO1
ERK5 Signaling	0.0117	0.1578	YWHAQ,IL6ST,FOS,YWHAB,CREB1,MRAS,YWHAZ,ATF4,WNK1
Gap Junction Signaling	0.0129	0.1648	ADCY9,GUCY1A3,TUBB4B,ACTB,TUBB2A,CSNK1A1,CSNK1D,TUBA4A,ACTG1,TUBA1B,GNAI2,TUBA1A,PPP3R1,PRKAR1B,MRAS,CTNNB1
Actin Cytoskeleton Signaling	0.0132	0.1648	ACTR2,PFN1,MYL6,CFL1,TMSB10/TMSB4X,ARPC1B,ACTB,PPP1CB,IQGAP1,CDC42,GSN,ACTG1,MYL12A,ACTR3,MYL12B,RHOA,MRAS,PPP1R12A,MYH9,ITGA4,MSN
Breast Cancer Regulation by Stathmin1	0.0135	0.1648	ADCY9,PPP1R14C,Calm1 (includes others),TUBB4B,TUBB2A,GNB2L1,TUBA4A,PPP1CB,CDC42,TUBA1B,GNG5,GNB1,GNAI2,TUBA1A,RHOA,PRKAR1B,MRAS,PPP1R12A,UHMK1
Chemokine Signaling	0.0158	0.1875	GNAI2,FOS,Calm1 (includes others),CFL1,CXCR4,RHOA,MRAS,PPP1R12A,PPP1CB
Clathrin-mediated Endocytosis Signaling	0.0174	0.1991	ACTR2,ARPC1B,ACTB,CHP1,CLTC,RAB7A,SH3GLB1,Ubb,CDC42,ACTG1,HSPA8,ARF6,ACTR3,PPP3R1,SH3GLB2,UBC,DNM1L,DNM2
Nur77 Signaling in T Lymphocytes	0.0195	0.2208	Calm1 (includes others),CYCS,PPP3R1,CHP1,NR4A1,HLA-DOB,SIN3A
Prostate Cancer Signaling	0.0204	0.2223	HSP90B1,NFKBIA,PA2G4,HSP90AB1,CREB1,MRAS,HSP90AA1,ATF4,CTNNB1,SIN3A
Antigen Presentation Pathway	0.0214	0.2265	B2M,CALR,HLA-C,HLA-DOB,CANX
Corticotropin Releasing Hormone Signaling	0.0229	0.2393	RAP1B,GNAI2,ADCY9,BRAF,FOS,Calm1 (includes others),GUCY1A3,CREB1,GNAO1,PRKAR1B,NR4A1,ATF4
Antiproliferative Role of Somatostatin Receptor 2	0.0251	0.2523	RAP1B,GNB1,BRAF,GUCY1A3,SSTR2,GNB2L1,MRAS,GNG5
NRF2-mediated Oxidative Stress Response	0.0288	0.2818	AKR7A2,FTL,PPIB,PRDX1,ACTB,DNAJA1,ACTG1,BACH1,GSR,FOS,AKR1A1,DNAJC1,MRAS,ATF4,TXN,GSTK1,FTH1
Mitotic Roles of Polo-Like Kinase	0.0302	0.2877	SLK,HSP90B1,HSP90AB1,PTTG1,ANAPC5,HSP90AA1,FZR1,KIF11
CXCR4 Signaling	0.0309	0.2924	ADCY9,MYL6,CXCR4,EGR1,GNB2L1,GNG5,GNAI2,GNB1,FOS,MYL12A,RHOB,MYL12B,RHOA,GNAO1,MRAS
Glucocorticoid Receptor Signaling	0.0417	0.3741	TGFBR1,HSPA1A/HSPA1B,CHP1,SMARCD2,KRT32,GTF2A1,HSPA5,TAF13,NCOA3,HSPA8,FOS,HSP90B1,NFKBIA,HMGB1,HSP90AB1,DUSP1,PPP3R1,CREB1,MRAS,HSP90AA1,IL4,CREBZF
Gαs Signaling	0.0417	0.3741	ADCY9,GNB1,BRAF,GPER,CREB1,GNB2L1,MRAS,PRKAR1B,ATF4,RAPGEF3,GNG5

Ingenuity Canonical Pathways	p value	B-H p-value	Molecules
Synaptic Long Term Potentiation	0.0427	0.3784	RAP1B,PPP1R14C,Calm1 (includes others),PPP3R1,CREB1,CHP1,MRAS,PRKAR1B,PPP1R12A,ATF4,PPP1CB,RAPGEF3
eNOS Signaling	0.0479	0.4036	ADCY9,HSPA8,AQP3,HSP90B1,Calm1 (includes others),GUCY1A3,HSP90AB1,HSPA1A/HSPA1B,PRKAR1B,HSP90AA1,HSPA5,DNM2
Granzyme A Signaling	0.0490	0.4036	SET,APEX1,ANP32A

Table 8: Upstream Regulators for Allogeneic Matings

Complete list of the statistically significant transcription factor pathways as identified by Ingenuity Pathway Analysis.

Upstream Regulator	p-value of overlap	Target Molecules in Dataset
IGF1R	3.70E-08	ACP1, ALDOA, ATP5A1, ATP5D, Atp5h, CD36, CD38, CD53, COL1A1, CYCS, FTH1, IVNS1ABP, NDUFV2, RPL10A, RPL3, RPL35A, RPL37A, RPL7, RPL9, RPS21, RPS24, RPS26, SCP2, SF3B5, TGFBI, TXN
INSR	3.82E-08	ATP5A1, ATP5D, Atp5h, Calm1 (includes others), CCND2, CD36, CD83, CDC5L, CFL1, COL6A3, CSTB, CYCS, ESRRA, FBLN1, GANAB, Gapdh/LOC100042025, HSPD1, IQGAP1, LCP1, LDB2, Lyz1/Lyz2, MARCKSL1, NDUFV2, PAX6, RAB7A, Rpl5, RPL7A, RPS16, SCP2, TSC22D1, UCP2, YBX1
NFE2L2	5.36E-08	ACTG1, AKR1A1, AKR7A2, ALDOA, ANG, Arf1, BHMT, Calm1 (includes others), CCRN4L, COL1A1, CREG1, CTSD, EIF4G2, FTH1, FTL, GAS2, GNB2L1, GSR, HSP90AA1, HSP90AB1, HSP90B1, IFNGR2, IL4, INMT, L1CAM, LY6E, M6PR, MORF4L2, PPIB, PRDX1, RAN, RPL18, RPLP0, RPS16, SERINC3, SRXN1, SYT1, THRSP, TMED2, TXN, UGDH
ADORA2A	3.39E-06	App, ATP2B1, Cd24a, DUSP1, EEF2, EIF1, Eif2s2/Gm9892, FOS, Gapdh/LOC100042025, HNRNPK, Ifitm3, KIF5B, NR4A1, PPP3R1, SPARC, SPTBN1, TJP1, TUBB2A
PSEN2	6.55E-06	ACTB, App, CTNNB1, CTSS, CYTIP, Gapdh/LOC100042025, GAS5, GJA1, GNB1, KIF5B, PSENEN, SLC38A2, UBC, UEVLD, XIAP
DYSF	9.33E-06	ACTG1, ACTR3, B2M, CD53, CD83, CORO1C, Ctla2a/Ctla2b, CTSS, FTL, Gp49a/Lilrb4, HLA-C, HSPA1A/HSPA1B, LCP1, Lyz1/Lyz2, PSAP
RHOJ	2.70E-05	ACTG1, ADIPOQ, AKAP12, CCNI, CNBP, GSN, MYH9
FAAH	5.07E-05	Atp5h, RPL17, Rpl5, RPL7, RPS18, RPS2, RPS3A, RPS6
IRS1	6.04E-05	ACTR3, ADIPOQ, ATP5A1, COL4A1, COL6A3, EFNB2, EGR1, ESRRA, FOS, GAS2, GAS5, GJA1, NDN, PRDM16, RAB9A, TGFBI, UCP2
PSEN1	6.51E-05	ACTB, App, CTNNB1, CTSS, CYTIP, DUSP1, FOS, Gapdh/LOC100042025, GAS5, GJA1, GNB1, KIF5B, L1CAM, PSENEN, SLC38A2, UBC, UEVLD, XIAP
RNA polymerase II	6.98E-05	ADIPOQ, CD83, CXCL11, FOS, Gapdh/LOC100042025, HSPA1A/HSPA1B, IGDCC3, IL17A, RPL13A, RPS21, RPS3, SLC6A2, TMSB10/TMSB4X, TXN, UBC, ZNF238
APOE	7.48E-05	ACTB, App, CALR, CCND2, CD36, COL1A1, CTDSP1, CTNNB1, CTSD, CTSS, CYB5R3, CYBB, EGR1, EMR1, HMMR, HSP90AB1, HSPA1A/HSPA1B, HSPD1, IL17A, IL4, M6PR, MGEA5
AFP	1.23E-04	EGR1, FOS, PTP4A1, TSC22D1
FOS	1.93E-04	A130040M12Rik, APLN, APLP2, AQP3, ARNT, CADM1, CASZ1, CLIP1, DDX3X, DLG1, ELOVL3, FOS, GAS2, GSR, HMMR, KIF5B, KLF6, MMRN1, MYH9, ODC1, PFN1, PTPN12, PTTG1, RAPGEF3, RBBP4, VIM, YWHAZ
Jnk	2.51E-04	APLN, COL1A1, DUSP1, EGR1, FOS, GJA1, IL17A, ITGA4, TGM2
MECP2	2.51E-04	ACTB, DPYSL2, HSPA5, Meg3, NR4A1, SLC6A2, UBE3A, YWHAB, YWHAZ

Upstream Regulator	p-value of overlap	Target Molecules in Dataset
CREB1	3.81E-04	BTG2, CREB1, EGR1, FOS, IDI1, KLF5, LSS, MCL1, MKNK2, NPC2, NR4A1, SPTY2D1
FLI1	3.89E-04	COL1A1, GNB2L1, HSPA8, NPM1, RPL18, TCP1
SMTNL1	5.24E-04	GJA1, PPP1R12A, Prl2c2 (includes others), Prl3b1
FMR1	6.03E-04	ALDOA, App, CFL1, CTNNB1, EEF2, Gapdh/LOC100042025, PPIA, RPSA
PRKAG3	6.14E-04	CD36, FTL, GDAP1, MAP4, NAP1L1, RPL13A, RPL22, Rpl5, Snhg8, XPR1
YY1	6.50E-04	API5, ATF4, BTF3, BTG2, COL1A1, EEF1B2, EIF4G2, FOS, GTF2A1, HNRNPA1, KIF11, KIF5B, LUC7L2, MAT2A, PNRC2, RBBP4, SFXN1, TGFBI, TGFBR1, TGM2, WSB1
Il3	8.86E-04	ARNT, CCND2, EMR1, FOS, IL4, Lyz1/Lyz2, PIM1, TCP1, TNFRSF1B
Igm	0.0013	CCND2, CFLAR, EGR1, IL17A, PIM1
E2F1	0.0016	ADIPOQ, Calm1 (includes others), CALR, COX7C, DUSP1, EGR1, FOS, HSPA1A/HSPA1B, INMT, NCL, RBBP4, ZFP36
VEGFA	0.0017	COL1A1, CST3, CSTB, CTSS, NR4A1
NR3C1	0.0021	ACTB, App, B2M, CD47, CXCL11, DDX5, DUSP1, EGR1, EPB41L4B, FOS, HSP90AB1, HTR1A, MKNK2, MTCH2, PTP4A2, SERINC3, TXN
PGF	0.0022	CXCR4, EGR1, ETS2, NRP2
CREM	0.0025	BTG2, EGR1, FOS, IDI1, KLF5, LSS, MARCKS, MCL1, MKNK2, NPC2, NR4A1, SPTY2D1
SERCA	0.0029	BTG2, EGR1, ZFP36
LIMS2	0.0029	CTNNA1, GJA1, TJP1
MAX	0.0030	AEBP2, CCND2, NCL, ODC1, RBBP4
HSPA1A/HSPA1B	0.0030	FOS, HSPA1A/HSPA1B
ABCB7	0.0030	FECH, TXN
NKX3-1	0.0032	BTG2, CA3, CTNNB1, FOS, PIM1, PTP4A2, PTPRC, VNN1
SPI1	0.0036	CTSS, EMR1, GNB2L1, HSPA8, IL4, MCL1, PTPRC, RPL18, TCP1
CCR1	0.0038	ATF4, CTSS, FOS, ITGAV, SPARC
TP53	0.0040	ACTB, APEX1, App, BTG1, BTG2, CCND2, CLIC4, COL1A1, COL4A1, CSNK1D, CSTB, CTNNB1, CYB5R3, DKK3, DUSP1, DUSP2, FKBP1A, Gapdh/LOC100042025, GMNN, GSN, GTF3C2, HADH, HSP90AA1, HSP90AB1, HSPD1, KPNB1, Lyz1/Lyz2, MAP4, MCM3, MYH9, NAP1L4, ND5, P4HA1, PFN1, PSAP, PTPRM, RBBP4, RHOB, TDO2, TGFBI, TGM2, TJP1, UBC, UGDH, VIM
SIN3A	0.0048	CCND2, MAP4, NCL, SET, TP53BP1
LIMS1	0.0049	CTNNA1, GJA1, TJP1
CAV1	0.0051	ADIPOQ, CTNNB1, HSPA8, NPM1, NR4A1, RPL17, RPS13, Rps9, TFPI, TJP1
CD44	0.0057	ACTB, CALR, CCND2, COL1A1, CTDSP1, CYB5R3, HMMR, HSP90AB1, MGEA5
ERK1/2	0.0069	ADIPOQ, APLN, BHMT, CCND2, EFNB2, EGR1, FOS, IL4
AMPK	0.0075	CTNNB1, EGR1, UCP2
CCKBR	0.0075	ADIPOQ, APLN, SPARC
LIPE	0.0077	ADIPOQ, COL1A1, EGR1, FOS, G0S2, Gapdh/LOC100042025, GJA1, H3f3a/H3f3b, HSPA1A/HSPA1B, INMT, NR4A1, SCARB2, THRSP
TCR	0.0078	CFLAR, EGR1, FOS, HSP90B1, HSPA5, IL4, LAMP1, MCL1
CTGF	0.0083	COL1A1, CTNNB1, HSD17B7, MBNL2, P4HA1, PI4K2B, WNK1
ANK2	0.0087	L1CAM, SPTBN1

Upstream Regulator	p-value of overlap	Target Molecules in Dataset
F2RL3	0.0087	EGR1, FOS
LCP2	0.0087	IL17A, IL4
IFNG	0.0091	ACTB, ADIPOQ, ADORA1, ATF4, BTG1, CASP12, CELSR2, CLIC4, CTSD, CTSS, CXCL11, CXCR4, CYBB, DUSP1, EIF2AK2, FTH1, GJA1, GNAI2, GNAO1, GNB2L1, GPER, HSPA1A/HSPA1B, IL17A, IL4, KCTD12, LY6E, NFKBIA, NTRK2, PIM1, PPIA, SAMHD1, TGFBR1
MAPK3	0.0107	CTNNB1, IL4, MCL1
RTN4	0.0126	CFL1, DPYSL2, GNAO1, RHOB, YWHAB, YWHAQ
IL5	0.0143	ALDOA, BNIP3L, CCND2, GPAM, HMMR, HSP90B1, HSPA5, IL4, ITGAV, MYADM, P4HA1, PGM1, PIM1, VIM
KITLG	0.0144	EGR1, FOS, GJA1, IL4, PIM1
IRAK4	0.0146	BTG2, CCRN4L, EGR1, FOS, IL4, NFKBIA, NR4A1, ZFP36
NQO2	0.0147	CFLAR, CXCR4, XIAP
MNT	0.0147	CCND2, NCL, ODC1
USF1	0.0148	AKAP12, DUSP1, GPAM, UCP2
TCOF1	0.0151	AZIN1, BCLAF1, BNIP3L, CNBP, HNRPDL, IQGAP1, Nptn, RBM10, STMN3
FADD	0.0161	CXCL11, EGR1, EIF2AK2, ELMOD2, FOS, KLF6, LY6E, PIM1
WT1	0.0163	IDI1, ITM2B, KLF4, LMAN1, NTRK2, ODC1
SLC6A4	0.0167	GNAO1, HTR1A
F2R	0.0167	EGR1, FOS
VAV1	0.0167	CCND2, IL4
CLU	0.0167	App, NFKBIA
ELK3	0.0167	EGR1, FOS
ATP7B	0.0184	App, H19, IDI1, LSS, PTTG1, THRSP
RAC2	0.0184	ALDOA, Cd24a, EFNB2, FOS, NR4A1, TSC22D1
DLL4	0.0194	EFNB2, IL4, UNC5B
WNT1	0.0194	CCND2, CTNNB1, KLF5
NHLH2	0.0194	EMR1, NDN, UCP2
FGFR1	0.0232	CCND2, DNAJC1, Eef1a1, NCK1, RPS6, XIAP
MKL2	0.0245	ACTB, CAMP, CXCR4, G0S2, Gp49a/Lilrb4, HLA-C, MYH9, PPBP, SERINC3
Mapk	0.0249	APLN, GJA1, ITGA4
COBRA1	0.0249	MKNK2, RPLP0, RPS3
mir-451	0.0249	ETS2, PGM1, YWHAZ
mir-144	0.0249	ETS2, PGM1, YWHAZ
HSP90B1	0.0249	CALR, CANX, HSPA5
PTEN	0.0260	ADIPOQ, BTG2, CA3, CTNNB1, EFNB2, EPAS1, FOS, MCL1, PIM1, PTP4A2, PTPRC, RPS6, VNN1
HAVCR1	0.0268	IL17A, IL4
CNTF	0.0268	IL6ST, VIM
DEF6	0.0268	FOS, IL17A
H2AFY	0.0268	CD36, THRSP
STK17B	0.0268	CFLAR, IL4
EIF2AK3	0.0284	ATF4, BTG2, CARS, EGR1, ETS2, KLF4, PON2, SLC1A4, ZFP36
BCR (complex)	0.0287	CCND2, CFLAR, EGR1, MCL1, XIAP
NOS2	0.0306	ADIPOQ, API5, CD53, COL4A1, CYCS, DDX3X, GJA1, Gp49a/Lilrb4, H19, KLF6, MB, SFXN1, TYROBP
MTORC1	0.0310	ATF4, IL4, KLF4
IGF2BP1	0.0310	ACTB, COL1A1, COL6A3
PTGER2	0.0310	App, EMR1, IL17A
ITGB3	0.0310	CD36, FOS, TGFBR1

Upstream Regulator	p-value of overlap	Target Molecules in Dataset
PIK3CD	0.0310	CCND2, IL17A, IL4
STAT3	0.0323	CREB1, EGR1, EIF2AK2, FFAR2, FOS, HLA-C, IL17A, IL4, IL6ST, MCL1, PEG10, TNFRSF1B, ZFP36
PPARA	0.0323	ADIPOQ, ANAPC5, APEX1, AQP3, CD36, CDS2, ELOVL3, FOS, G0S2, GPAM, GSTK1, H2AFZ, HADH, Hmgn1, IDI1, Ifitm3, IL4, LSS, LY6D, NFKBIA, PLTP, SAT1, SCP2, UCP2, VNN1
IL2	0.0324	CFLAR, HSP90B1, HSPA5, IL17A, IL4
CD3	0.0328	CCND2, CFLAR, FOS, HSP90B1, HSPA5, IL17A, IL4, LAMP1, PTPRC, TGM2
TICAM1	0.0344	CD38, CFLAR, CXCL11, DUSP1, EGR1, ETS2, IL17A, NFKBIA, RHOB, SAMHD1, TSC22D1
CLDN6	0.0345	ATF4, CLDN14, HSPA5, KLF4
NPR1	0.0345	ABCC8, COL1A1, GUCY1A3, PPP3R1
MKL1	0.0350	ACTB, CAMP, CXCR4, G0S2, Gp49a/Lilrb4, HLA-C, MYH9, PPBP, SERINC3
PTPN1	0.0363	CFLAR, CXCL11, DUSP1, DUSP2, NFKBIA
Alpha catenin	0.0364	COL1A1, COL6A3, EPHA3, IL36A, IL6ST, Lyz1/Lyz2, NFKBIA, Prl2c2 (includes others), TGM2, VIM, ZEB2
ELOVL5	0.0379	GPAM, INSIG2, PLTP
SPTLC2	0.0379	ATF4, COL1A1, HSPA5
ZBTB7B	0.0379	COL1A1, IL17A, IL4
GNAI2	0.0379	CXCR4, IL4, ITGA4
ARNT	0.0384	CCND2, ITGAV, MYL6, OAZ1, TUBA4A, VIM
SCGB3A2	0.0388	CTSD, CTSS
miR-16-5p (and other miRNAs w/seed AGCAGCA)	0.0388	CCND2, UCP2
IKBKAP	0.0388	CTNNB1, RHOA
ADCY5	0.0388	ADCY9, Gnas
Trbv13-2	0.0388	IL17A, IL4
DBH	0.0388	FOS, UCP2
SERPIND1	0.0388	EGR1, KLF5
GFI1	0.0415	CFLAR, EIF2AK2, GJA1, HSP90AB1, IRAK2, Lyz1/Lyz2, NFKBIA
ICMT	0.0452	GJA1, RCN2, RHOA, TGFBI
ATF2	0.0452	ACTB, ARNT, CTNNB1, DUSP1
GLIS2	0.0455	COL1A1, SPARC, VIM
EHHADH	0.0455	CD36, LY6D, SCP2
miR-155-5p (miRNAs w/seed UAAUGCU)	0.0455	BACH1, SLA, TAB2
IL2RG	0.0455	HLA-C, IL17A, IL4
FAS	0.0460	CFLAR, COL1A1, COL4A1, COL6A3, EGR1, NFKBIA
Histone h3	0.0471	ADIPOQ, AKAP12, CTNNB1, FOS, GAS2, Ifitm3, IL17A, IL4, L1CAM, SLC6A2

Table 9: Partial List of Genes of Interest in the Allogeneic Fetal Cell Core Transcriptome

Reproduction (28)

Male Reproductive System (10)

- *Acrv1*
- *Ddx17*
- *Ddx39*
- *Ddx5*
- *Ddx54*
- *Ddx59*
- *Ddx6*
- *Ddx3x*
- *Ptma*
- *Tuba1a*

General Pregnancy (6)

- *Adam23*
- *Deptor* (*Depdc6*)
- *Gpr30*
- *Plscr3*
- *Psg28*
- *Tdo2*

Female Reproductive System (4)

- *Gpr30*
- *Pkd2l2*
- *Ptges3*
- *Tmsb10*

Placenta (8)

- *Ctsq*
- *Notch2*
- *Peg10*
- *Prl2b1*
- *Prl2c2/Prl2c3/Prl2c4*
- *Prl3b1*
- *Smurf2*
- *Tmed2*

Endothelial (13)

Blood Vessels (10)

- *Akap12*
- *Cd36*
- *Cd47*
- *Cxcr4*
- *Egfl7*
- *Epas1*
- *Klf4*
- *Rhoa*
- *Sepp1*
- *Tgfbr1*

Hematopoietic Cells (3)

- *Efnb2*
- *Epb4.1l4b*
- *Ybx1*

Immune (36)

Innate Immunity (23)

- *B2m*
- *Camp*
- *Cxcl11*
- *Cxcr4*
- *H2-D1*
- *H2-K1*
- *H2-Ob*
- *Hspd1*
- *Il1f6*
- *Il17ra*
- *Il17a*
- *Il4*
- *Il6st*
- *Ilf3*
- *Irak2*
- *Klf4*
- *Lyz1*
- *Lyz2*
- *Nfkbia*
- *Ppbp*
- *Tab2*
- *Tgfbr1*
- *Tm9sf3*

Acquired Immunity (13)

- *Cd24a* (*Hsa*)
- *Cd38*
- *Cd47*
- *Cd53*
- *Cd83*
- *Dusp1*
- *Gas5*
- *Igha/Igh-VJ558*
- *Igk-V28/Igkc/Igkj1/Igkv4-53/Igkv6-23/Igkv8-30*
- *Ighmbp2*
- *Pim1*
- *Rnf128*

Mesenchymal (7)

Expressed in Mesenchyme (3)

- *Ahnak*
- *Csnk1a1*
- *Epas1*

Epithelial-Mesenchymal Transition (4)

- *Ctnnb1*
- *Klf4*
- *Notch2*
- *Vim*

Table 10: Comparison of Fetal Cells in the Maternal Lung in Syngeneic and Allogeneic Pregnancies.

Comparison of tissue types identified by the three primary analyses used in the gene expression experiments. Syn. = syngeneic pregnancies; Allo. = allogeneic pregnancies; PCA = Principal component analysis.

	Lattin PCA		Thorrez PCA		BioGPS	
	Syn.	Allo.	Syn.	Allo.	Syn.	Allo.
Adrenal Gland			x	x		
Embryonic Stem Cells		x	x			
Eye				x	x	x
Immune Cells	x	x			x	x
Liver						x
Lung			x	x	x	x
Nervous System					x	x
Osteoblasts	x	x				
Ovary			x	x		
Pancreas	x	x				
Placenta	x	x	x	x	x	x
Testis		x		x	x	x

CHAPTER FOUR: ISOLATION OF FETAL MESENCHYMAL STEM CELLS FROM THE MATERNAL ORGANS DURING PREGNANCY

INTRODUCTION

Our analysis of the core transcriptome of fetal cells in the maternal lung demonstrated similarity to trophoblasts, mesenchymal stem cells (MSCs), and cells of the immune system (Chapters Two and Three). Trafficking of all three cell types has been demonstrated previously in humans (Adams Waldorf et al., 2010; Chamley et al., 2011; O'Donoghue et al., 2003). Although fetal immune cells and MSCs have been identified in pregnant mice (Bou-Gharios et al., 2011; Khosrotehrani et al., 2008), trophoblast deportation has previously only been reported in humans. Recent evidence from both our laboratory and others (Kara et al., 2012) suggests that it also occur in mice.

To verify and expand on our gene expression results, we aimed to more precisely identify these cell types in the organs of pregnant mice. We were specifically interested in understanding any differences between adult and fetal cells of the same type. We focused on immune and MSCs for this reason, as well as the fact that these cells are more likely than trophoblasts to persist long-term and impact maternal health. The experiments regarding immune cells will be discussed in the next chapter.

There is no strict consensus about the constellation of cellular markers that define the MSC population. Various cell markers have been identified to define MSCs, although none are specific, thus constraining their usefulness (Summer and Fine, 2008). One potential alternative is the side population, a group of cells visible on flow cytometric analysis due to their unique Hoechst-33342 fluorescence. The side population is highly enriched for stem cells, such that their in vivo reconstitution activity is more than 1,000-

fold greater than unfractionated bone marrow (Goodell et al., 1996). These cells are found in solid organs including muscle (Gussoni et al., 1999) and lung (Summer et al., 2007).

Along with other criteria, the side population can be used to isolate MSCs. Summer and colleagues (Summer et al., 2007) define four characteristics of a murine mesenchymal stem cells: 1) They are CD45-/CD31- and present in the side population; 2) They can be serially cultured in an undifferentiated state; 3) They express Sca-1, CD106 and CD44; and 4) They can be induced to differentiate into smooth muscle, cartilage, bone and fat. We used these criteria to identify and collect both fetal and maternal MSCs from the lungs of pregnant female mice for comparison of in vitro differentiation characteristics. We hypothesized that fetal MSCs would have greater capacity for proliferation and differentiation compared to adult MSCs.

METHODS

MICE

Female C57BL/6J wildtype mice were mated with male mice homozygous for GFP (syngeneic matings). Ten days later female mice were weighed. Any females with at least 10% weight gain over baseline were assumed to be pregnant (Johnson et al., 2010). Eighteen days after mating females were euthanized and their lungs were collected using the methods described previously in this thesis (page 34). Virgin wildtype females served as controls.

FLOW CYTOMETRY

In order to analyze the side population, single cell suspensions were incubated in the presence of 5μg/mL Hoechst-33342 dye (Sigma Aldrich, St. Louis, Missouri). Bone

marrow from a non-mated female served as a positive control, as the side population in bone marrow is very prominent (Figure 13A). As a negative control, bone marrow samples were incubated with 500μM verapamil (Figure 13B), a calcium channel blocker that inhibits Hoechst efflux, which eliminates the side population. Single cell suspensions were incubated with 1:40 dilutions of PE-Cy7 rat anti-CD31 (Clone MEC 13.3, BD Pharmingen) and PE rat anti-CD45 (Clone 30-F11, BD Pharmingen) antibodies. PE-Cy7 rat anti-IgG2b-k (clone A95-1, BD Pharmingen) and PE rat anti-IgG2a-k (clone R35-95, BD Pharmingen) were used as isotype controls. The side population gate was applied to the maternal lung cells (Figure 13C and Figure 14). Cells in the side population gate were further assessed for expression of CD31 and CD45 (Figure 14B). CD31-, CD45- cells were then assessed for GFP.

SORTED CELL CULTURE

Putative fetal MSCs were directly sorted into either DMEM or α-MEM media supplemented with 10% fetal bovine serum, penicillin-streptomycin, HEPES and L-glutamine. Cells were sorted directly into either a 6-well or 96-well plate and incubated at 37°C, 5% CO_2 overnight. After 24 hours cultures were washed once gently with DPBS to remove non-adherent cells and fresh media was replaced. Cells were observed under a fluorescent microscope every 48 hours.

Some stem cells require a feeder layer of cells, typically bone marrow-derived MSCs, to receive necessary growth factors, (Wagner et al., 2008). To test the hypothesis that fetal cells require a feeder layer of cells for growth, lung cells from virgin wildtype C57BL6 females were cultured for three days. 6,000 GFP+ fetal cells pooled from multiple female mice were directly sorted into this feeder layer and allowed to

incubate for 48 hours. Fetal cells would be identified among the feeder cells by their green fluorescence.

Whole Organ Culture

Since the number of fetal MSCs was low, we cultured whole lungs to try to enrich for adherent cells and thus MSCs. Lungs were collected from two virgin female mice and physically dissociated to create single cell suspensions. Cells were filtered, pelleted, and resuspended in pre-warmed supplemented DMEM or α-MEM. Cells were cultured for 24 hours at which time the media was removed, the adherent cells were washed with DPBS and fresh media was replaced. Cells were cultured for three weeks, during which time they were passaged four times. At the end of this period, adherent cells were removed from the flasks using trypsin. Cells were washed and pelleted. Cell pellets were incubated with 1:40 dilutions of anti-CD31, anti-CD45, APC rat anti-Sca1 (Clone RB6-8C5, BD Pharmingen) and PE-Cy5.5 rat anti-CD44 (Clone IM7, BD Pharmingen) antibodies. Cell pellets were washed and resuspended in flow cytometry buffer. Two additional antibody cocktails were also used to look for MSCs in cultured whole organs: The “International” cocktail, derived from the The International Society for Cellular Therapy position statement, defines MSCs as positive for CD105 and Thy-1 (CD90), and negative for CD45, CD34 and CD11b (Dominici et al., 2006). The “Quad” cocktail, previously developed in our laboratory after an extensive literature review, looked for cells that were Sca-1, Thy-1 and CD44 positive, and CD34 and CD45 negative.

RESULTS

SORTED CELL CULTURE

The goal of this experiment was to study the fetal MSC population of the murine maternal lung. Cells of interest were defined as Hoechst-, GFP+, CD31-, and CD45-. Due to an artifact of Hoechst staining, some cells appeared to have low green fluorescence. These were not considered to be fetal. Almost immediately we noticed the absence of a discrete side population within the murine lung (Figure 13), in contrast to previously published accounts (Summer et al., 2007).

Low numbers of fetal MSCs were identified. Per lung pair, we saw 2-60 putative fetal MSCs. Because so few cells could be collected, we attempted to culture the cells so that more experiments could be performed. After 48-hours in culture, cells could be seen (Figure 15). However, after several days of observation, the cells did not appear to be growing or replicating. In contrast, cells from $GFP^{+/+}$ control animals adhered and proliferated in the same conditions (Figure 15E and F). In co-culture with a feeder layer of GFP- lung cells, no GFP+ cells could be observed by fluorescent microscopy after 48 hours.

WHOLE ORGAN CULTURE

Cultured adherent cells were stained using three antibody cocktails and analyzed by flow cytometry. For single antibodies, 88.6% of the cells were CD44+, 26.1% were CD45+, 57.7% of cells fulfilled the “International” criteria, 0.5% of cells fulfilled the “Quad” cocktail criteria, and 0.57% of cells fulfilled the criteria described by Summer et al. (2007).

DISCUSSION

There are several reasons as to why the putative fetal MSCs may not have grown. First, one major obstacle was the absence of a clear side population. This is likely the main reason that so few fetal MSCs were identified. This is in contrast to the clear side population previously reported where similar experimental conditions were employed (Summer et al., 2007). Discussions with the lead author of that paper did not uncover the reason for these differences.

We also encountered difficulties due to the lack of standardization in the MSC field as to how to concretely define this population. While hematopoietic stem cells are somewhat specifically defined by cell surface markers, the defining characteristics of MSCs vary between investigators and organs (Dominici et al., 2006). Of the proposed surface markers, none are specific to MSCs, complicating their isolation (Chamberlain et al., 2007; Tarnok et al, 2010). There are further discrepancies between MSCs in humans versus mice, in different organs, and between murine strains (Peister et al., 2004; Dominici et al., 2006).

A proportion of the fetal cells in maternal lung are not viable (see Chapter Seven) and therefore unable to grow. The presence of dead cells may have artificially elevated the number of fetal cells placed into culture. Because of this as well as because of the low number of cells in general, the size of the culture wells was potentially too large to allow adequate cell communication and growth.

Lastly, our media conditions may not have been optimal. Conditions known to grow murine adult (Summer et al., 2007) and human fetal (O'Donoghue et al., 2003) MSCs were tested, as well as another popular growth medium, but perhaps murine fetal MSCs have unique needs in culture. We additionally tested the hypothesis that fetal cells were not receiving needed growth signals when cultured alone. Adding a feeder layer of

plastic-adherent cells also did not result in growth of the collected fetal cells. This may be in part due to our use of adherent lung cells instead of the more standard bone marrow-derived population (Wagner et al., 2008). MSCs from different organs may have different properties (Dominici et al., 2006).

Figure 13: Establishment of the Side Population Flow Cytometry Gate

All samples are stained with Hoechst dye. **(A)** Bone marrow serves as a positive control and is used to draw the side population gate R1 as shown. **(B)** Bone marrow incubated with verapamil serves as a negative control and the side population disappears. **(C)** Adult lung with the same side population gate as in (A) and (B). **(D)** Adult lung incubated with verapamil.

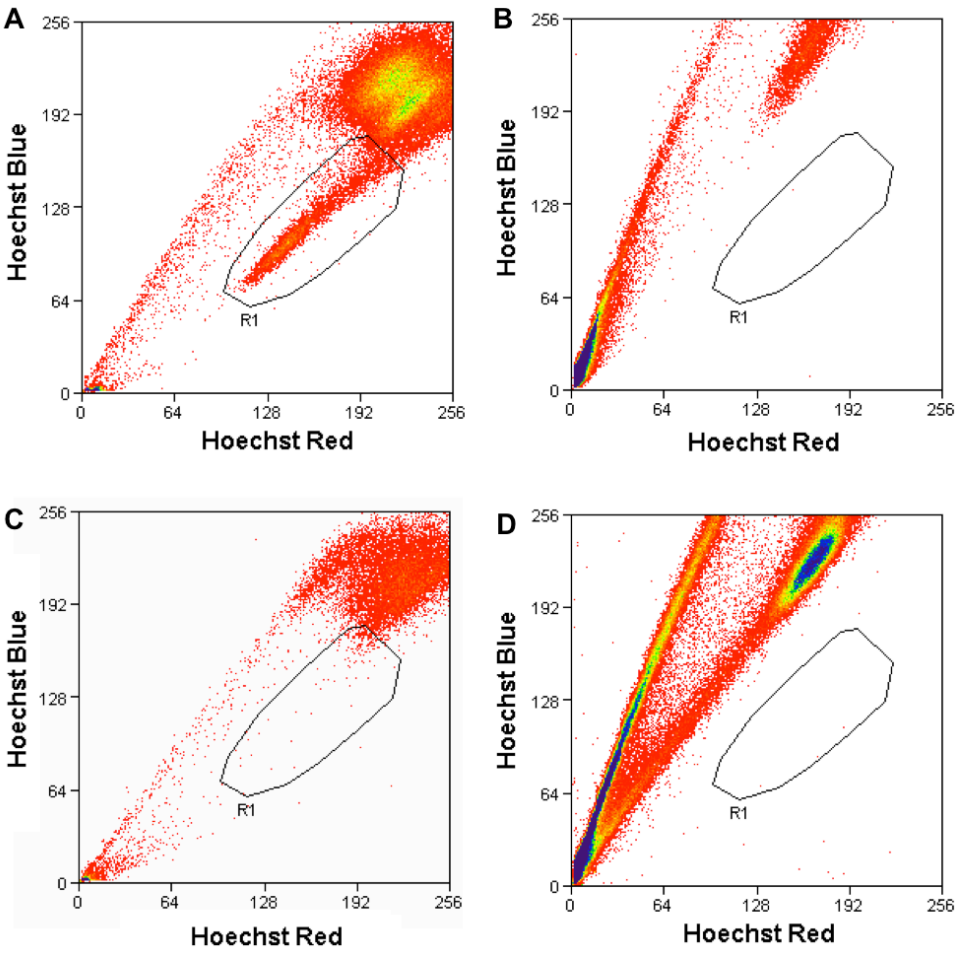

Figure 14: Flow Cytometry Gates for the Isolation of Fetal Mesenchymal Stem Cells

(A) Pregnant female lung stained with Hoechst dye. The R1 gate represents the putative side population and was drawn using the bone marrow control as shown in Figure 13A. **(B)** and **(D)** Pregnant female lung stained with anti-CD45 and anti-CD31 antibodies. The R2 gate represents cells negative for both markers. In (D) the R1 gate from (A) has been applied so that only cells in the side population are shown. **(C)** and **(E)** Pregnant female lung showing GFP+ fetal cells. Here the GFP- (adult) and GFP+ (fetal) populations can be seen in gates R3 and R4 respectively. The cells between the two gates appear to be GFP+ but it is an artifact of Hoechst staining. In (E) the R1 and R2 gates have been applied so that only cells in the side population that are also negative for CD31 and CD45 are displayed.

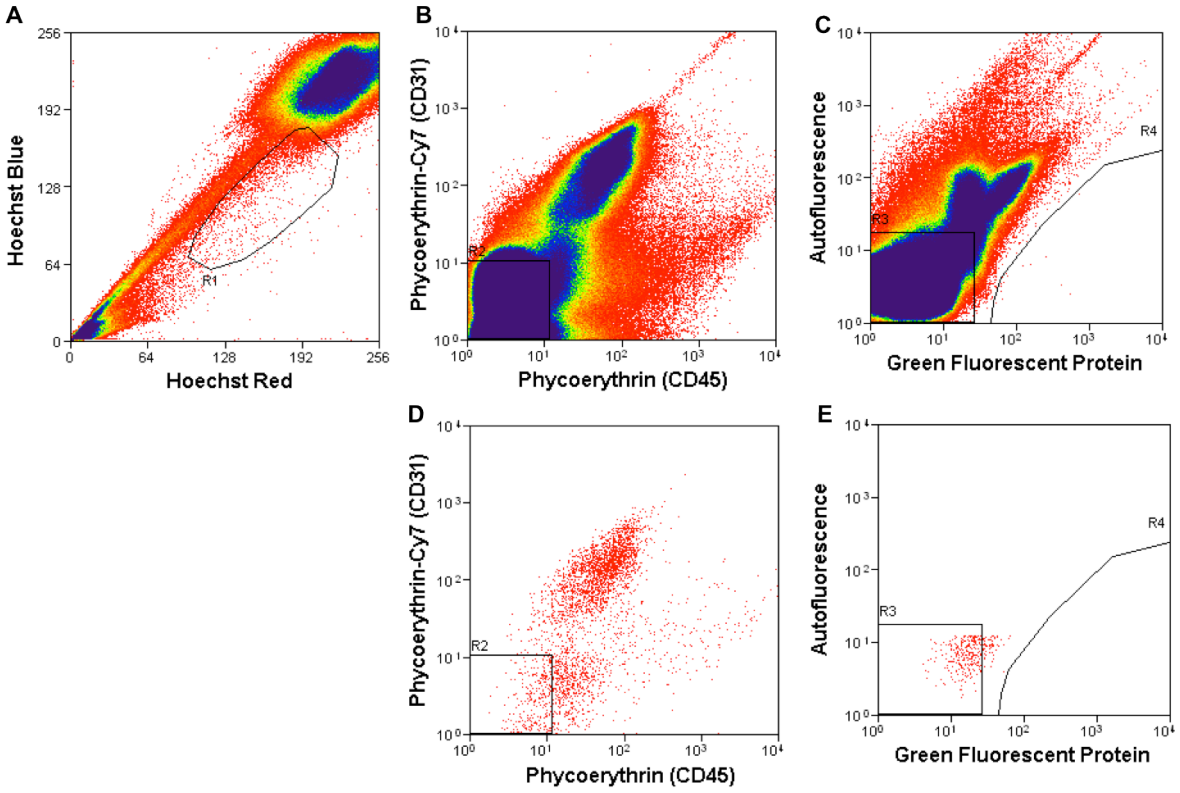

Figure 15: Fetal and Adult Cells in Culture

(A-D) Fetal cells were flow-sorted from maternal lungs and plated in supplemented media. Non-adherent cells were removed after 24 hours, and fresh media was replaced. Although GFP+ cell fragments could be observed, no large cells or growth was seen over the course of one week. Images (A) and (C) were taken on day two of culture, while (B) and (D) were taken on day 5. (C) and (D) show the same cell at these two time points. **(E)** and **(F)** $GFP^{+/+}$ female lung adherent cells have the appearance of MSCs and grew well in the same culture conditions, serving as a positive control.

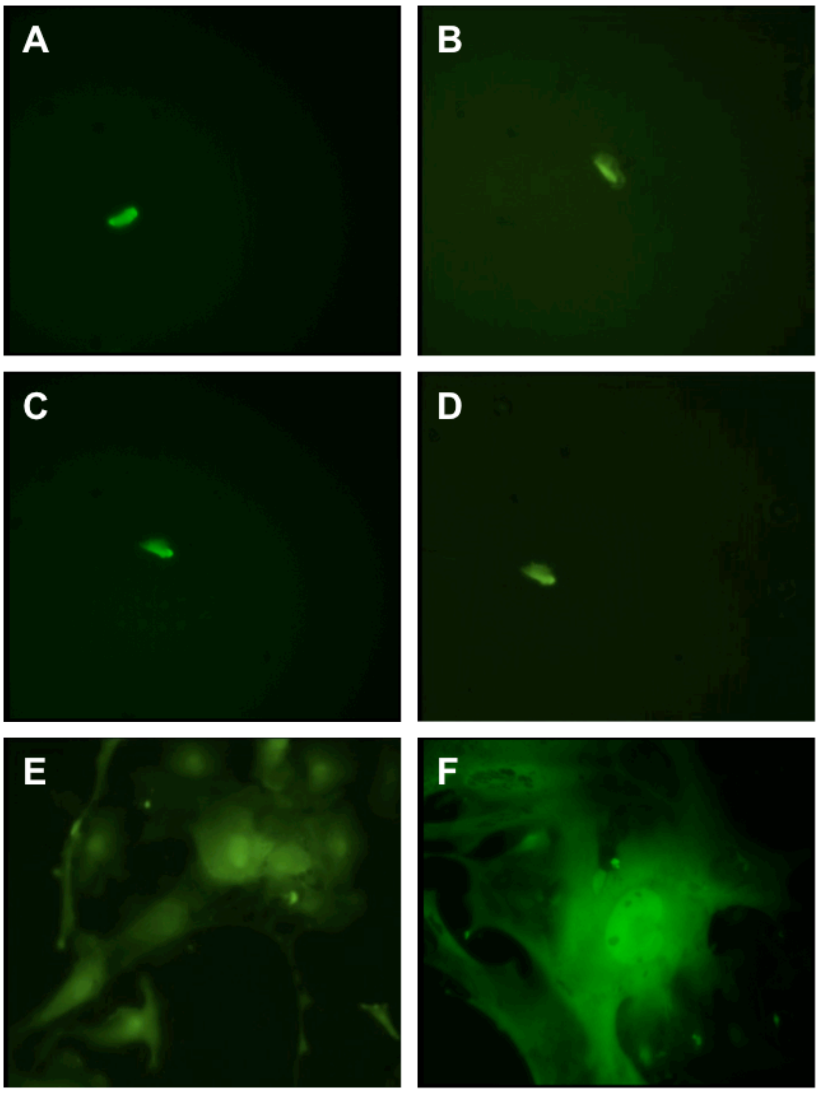

CHAPTER FIVE: THE ROLE OF MICROCHIMERIC FETAL CELLS IN RECOVERY FROM UNILATERAL PNEUMONECTOMY IN A MOUSE MODEL

INTRODUCTION

Fetal cells are present in injured maternal tissues in both humans and mice (Artlett, 2005; Bianchi, 2004; Bianchi, 2000; Dawe et al., 2007; Lee et al., 2010; Pritchard et al., 2011). It is currently unknown if the fetal cells are augmenting the mother's natural repair mechanisms and have a measurable effect on physiology, or whether the fetal cells are recruited to but have no significant impact on damaged tissues. We wished to examine whether fetal cells contribute to injury repair in the maternal lung. This maternal organ was selected because it contains the greatest number of fetal cells during pregnancy. Unlike humans, mice are capable of compensatory lung growth following unilateral pneumonectomy. Pulmonary function tests return to baseline after a recovery period of approximately two to three weeks (Paxson et al., 2009). We hypothesized that after unilateral pneumonectomy, postpartum mice would have an increased presence of fetal cells in their lungs compared to the sham mice. We further hypothesized that postpartum mice would recover pulmonary function quicker and to a greater extent than virgin females undergoing the same procedure.

METHODS

MICE

All protocols were approved by the Institutional Animal Care and Use Committee. Eight to 12 week-old C57BL/6J female mice were mated to C57BL/6J $GFP^{+/+}$ males in syngeneic matings. Mice delivered litters of $GFP^{+/-}$ pups, which were weaned at 21 days of life. Mice were housed in standard conditions and provided food and water *ad libidum*.

PNEUMONECTOMY

Three weeks after parturition, postpartum and virgin mice underwent either a unilateral pneumonectomy or a sham procedure (Figure 16). Unilateral pneumonectomies were performed by an experienced member of a collaborating laboratory at the Tufts School of Veterinary Medicine using the technique previously described (Nolen-Walston et al., 2008). Briefly, mice were anesthetized by intraperitoneal injections of ketamine and xylazine. Mice were mechanically ventilated, and the left thoracic wall was clipped and disinfected. The skin, chest wall, and pleura were incised at the fifth intercostal space. The left lung was gently lifted through the incision and ligated at the hilum. The remaining right lung was then inflated and the chest wall closed with a single interrupted suture. At the onset of vigorous spontaneous breathing the mice were extubated. Postoperative pain was managed with subcutaneous buprenorphine as soon as mice showed conscious motor control, and every 12 hours thereafter as needed (<3 days). The mice were allowed to recover for two weeks to allow for lung regrowth.

COMPARISON OF VIRGIN AND POSTPARTUM FEMALES

Pulmonary function tests were performed before the surgery and after the two-week recovery period in order to assess vital capacity, functional residual capacity, total lung capacity, residual volume, and lung compliance. We also performed flow cytometric analysis on the maternal lungs to look for the presence of the fetal cells (protocol described on page 35). The removed left and expanded right lungs from the mice that underwent pneumonectomy, as well as lungs from the sham mice, were analyzed.

RESULTS

Mated mice delivered litters of 6-8 pups. Ten mice were used in this preliminary experiment (Table 11): four postpartum and three virgin mice underwent pneumonectomies (PNX and Virgin groups, respectively), and three postpartum mice had the sham procedure (Sham group). The results of our pilot experiment did not show any consistent significant differences between the three experimental groups (Figure 17). Although not significant, the pulmonary function test changes in the sham group were larger than previously seen with this procedure (Dr. Andrew Hoffman, personal communication). The number of GFP+ fetal cells present in the maternal lungs was low in most females and highly variable (Table 11 and Figure 18).

DISCUSSION

We did not observe a role for microchimeric fetal cells in maternal compensatory lung growth following unilateral pneumonectomy. No differences in pulmonary function tests were noted between the virgin and postpartum females. Previous work demonstrated that exposure to CCl_4 resulted in elevated numbers of fetal cells in the maternal liver, while a partial hepatectomy had no such response (Khosrotehrani et al.,

2007). This may be because liver regrowth after partial hepatectomy involves replication of hepatocytes, while CCl_4 injury recruits bone marrow stem cells to the liver. This suggests that an inflammatory reaction and recruitment of bone marrow cells may be a necessary step for fetal cell trafficking to the injured tissue.

The number of fetal cells in each maternal lung pair varied widely. Variability between animals has been previously noted (Fujiki et al., 2008a; Kallenbach et al., 2011a; Khosrotehrani et al., 2005; Pritchard et al., 2012a) and the reason for it remains unknown. Some correlation with litter size has been noted (Fujiki et al., 2008a; Pritchard et al., 2012a) while others have shown no differences (Kallenbach et al., 2011a). It is possible that these differences are due to the underlying biology of fetal cell trafficking during pregnancy, but more research is needed to determine the precise cause.

The unilateral pneumonectomy model was chosen for several reasons. Firstly, we had collaborators at the Tufts University School of Veterinary Medicine who had significant experience with this injury model in mice. Their expertise on the surgical procedure as well as the typical recovery timeline was indispensible during this project. Secondly, it was essential to select an injury model with associated objective functional testing that could be used to quantify recovery following the procedure. The availability of pulmonary function tests permitted such quantification and would allow detection of fetal cell physiologic contribution to maternal recovery. Finally, although a previous experiment comparing an inflammatory and a surgical model in the liver did not show fetal cell contribution in the surgical injury (Khosrotehrani et al., 2007), not all surgeries are the same. In addition, different organs have different recovery mechanisms and may respond to similar injuries in different ways. For all of these reasons we felt that the unilateral pneumonectomy was a good model in which to study the role of fetal cell microchimerism in maternal tissue repair.

There are inflammatory injuries of the lung that may be better models for future experiments. For example, intranasal lipopolysaccharide (LPS) is a well-accepted model of inflammatory injury in the lung. A second model would be an elastase exposure to induce emphysema. There are noted sex differences in humans with emphysema (Sverzellati et al. 2009) making this model a good choice to study whether microchimeric fetal cells are responsible for these noted differences in disease presentation. In both LPS and elastase exposures, bone marrow-derived progenitor cells are mobilized to inflammation sites within the lungs (Yamada et al. 2004, Ishizawa et al. 2004). Thus, we hypothesize that naturally acquired PAPCs might exert a beneficial effect in females by either minimizing the development of injury or by accelerating the regeneration of alveoli.

Due to the absence of differences between the virgin and postpartum mice, both in terms of pulmonary function tests and the number of fetal cells, further studies were not pursued. Combined with our previous results showing absence of fetal cell participation in partial hepatectomy, we conclude that surgical models may not be ideal for this field of study. We therefore recommend that future experiments focus on models that involve inflammation and recruitment of bone marrow cells.

Figure 16: Experimental Outline for Postpartum Pneumonectomy Studies.

Three experimental groups were involved in this project. The sham and pneumonectomy (PNX) group consisted of wildtype C57BL/6 mice mated to males homozygous for the GFP transgene. The third group was virgin C57BL/6 females. Sham and PNX mice were allowed to deliver $GFP^{+/-}$ pups. Three weeks later, PNX and Virgin groups underwent a unilateral pneumonectomy while the Sham group had a sham surgery. Baseline pulmonary function tests were performed immediately prior to surgery and the removed lungs were analyzed by flow cytometry for the presence of GFP+ fetal cells. After a two-week recovery period, pulmonary function tests were repeated, the mice were euthanized, and the lungs were again analyzed by flow cytometry.

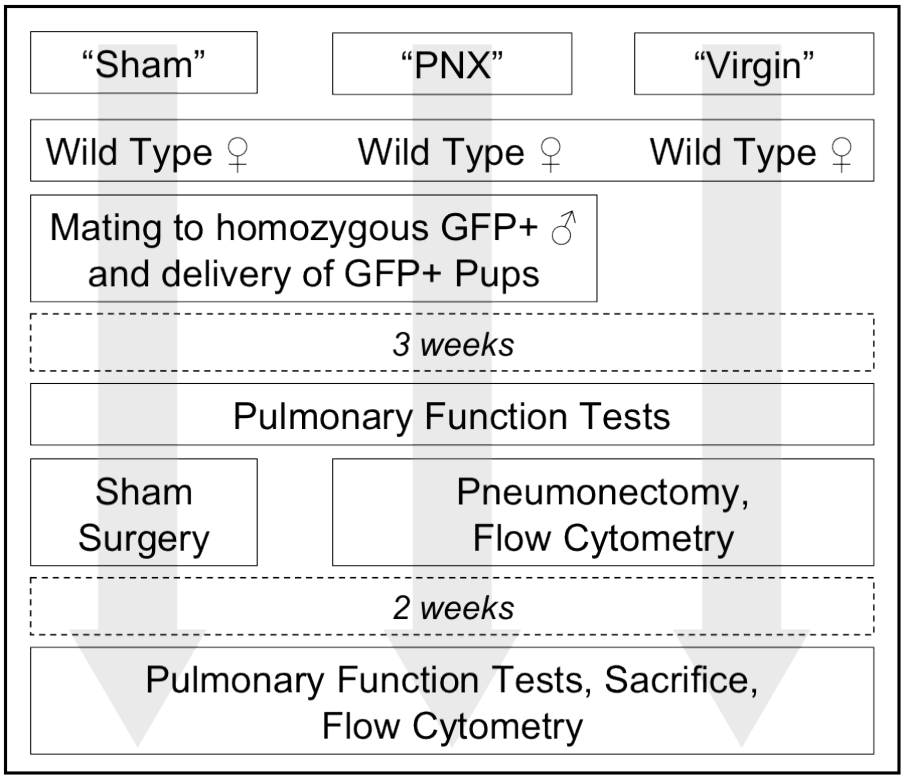

Figure 17: Average Percent Change in Pulmonary Function Tests.

Percent change in pulmonary function tests following sham or pneumonectomy surgery was calculated for each mouse. Results were averaged for each group. Error bars: standard deviation. * = $p<0.05$

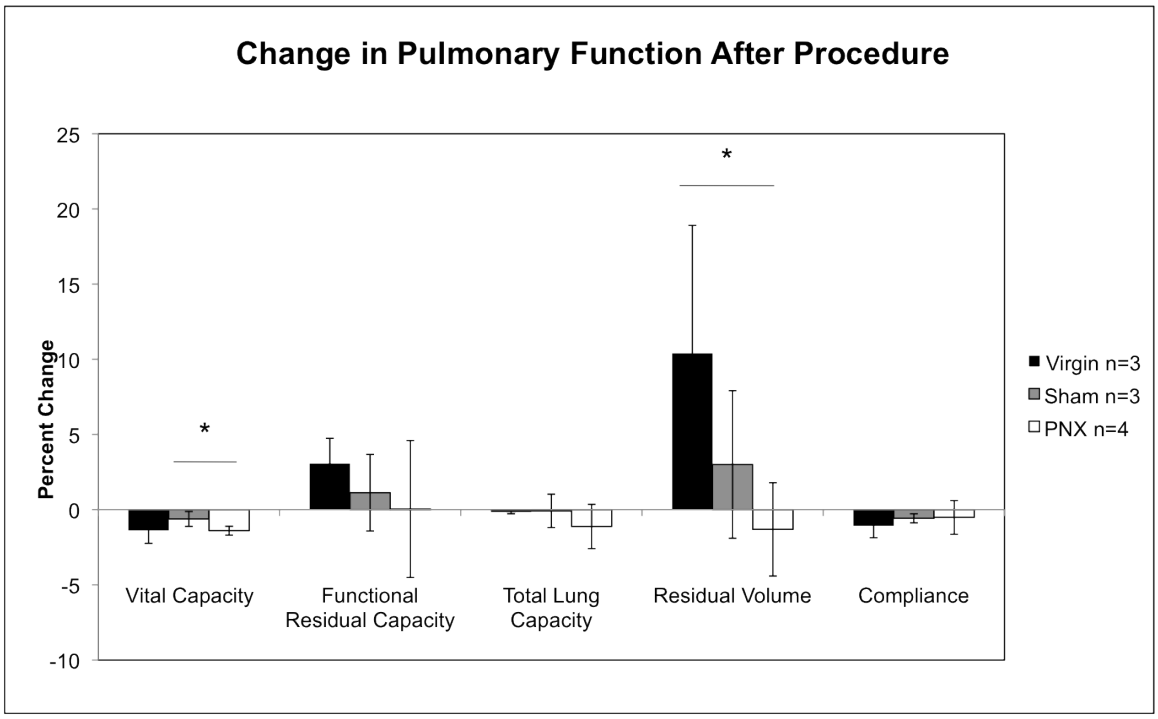

Figure 18: GFP+ Fetal Cells in the Lungs of Mice in the Pneumonectomy Study

Average number of fetal cells normalized per 10 million total flow cytometry events. Microchimerism was highly variable between individuals. See Table 11 for raw data.

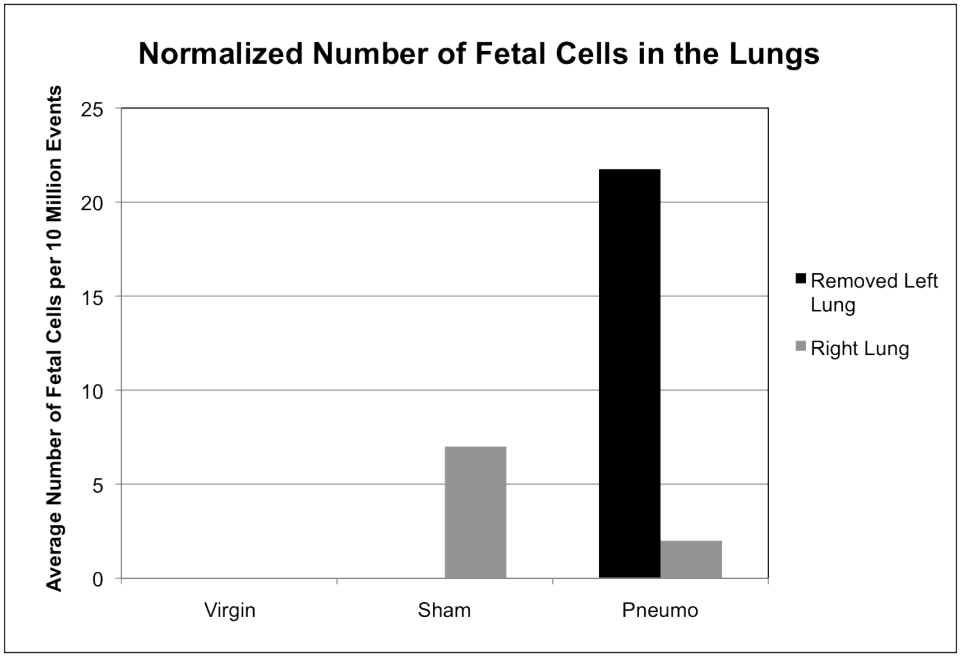

Table 11: Mice in Each Experimental Group for Pneumonectomy Study

Characteristics of the mice used each experimental group, including their pregnancy history and the number of fetal cells present in the lungs at various points of the experiment. The “Raw” column lists the total number of GFP+ cells observed, while the “Corr.” column contains the corrected number of fetal cells (total observed per 10 million total events). Days PP refers to the number of days after delivery on which the surgery was performed. *For Mouse 7 the two lungs were not analyzed separately. These numbers therefore represent the total and corrected numbers of GFP+ fetal cells in both lungs.

Mouse ID	Study Group	No. of Pups	Days PP	No. GFP Cells PNX Lung		No. GFP Cells Left Lung		No. GFP Cells Right Lung	
				Raw	Corr.	Raw	Corr.	Raw	Corr.
1	PNX	6	21	13	6.5	-	-	3	1
2	PNX	7	22	24	8.5	-	-	2	1
3	PNX	6	28	70	35	-	-	78	33.3
4	PNX	8	11	617	205.7	-	-	12	3
5	Sham	8	21	-	-	1	1	6	6
6	Sham	7	21	-	-	2	2	0	0
7	Sham	Unkn.	34	-	-	-	-	1526*	580.7*
8	Virgin	-	-	0	0	-	-	0	0
9	Virgin	-	-	0	0	-	-	0	0
10	Virgin	-	-	0	0	-	-	0	0

CHAPTER SIX: FETAL IMMUNE CELLS IN MATERNAL ORGANS AND THEIR IMPACT ON CONTACT HYPERSENSITIVITY REACTION

INTRODUCTION

Our analysis of the core transcriptome of fetal cells in the maternal lung demonstrated gene expression profiles consistent with trophoblasts, mesenchymal stem cells (MSCs), and cells of the immune system. Fetal immune cells of different lineages have been collected from pregnant and postpartum females (Adams Waldorf et al., 2010; Artlett et al., 2002; Huu et al., 2007; Khosrotehrani et al., 2008; Leduc et al., 2010; Loubiere et al., 2006; Schroder and Chapelle, 1972). Unlike other types of immune cells, like macrophages and NK cells, T lymphocytes have a long lifespan. Fetal T cells acquired during pregnancy could thus survive within the mother and potentially impact her health (Adams Waldorf et al., 2010). Acquired fetal T cells activated against maternal antigens could be responsible for fetal graft versus maternal host reactions (Adams Waldorf et al., 2010; Nelson, 2008). The autoimmune disease scleroderma has many clinical similarities to graft versus host disease and the role of fetal cells in this process has been examined by others (Evans et al., 1999; McNallan et al., 2007; Nelson et al., 1998).

Using a knockout model would allow not only allow verification of our earlier transcriptome data, but also potentially provide insight as to how fetal cells impact maternal health during and following pregnancy. We hypothesized that female mice lacking one of the genes expressed by the fetal cells, when mated to $GFP^{+/+}$ males, would have at least partial alleviation of their phenotype compared to knockout females mated to knockout males.

METHODS

SELECTION OF A KNOCKOUT MODEL

During our microarray analysis of fetal cells collected from the maternal lungs, 79 genes of interest were identified (Table 5). For each of these 79 genes, a search was performed using the JAX® Mice Database Search from the Jackson Laboratories (http://jaxmice.jax.org/query) to look for a homozygous knockout mouse model. Mouse models were eliminated if there were additional requirements such as doxycycline treatment or mating to a $Cre^{+/+}$ animal, if the females were infertile, or if homozygous mice did not survive to reproductive age (Figure 19). Nine knockout models were identified (Table 12). We ultimately selected the Beta-2 microglobulin (*B2m*) knockout model since objective quantification of an immune phenotype using antibody staining and flow cytometric analysis could be performed.

QUANTITATIVE REAL TIME POLYMERASE CHAIN REACTION

To confirm fetal cell expression of B2m, qRT-PCR was performed on four fetal cell cDNA samples. B2m TaqMan Gene Expression assay ID Mm00437762_m1 and ActB assay ID Mm00607939_s1 (Applied Biosystems) were used with TaqMan Fast Universal PCR Master Mix according to the manufacturer's instructions.

MICE

The Institutional Animal Care and Use Committee of the Tufts University School of Medicine Division of Laboratory Animal Medicine approved all protocols. All institutional and standard guidelines regarding the ethical use of experimental animals were followed. B6.129P2-$B2m^{tm1Unc}$/J (stock number 2087, Jackson Labs, Bar Harbor,

Maine) B2m knockout mice, wildtype C57BL/6J mice and homozygous GFP mice were housed in standard conditions. For the study of fetal CD8+ cells in the maternal organs, females were mated at 8-12 weeks of age in syngeneic matings.

Flow Cytometric Analysis of Fetal Cells from Maternal Organs

Female mice were euthanized 19 days after mating. Gestational ages of the pups studied were 15.5-17.5 days as determined by Theiler staging (Theiler, 1989). The thoracic cavity was opened and blood was collected by cardiac puncture and immediately mixed with EDTA to prevent clotting. The lungs, spleen, and liver were harvested.

A single cell suspension was separately created from each organ using a GentleMACS dissociator (Miltenyi Biotech) following the manufacturer's protocol. Maternal lungs were dissociated as described earlier (page 34). Livers were incubated at 37°C in pre-warmed Krebs-Ringer buffer (154 mM NaCl, 5.6 mM KCl, 5.5 mM Glucose, 20.1 mM HEPES, 25 mM $NaHCO_3$, adjusted to pH 7.4 with NaOH), with 2mM $CaCl_2$, 2mM $MgCl_2$, Collagenase IV (500 CDU/mL) and DNase I (150 U/mL) and then physically dissociated. Spleens were physically dissociated without prior enzymatic incubation.

All samples were filtered at 100µm and 70µm. Cell suspensions were spun at 300xg to pellet, and lysis buffer (0.15M NH_4Cl, 1.0mM $KHCO_3$, 0.1mM Na_2-EDTA in dH_2O) was used to eliminate red blood cells in all samples. Samples were washed once in PEB buffer (0.5% bovine serum albumin and 2mM EDTA in DPBS) and centrifuged again. Anti-CD8 antibody (clone 53-6.7, isotype Rat IgG2a,κ; BD Biosciences, San Jose, California) was applied for 30 minutes at 4°C. Cells were washed once with flow cytometry buffer, and centrifuged. Cell pellets were then resuspended again in flow cytometry buffer and propidium iodide (PI) was added to exclude dead cells. On a MoFlo

high-speed flow cytometer (DAKO, Fort Collins, Colorado), a 488nm laser was used to excite the fluorophores. Green fluorescence was collected with a 530/40 filter, APC with a 680/30 filter, and PI with a 670/40 filter. Fetal liver from euthanized pups was used as a GFP+ control. Organs from C57BL/6J and $B2m^{-/-}$ virgin females were used as negative controls (Figure 20).

Quantification of Cells and Statistical Analysis

GFP and PI gates (Figure 20) were drawn after data collection using Summit V4.3 Build 2445 software (DAKO). The GFP gate was drawn to exclude all cells in the virgin female organs. CD8 gates were drawn for individual organs separately to account for the unique autofluorescence patterns of each organ. Cells positive for either CD8+ or GFP+ as well as those double positive for CD8 and GFP were counted for each sample. Propidium iodide staining was also assessed for each cell type. Cell numbers were normalized per one million total events counted by the flow cytometer. A two-tailed student's T test was used to compare organs and mating groups.

Contact Hypersensitivity

Contact hypersensitivity (CHS) was elicited using a previously described protocol (Huu et al., 2007). In brief, fur was removed from the lower back by shaving. Mice were sensitized to 50µl of 2% oxazolone (4-Ethoxymethylene-2-phenyl-2-oxazolin-5-one, Sigma Aldrich) in 4:1 vol/vol acetone:olive oil by topical application. Six days after sensitization, right ears were challenged with 10µl 2% oxazolone in the same vehicle while left ears were exposed to vehicle alone. A second oxazolone dose was given 24 hours later (Figure 21). Response to treatment was measured using the mouse ear-swelling test (MEST), a standard in the field. At 24-hour intervals, a micrometer

(Marathon Management Company, Richmond Hill, Canada) was used to measure changes in the thickness of the mouse's ear, which occurs with inflammation. At each time point, four measurements were taken and averaged to ensure accurate assessment of inflammation. The researcher was blinded regarding wildtype or knockout strain status in order to eliminate any potential bias. For each animal, the change in ear thickness (= [Thickness on day *n*] – [Thickness on day -6]) was calculated for the left and right ears. The thickness change from the left (vehicle) ear was subtracted from that of the right (treated) ear to control for any age- or vehicle-related changes. A two-tailed student's T test was used to determine significance between knockout and wildtype females.

RESULTS/DISCUSSION

B2M KNOCKOUT MODEL

B2 microglobulin is required for the normal expression of major histocompatibility class I proteins, which are expressed on all nucleated cells. MHC class I proteins display fragments of cytosolic proteins to T cells; cells containing foreign proteins (such as from viruses or bacteria) will trigger an immune response while healthy cells will be ignored. MHC class I proteins on thymic epithelial cells educate double positive (CD4+ and CD8+) T cells to become CD8+ cytotoxic T lymphocytes. Because B2m knockout mice have little to no MHC class I protein expression, there are few CD8+ T cells (Koller et al., 1990). Immune responses involving CD8+ T cells are severely impaired (Tarleton et al., 1992). All fetal cell cDNA samples had amplification of *B2m* by qRT-PCR, confirming expression by the fetal cells (Figure 22). This model was chosen to investigate the transfer of fetal CD8+ immune cells to the maternal organs during pregnancy and their potential impact on maternal health.

Oxazolone is a topical chemical used to elicit a delayed-type immune reaction on the skin. This reaction is primarily mediated by MHC class I restricted CD8+ T cells (Bour et al., 1995). Mice lacking MHC class I molecules and/or CD8+ lymphocytes have impaired reactions and reduced ear swelling. In a previous study it was shown that microchimeric fetal cells participate in the repair of tissues during contact hypersensitivity induced during pregnancy (Huu et al., 2007). Fetal cells preferentially trafficked to the injured skin and CD31+ fetal cells could be seen contributing to angiogenesis. We therefore hypothesized that *B2m* knockout females mated to $GFP^{+/+}$ males would have an increased CHS reaction compared to virgin females or females mated to knockout males.

CD8+ T Cells in B2m Knockout Mice

CD8+ cells were present in the lungs, liver, spleen and blood of both wildtype and B2m knockout females (Figure 23). Two-tailed T test was used to assess differences in the different organs and groups. Only wildtype virgin, knockout virgin, and knockout mated to $GFP^{+/+}$ groups could be analyzed statistically due to the low number of samples in the other two groups. Compared to wildtype virgin females, the number of CD8+ cells per million total events was significantly lower in the lungs of virgin knockout females ($p = 0.04$; Table 13) and females mated to GFP homozygous males ($p = 0.04$). Virgin females also had significantly lower levels of CD8+ cells in the blood ($p = 0.03$). Females mated to $GFP^{+/+}$ males did not have significantly different CD8+ cell numbers compared to virgin wildtype females ($p = 0.86$) or virgin knockouts ($p = 0.37$). Neither spleen nor liver showed any significant differences between the three groups. Although not surprising that CD8+ cells are more prevalent in specific organs, it was unexpected to see conflicting CD8+ deficiencies between organs in the knockout compared to

wildtype mice. Others have reported significantly lower CD8+ cells in the thymus, lymph nodes, and spleens of B2m$^{-/-}$ mice and the deficit was consistent between organs (Koller et al., 1990). If future experiments are pursued, the genotype of the mice should be verified and cellular levels of MHC class I should be quantified by flow cytometry.

The number of GFP+ fetal cells present in the organs of knockout females was similar to previously observed results in our laboratory although differences between organs were noted as expected (Figure 24 and Table 13). We did note that the number of GFP+ cells was highest in the maternal liver compared to the other organs. Previous results showed the greatest number of fetal cells in the maternal lung (Fujiki et al., 2008a). This may reflect differences in how the livers were processed. In this work, red blood cells were eliminated by use of a lysis buffer, a step not included in our prior experiments. Since the liver contains a high number of erythrocytes, their detection on flow cytometry would elevate the total number of events counted. The fetal erythrocytes are not GFP+ and thus would not be counted in the number of GFP+ cells. Therefore the normalized number of GFP+ fetal cells would seem lower when a lysis step is not included.

CD8+ GFP+ fetal cells were not observed in any of the GFP-mated females. This was unexpected, as the transfer of CD8+ fetal cells to the mother during pregnancy has been well documented in human pregnancies (Adams Waldorf et al., 2010; Artlett et al., 2002; Imaizumi et al., 2002; Lepez et al., 2011). The reasons for this discrepancy are not known at this time.

CONTACT HYPERSENSITIVITY IN B2M KNOCKOUT MICE

Because of the suspected involvement of fetal cell microchimerism in maternal autoimmune diseases and cancers, models of these diseases are of special interest.

However, most of these animal models do not have discrete objective disease measures other than presence or absence of disease. It would be difficult to appreciate small changes in disease progression or presentation in many of these models. Although not directly testing an autoimmune process, the contact hypersensitivity model was appealing for multiple reasons. The first is that the mouse-ear swelling test is a quick, objective, quantitative assessment of inflammation. Secondly, other authors have published on the presence of fetal cells in the tissues in response to oxazolone exposure. Finally, and most importantly, showing a significant fetal cell contribution to the maternal immune response as measured by ear thickness would have far-reaching implications for maternal health.

No statistically significant difference was observed in ear swelling between wildtype and knockout virgin females after oxazolone treatment (Figure 25, Figure 26). There are several possibilities for these results. Firstly, low molecular weight chemicals can be presented by MHC molecules in two ways: 1) a chemical can bind to extracellular proteins, enter the cell, and be presented by MHC-II molecules to CD4+ cells; or 2) a chemical may be able to enter the cell on its own, bind to intracellular proteins, be processed in the endoplasmic reticulum, and be presented by MHC-I molecules to CD8+ cells (Bour et al., 1995). As a lipid-soluble compound, oxazolone would be expected to follow either the second or both pathways. However, if it does not enter the cells for some reason, CD4+ cells may dominate the reaction. Since there is no CD4+ cell defect in the $B2m^{-/-}$ mice, this could explain why no differences were noted between knockout and wildtype females.

The original report showing limited CHS response in $B2m^{-/-}$ mice used dinitrofluorobenzene instead of oxazolone (Bour et al., 1995). It is possible that these two chemicals are treated differently by the murine immune system. Further research would be needed to determine if this is the case.

Finally, we did not observe significant differences in CD8+ cells in all organs investigated (Table 13 and Figure 23), a difference from previous accounts (Koller et al., 1990). As stated above, the reasons for this inconsistency are not known at this time. The relatively robust CD8+ cell populations in some $B2m^{-/-}$ mouse organs may be responsible for the vigorous CHS response seen here. Future work is needed to explore this possibility.

Figure 19: Selection of a Knockout Model

Genes of interest were identified by microarray analysis of fetal cells collected from the maternal lungs. For each gene, a search was performed using the JAX® Mice Database Search from the Jackson Laboratories to look for a homozygous knockout mouse model. Mouse models were eliminated if there were additional requirements such as doxycycline treatment or mating to a $Cre^{+/+}$ animal, if the females are infertile, or if homozygous mice do not survive to reproductive age. Nine knockout models were identified (Table 12).

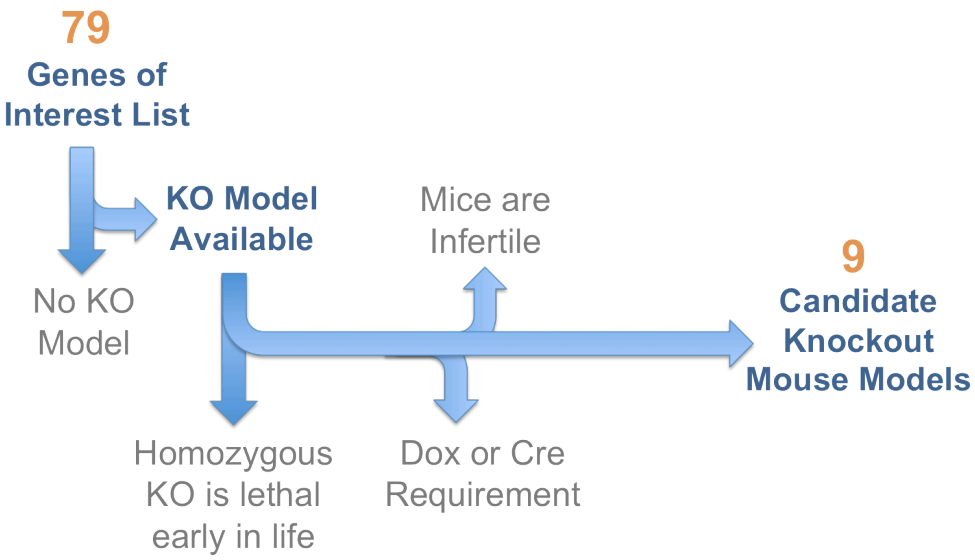

Figure 20: Sample Flow Cytometry Gates for Isolation of CD8+ Cells

Flow cytometry gates used to measure CD8+ and GFP+ cells in maternal organs. **(A)** Cells in the R1 gate are GFP+ fetal cells. **(B)** Gate R2 on the bottom of the image contains PI- (live) cells. **(C)** Gate R3 surrounds CD8+ cells identified with an APC-conjugated antibody. The individual organs required a different R3 gate as autofluorescence is different in each. The gates and sample shown here are maternal lung.

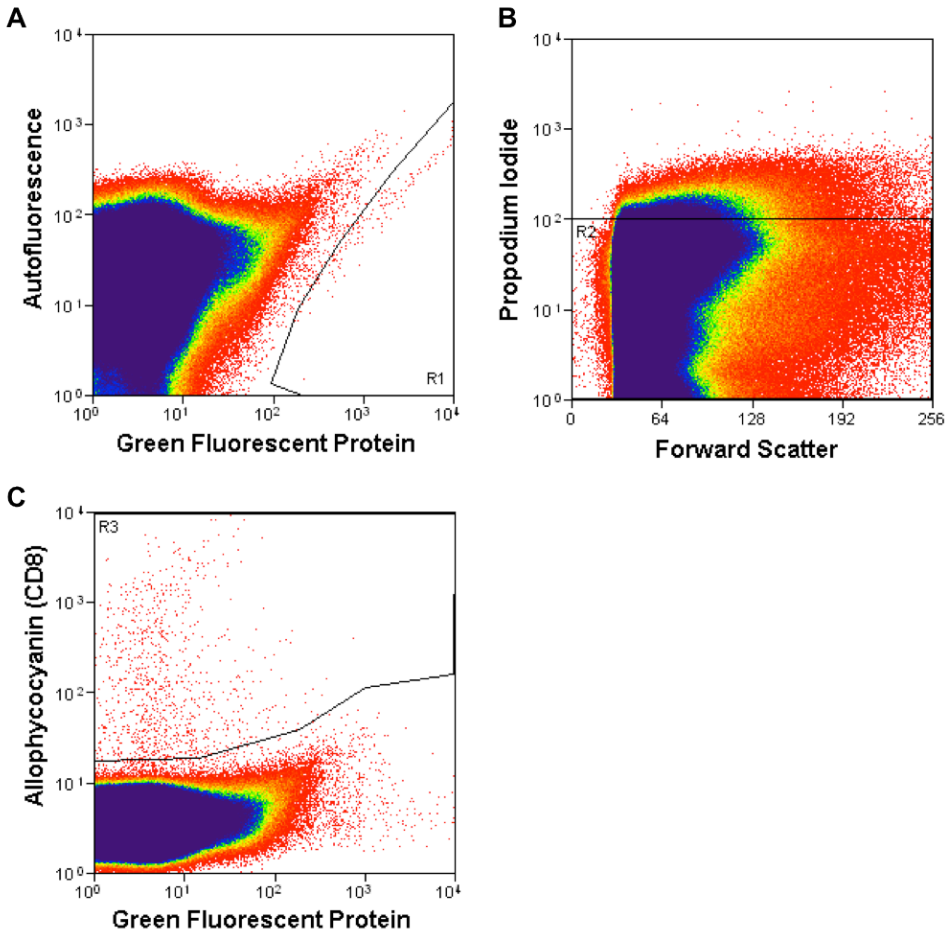

Figure 21: Injury Experiment Protocol.

Knockout (KO) females were to be placed in one of three experimental arms: virgins, mated to knockout males, or mated to GFP homozygous males. Wildtype (WT) females would be either mated to GFP homozygous males or not mated. Ten days after mating females would be sensitized to oxazolone. Six days later, oxazolone was to be applied to the right ear, while the left ear would receive vehicle only. This would be repeated after 24 hours. Due to complications with this model, only the Virgin experimental arm was completed. Ear thickness was measured at the start of the experiment (Day -6), before oxazolone exposure (Day 0), and then every 24 hours.

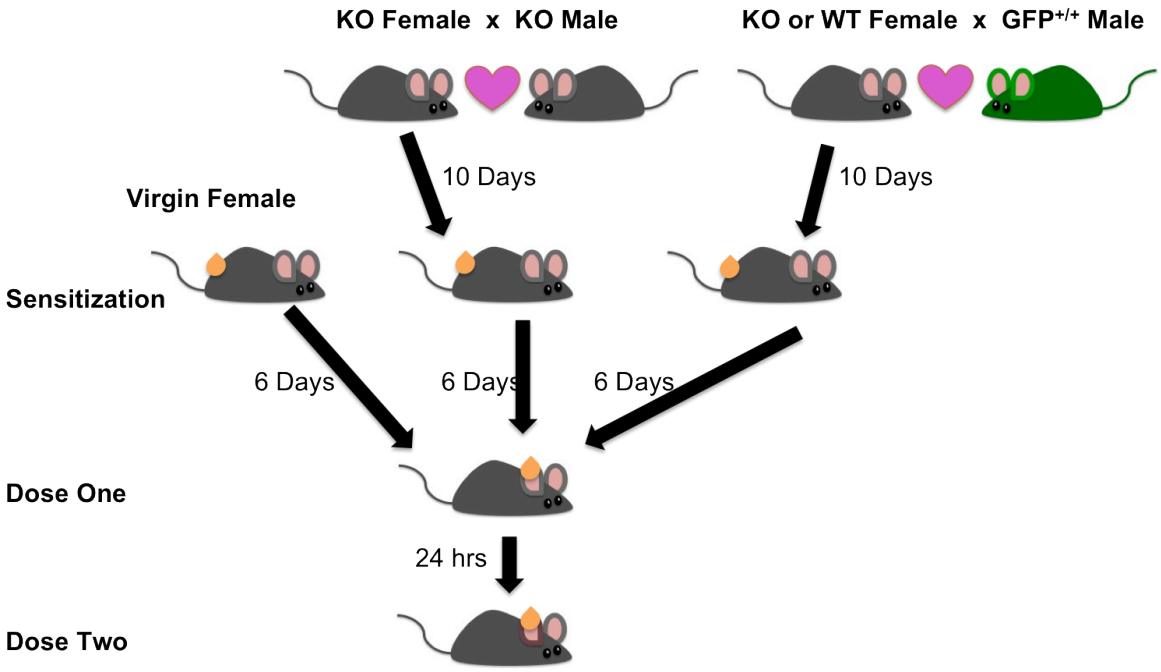

Figure 22: Quantitative Reverse Transcriptase PCR Amplification of B2m and ActB in Microchimeric Fetal Cell Amplified cDNA

GFP+ positive samples are from cDNA amplified from GFP+ fetal cells flow-sorted from maternal lung. GFP- sample was cDNA amplified from GFP- maternal cells also sorted from maternal lung. It was used as a positive control.

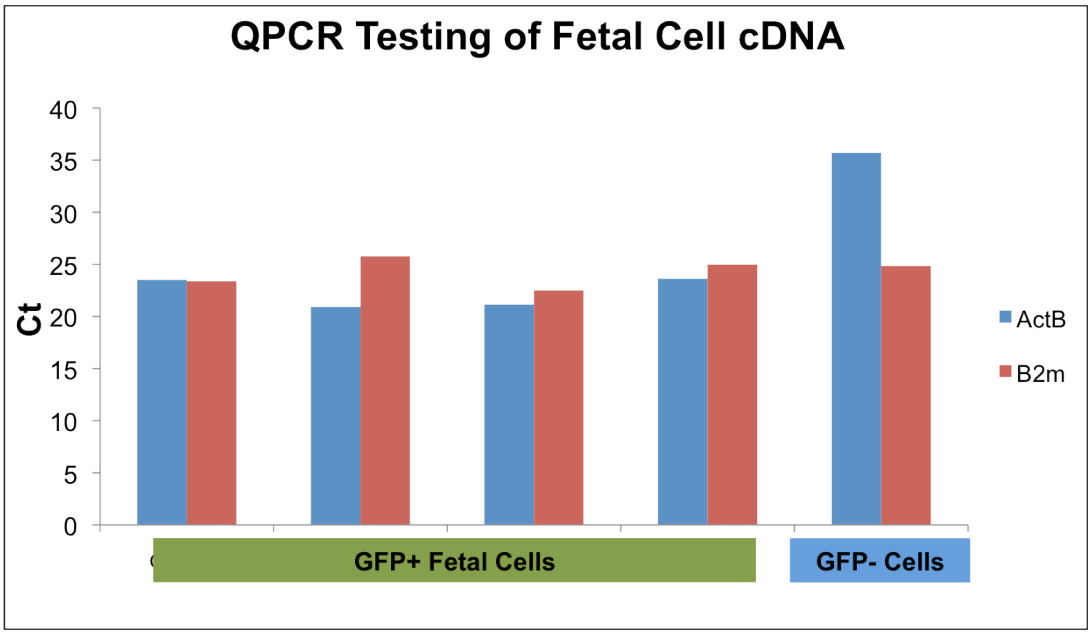

Figure 23: CD8+ Cells in Wildtype and Knockout Virgin and Pregnant Females

The number of CD8+ cells in each organ was quantified using the gates drawn in Figure 20. Cell numbers shown are normalized per one million total events counted by the flow cytometer. Note that the Y-axis is log scale.

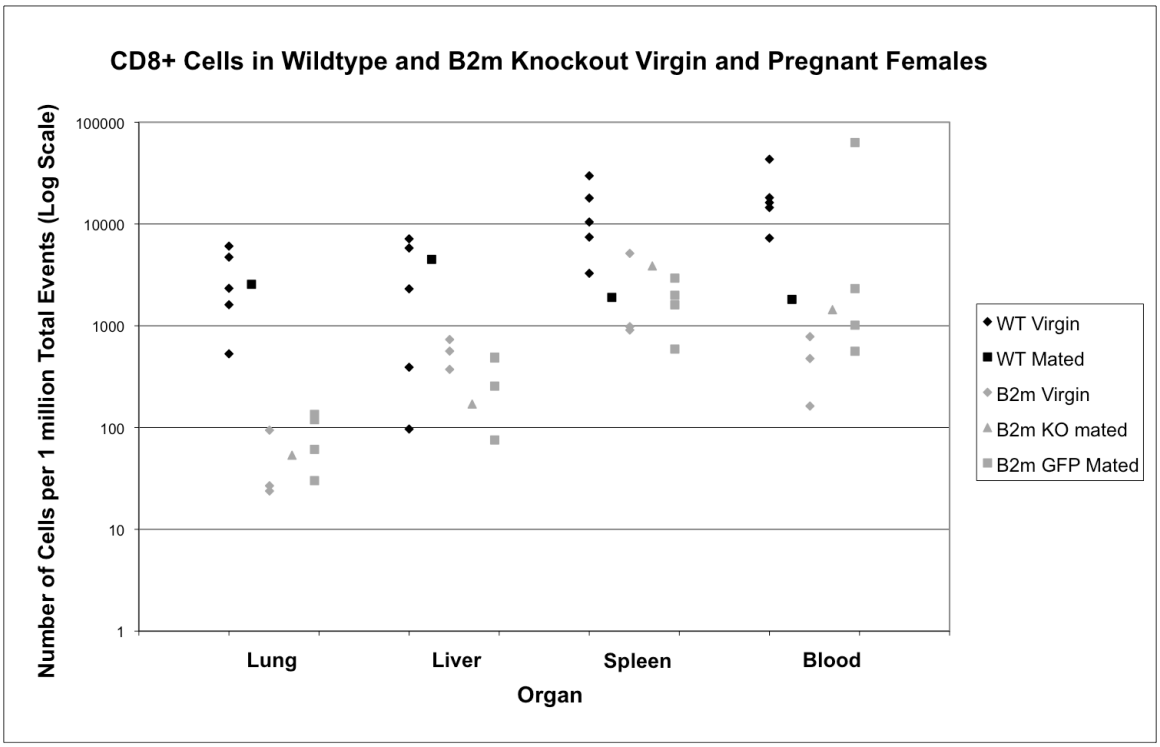

Figure 24: GFP+ Fetal Cells in Wildtype and Knockout Virgin and Pregnant Females

The number of GFP+ fetal cells in each organ was quantified using the gates drawn in Figure 20. Cell numbers shown are normalized per one million total events counted by the flow cytometer.

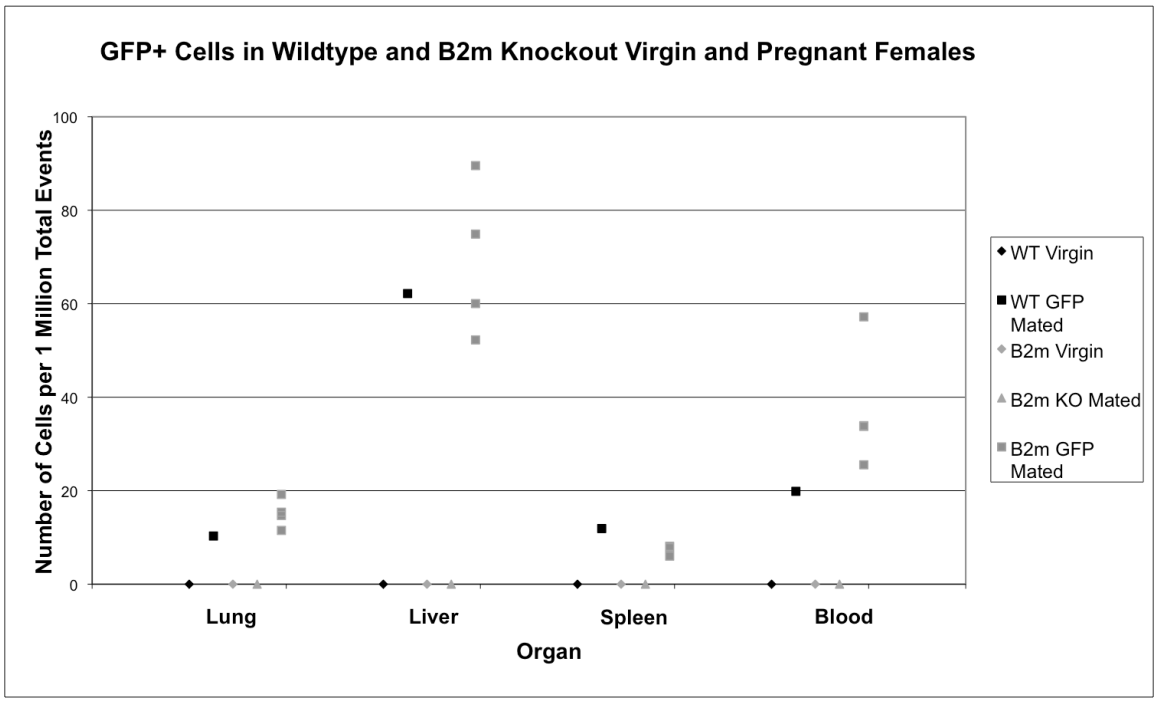

Figure 25: Ear Thickness of Animals After Oxazolone Exposure

Five knockout (KO) females and three wildtype (WT) females received oxazolone sensitization on Day -6, and then exposures on Day 0 and Day 1. Their genotypic status was blinded during all measurements. For each animal, the change in ear thickness (∆= [Thickness on day *n*] – [Thickness on day -6]) was calculated for the left and right ears. The thickness change from the left (vehicle) ear was subtracted from that of the right (treated) ear to control for any age- or vehicle-related changes. The average adjusted ear thickness change is shown for both wildtype and knockout animals. Error bars show standard deviation. A two-tailed unpaired student's t-test was used to determine significance between knockout and wildtype females. * $p<0.05$

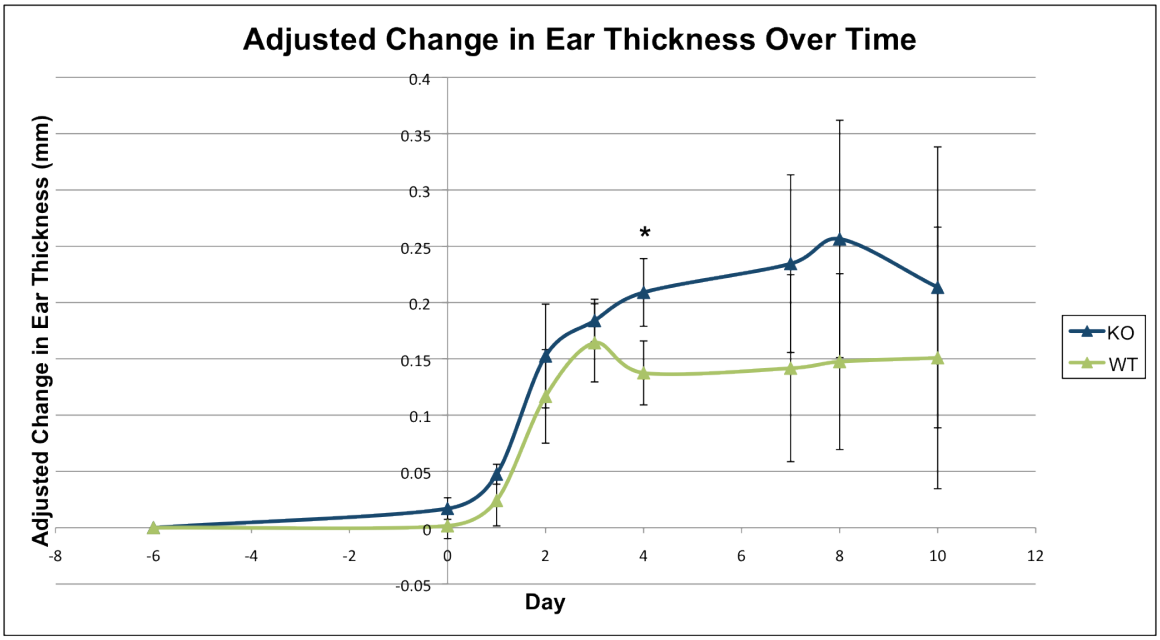

Figure 26: Representative Images of Wildtype and Knockout Ears from Oxazolone-Exposed Animals.

Right ears were exposed to 2% oxazolone in 4:1 vol/vol acetone:olive oil while left ears were treated with vehicle alone. Images were taken two days following the second exposure (Day 4). **(A)** Wildtype; **(B)** B2m Knockout

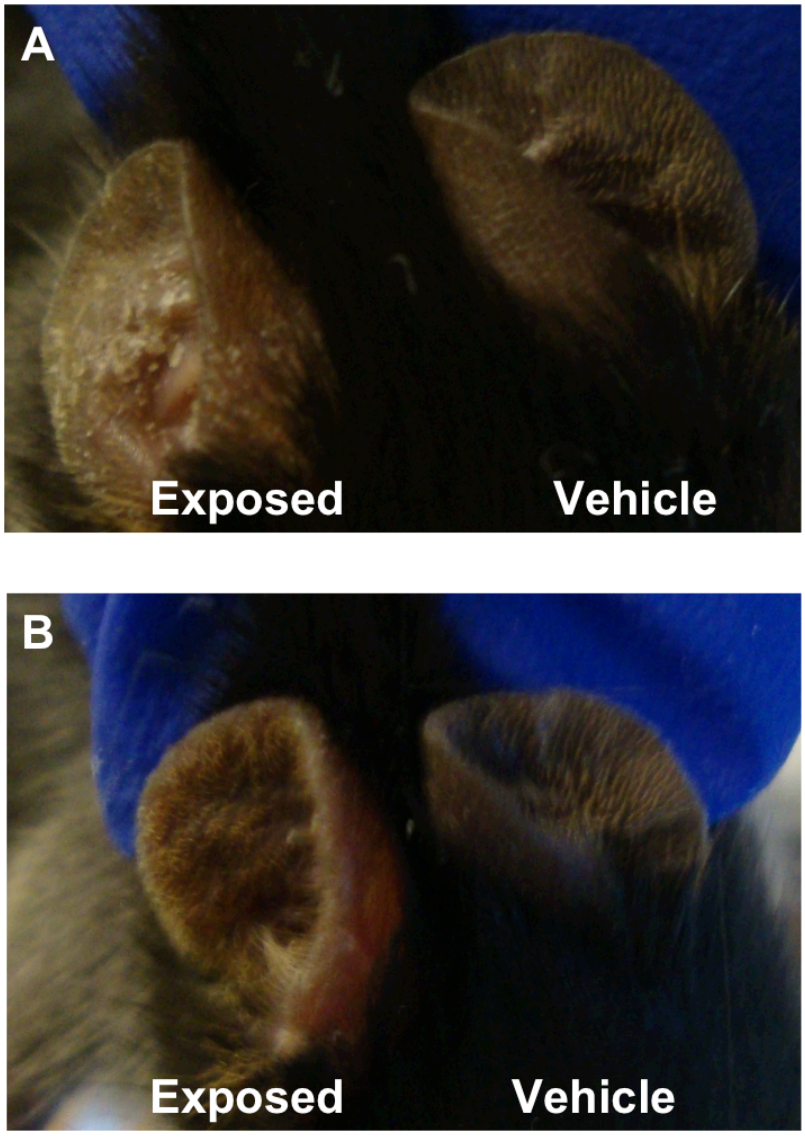

Table 12: Relevant Knockout Models Available from Jackson Laboratories

Genes of interest were identified by microarray analysis of fetal cells collected from the maternal lungs. For each gene, a search was performed using the JAX® Mice Database Search from the Jackson Laboratories to look for a homozygous knockout mouse model. Mouse models were eliminated if there were additional requirements such as doxycycline treatment or mating to a $Cre^{+/+}$ animal, if the females are infertile, or if homozygous mice do not survive to reproductive age. (See also Figure 19.) Colony status refers to the availability of the mice from the Jackson Laboratories.

Gene	Colony Status	Phenotype
Ahnak	Cryopreserved	Defects in T cell activation and proliferation, increased IL-4 secretion, decreased IL-2 and IFNgamma secretion.
Aicda	Cryopreserved	B cells are impaired but not ablated in their ability to undergo class switch recombination and somatic hypermutation.
B2m	Live	Little if any MHC class I protein expression on the cell surface. Few CD8+ cytotoxic T cells; immune responses involving CD8+ T-cells are deficient
Cav1	Live	Exercise intolerance and slight hyperphagia. Resistant to diet-induced obesity. In lung: thickened alveolar septa, hypercellularity, reduced alveolar spaces and increased densiy of basement membrane and reticulin fibers, more endothelial cells. 3-6mo mice have some characteristics of Alzheimer's disease.
Pkd2l2	Cryopreserved	Higher total distance traveled scores on the Open Field Test
Rnf128	Cryopreserved	Hyperactivation of primary CD4+ T cells. Multiple defects in naïve, helper and anergic T cell states affective survival, proliferation and cytokine secretion. Normal levels of T and B cells, dendritic cells, macrophages, neutrophils and other differentiated cell lineages.
Sepp1	Cryopreserved	Altered selenium metabolism. Increased susceptibility to parasitic infection. Decreased liver function and increased hepatocyte apoptosis.
Smad1	Cryopreserved	Abnormal gastric musoca cell population ratios. Cytoskeleton shows loss of adhesion zippers, decreased stress fibers and actin accumulation.
Zap70	Cryopreserved	Thymic development is arrested at the CD4+/CD8+ double positive stage. No peripheral T lymphocytes.

Table 13: T Test p-Values of CD8+ and GFP+ Cells in Organs of Wildtype and Knockout Females

(A) Comparison of CD8+ cell numbers in the four organs within each cohort.

(B) Comparison of CD8+ cells in each tested organ between the three cohorts.

(C) Comparison of CD8+ cells in the four tested organs within the B2M cohort.

WTV = Wildtype virgin females; B2V = B2m knockout virgin females; B2M = B2m knockout females mated to $GFP^{+/+}$ males. Statistically significant p-values are underlined.

A **CD8+ Cells**

WTV

	LUNG	LIVER	SPLEEN
LIVER	0.957	-	-
SPLEEN	0.082	0.084	-
BLOOD	0.051	0.051	0.453

B2V

	LUNG	LIVER	SPLEEN
LIVER	<u>0.034</u>	-	-
SPLEEN	0.243	0.330	-
BLOOD	0.138	0.715	0.313

B2M

	LUNG	LIVER	SPLEEN
LIVER	0.093	-	-
SPLEEN	<u>0.040</u>	0.055	-
BLOOD	0.360	0.366	0.404

B **CD8+ Cells**

LUNG

	B2V	B2M
WTV	<u>0.042</u>	<u>0.044</u>
B2V	-	0.310

LIVER

	B2V	B2M
WTV	0.143	0.119
B2V	-	0.175

SPLEEN

	B2V	B2M
WTV	0.069	0.061
B2V	-	0.735

BLOOD

	B2V	B2M
WTV	<u>0.034</u>	0.860
B2V	-	0.370

C **GFP+ Cells**

B2M

	LUNG	LIVER	SPLEEN
LIVER	<u>0.006</u>	-	-
SPLEEN	<u>0.012</u>	<u>0.005</u>	-
BLOOD	<u>0.027</u>	<u>0.027</u>	<u>0.021</u>

CHAPTER SEVEN: POSTPARTUM KINETICS OF FETAL CELLS IN THE MATERNAL LUNGS AND BONE MARROW

INTRODUCTION

Evidence from mice and humans suggests that persistent fetal cells can contribute to maternal tissue repair during injury. In mouse models, most injury experiments are performed during pregnancy since the number of fetal cells is highest immediately prior to delivery (Fujiki et al., 2008a; Sunami et al., 2010). In a clinical setting, however, most injuries or diseases occur postpartum. Therefore, experiments using animal models should be designed to address questions in the time period following delivery. In order to provide a baseline for such experiments, a comprehensive analysis of the natural history of fetal cells in the postpartum maternal organs is needed.

Our laboratory previously described the natural history of fetomaternal trafficking in mice during pregnancy (Fujiki et al., 2008a) and suggested that the number of fetal cells would likely increase in the postpartum period. Other laboratories have examined fetal cell presence at specific time points postpartum (Bonney and Matzinger, 1997; Sunami et al., 2010; Vernochet et al., 2007; Zeng et al., 2010). This chapter presents a detailed analysis of the natural history of fetal cells in the murine maternal lungs and bone marrow in the postpartum period. The maternal lungs contain the largest number of fetal cells during pregnancy (Fujiki et al., 2008a). For this reason, we chose the lungs for this experiment. Furthermore, since fetal cells have some similar properties to bone marrow stem cells, such as the ability to respond to injury and inflammation (Khosrotehrani et al., 2004; Pritchard et al., 2011), we also examined bone marrow. Finally, we used flow cytometry since it is the most sensitive and specific method for detection of rare microchimeric fetal cells (Fujiki et al., 2008a; Fujiki et al., 2008b).

MATERIALS AND METHODS

MICE

Wildtype females were mated to $GFP^{+/+}$ males as described earlier. With the *Egfp* homozygous male, all pups inherit one copy of the *Egfp* transgene. *Egfp* expression was used as a marker for all fetal cells and is independent of gender. Female mice delivered $Egfp^{+/-}$ litters. The pups were counted and euthanized during the first week of life. A total of 52 females were housed for 0.5-91 days postpartum in standard conditions with food and water provided *ad libitum*.

FACS ANALYSIS OF FETAL CELLS IN MATERNAL LUNG AND BONE MARROW

During the postpartum period, female mice were euthanized. Bone marrow cells were isolated from bilateral femoral and tibial bones. The marrow cavities were flushed with flow cytometry buffer. The lungs were collected and processed as described in Chapter One (page 34). Cell suspensions from both organs were filtered, spun at 300xg and resuspended in flow cytometry buffer with PI to assess dead cells. On a MoFlo high-speed flow cytometer (DAKO), a 488nm laser was used to excite the fluorophores. Green fluorescence was collected with a 530/40 filter, and PI with a 670/40 filter.

QUANTIFICATION OF FETAL CELLS

GFP and PI gates (Figure 27) were drawn after data collection using Summit V4.3 Build 2445 software (DAKO). Bone marrow and lungs from homozygous GFP+ mice were used as GFP+ controls. C57BL/6J virgin female lungs and bone marrow were used as a negative control and the GFP gate was drawn to exclude all cells in the virgin female samples (Figure 27C). The PI gate was drawn by comparing PI-stained and

unstained lung and bone marrow control samples from both $GFP^{+/+}$ and wildtype animals (Figure 27A, B). To account for differences between organs and different animals, the total number of GFP+ fetal cells (Figure 27D) in each sample is given as the number of fetal cells per $1x10^7$ total cells. Dead fetal cells were defined as cells that were both GFP+ and PI+ (Figure 27E). Live fetal cells were GFP+ and PI- (Figure 27F).

STATISTICAL ANALYSIS

Fetal cell counts were compared between the lung and bone marrow using the Wilcoxon rank-sum test to address a skewed distribution of the data. Partial Spearman correlation analysis was used to detect the association of fetal cell counts with duration of postpartum and litter size. All statistical analyses were performed using SAS/STAT software (SAS Institute, Inc., Cary, North Carolina). Statistical significance was assigned at $p<0.05$. A regression model was fit to the log-transformed fetal cell counts for each organ in order to describe the relationship with duration of postpartum.

RESULTS

Forty-eight lung and 40 bone marrow samples were analyzed between postpartum days 0.5 to 91. For most samples 10-30 million events were analyzed per lung pair, and 8-20 million per bone marrow.

Fetal cells were detectable in the pregnant mice for the duration of the experiment, which was up to 90 days postpartum in both lungs and bone marrow (Figure 28). In the lungs (Figure 28A), there was a steep decline in the number of fetal cells immediately following delivery ($r = -0.76$, $p < 0.0001$). This was followed by a slower decrease that started around days 17-18 but did not reach statistical significance ($r = -$

0.21 and p = 0.32). In the bone marrow (Figure 28B), the pattern was similar (r = -0.65, p = 0.0025 in early postpartum and r = -0.30, p = 0.20 after days 17-18).

The number of fetal cells detected was consistently higher in the lungs (median [interquartile]: 27 [13-51]) compared to bone marrow (7 [3-16]; p < 0.0001), with a strong positive correlation between the total number of fetal cells in each organ for a given animal (r = 0.58, p = 0.0001). Over time, the ratio of live to dead cells in bone marrow significantly decreased (Figure 29), particularly during early postpartum (r = -0.58, p = 0.0075) with a similar trend detected thereafter (r = -0.33, p = 0.16). An opposite pattern was observed for the lung with no change in the ratio of live to dead cells during early postpartum (r=-0.07, p=0.74) followed by a significant increase between 18 and 90 days (r=0.42, p=0.035).

After adjusting for the number of days postpartum, the number of pups in the litter negatively correlated with the total number of fetal cells in the bone marrow (r = -0.36, p=0.028). There was no statistically significant relationship between litter size and cell number in the lungs (r = -0.19, p=0.24).

DISCUSSION

Here we report a two-stage pattern in the number of fetal cells in postpartum murine organs. The first stage is characterized by a rapid clearance of fetal cells during the two-and-a-half weeks immediately following delivery. This is followed by a gradual trend through at least day 90 postpartum. Although the quick decline immediately postpartum has been previously reported in both humans and mice (Ariga et al., 2001; Fujiki et al., 2008a; Kolialexi et al., 2004), the two-stage pattern is a novel finding. These results inform study design, and we recommend that murine injury experiments investigating the potential postpartum effects of fetal cells on maternal tissue repair

should start at a minimum of 17-18 days after delivery to be sure that the initial clearance stage has been completed.

We further showed a positive correlation between the number of fetal cells in the lung and bone marrow for an individual animal. The strong positive correlation between the numbers of fetal cells in each organ for an individual animal suggests that an animal with high levels of fetal cells in one organ will also have high levels in other organs. This may simplify study design by eliminating the need to test multiple organs in healthy animals when assessing levels of microchimerism. There was substantial variability between individual animals, similar to other reports (Fujiki et al., 2008a; Kallenbach et al., 2011a; Khosrotehrani et al., 2005). The reason for this variability is not known at this time. It raises important biological questions about fetal cell trafficking.

In addition, we found the ratio of live to dead cells changes over time, with different patterns observed for the lung and bone marrow cells. The increased presence of live fetal cells in the maternal lung suggests that the fetal cells may be actively dividing after days 17-18. Such a finding would have positive implications for the potential use of fetal cells to treat maternal disease (Pritchard et al., 2011) or negative implications if parous females serve as organ donors due to the risk of graft versus host disease (Bianchi and Fisk, 2007). Previous work has demonstrated proliferation by looking at mitoses in fetal cells in postpartum female mice (Liegeois et al., 1981). Future work could use a marker of DNA replication such as bromodeoxyuridine to determine what percent of the fetal cells are actively proliferating.

Our results showed a negative correlation between litter size and microchimeric fetal cells in bone marrow, which did not reach statistical significance in the lung. Previous work in our laboratory used a hemizygous GFP male so that approximately half of the pups inherited *Egfp*. Using this model we noted a statistically significant positive association between the number of GFP+ fetuses and fetal cells in the lung and kidney

(Fujiki et al., 2008a). Others have found no significant relationships between litter size and fetomaternal cell trafficking (Kallenbach et al., 2011a). These conflicting results suggest that overall there may not be an effect, but that individual studies show an association due to small sample sizes. However, it is possible that an inverse relationship may reflect different efficiencies of fetal cell clearance. One limitation of determining the true effect of litter size on the microchimeric fetal cell population is that most studies count the number of pups that were delivered, not the number of pups present at the beginning of pregnancy. In order to thoroughly address this question, sonographic assessment of the number of pups, combined with measurement of fetal cells in maternal blood, would need to be performed repeatedly during gestation.

CONCLUSIONS

We report here on postpartum fetal cell trafficking in mouse lungs and bone marrow. We show that there is a rapid decline immediately after delivery, followed by a slower decline after the second week. Fetal cells were present in both organs for the 90-day duration of the experiment, and they likely persist for an even longer time in mice. Our results have implications for the design of murine postpartum injury experiments studying potential effects of fetal cells on maternal tissue repair. Such experiments should start at least 17-18 days after delivery to ensure that the initial postpartum clearance is complete. Lastly, the increased ratio of alive to dead cells in the maternal lung is suggestive of fetal cell proliferation, which, if proven, may impact women's health following pregnancy.

Note: The results of this study were published in *Chimerism* in July 2012.

Figure 27: Gates used During Flow Cytometery Experiments to Quantify Fetal Cells in Postpartum Females

(A) Unstained virgin female lung sample showing gate R1 used for PI. **(B)** Virgin female lung sample stained with PI showing gate R1 used for PI. The cells in the upper region (gate R1) are PI positive, and therefore dead. Cells not contained within the R1 gate (at the bottom of the image) are PI negative, and therefore alive. **(C)** Virgin female lung sample stained with PI showing gate R2 used for GFP+ cell counting. **(D-F)** Postpartum female lung sample stained with PI showing gate R2 used for GFP+ cell counting. Cells within the R2 gate (at the right of the image) are GFP+ and therefore fetal. (D) Ungated window displaying the total number of fetal cells in gate R2. (E) The same sample gated for PI (Gate R1), showing GFP+ PI+ dead fetal cells in area R2. (F) The same sample gated to exclude PI, showing GFP+ PI- live fetal cells in area R2.

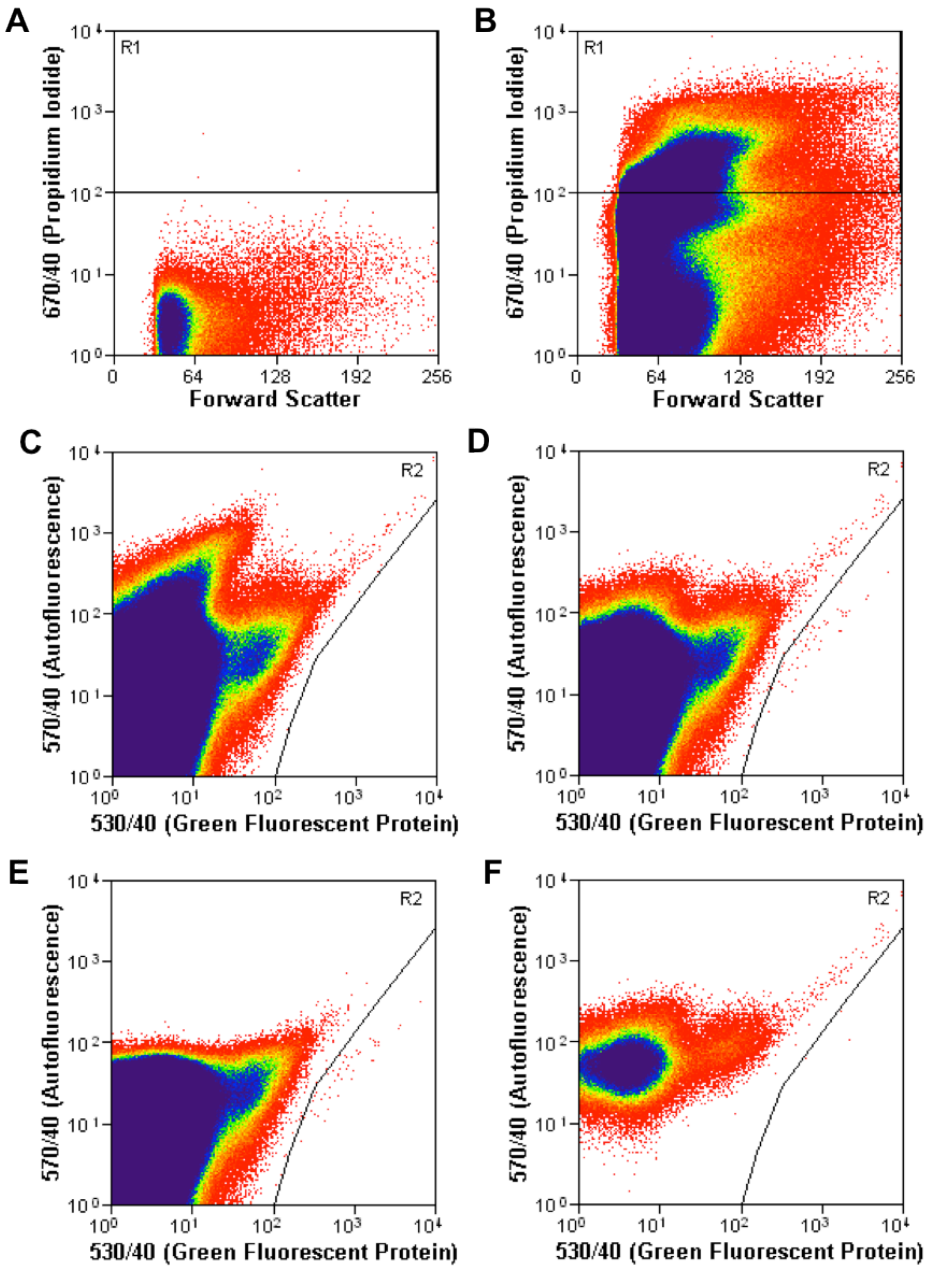
A
B
C
D
E
F
R1
R2
670/40 (Propidium Iodide)
Forward Scatter
570/40 (Autofluorescence)
530/40 (Green Fluorescent Protein)
0
64
128
192
256

Figure 28: Log-transformed Normalized Total Fetal Cells in the Maternal Postpartum Organs.

Log-transformed normalized total number of GFP+ fetal cells in the maternal organs during the postpartum period. **A)** Lung; regression function: f(y)=3.0+1.7*exp(-0.2x), R^2=0.34; **B)** Bone marrow; regression function: f(y)=2.2+53.8*exp(-6.5x), R^2=0.18.

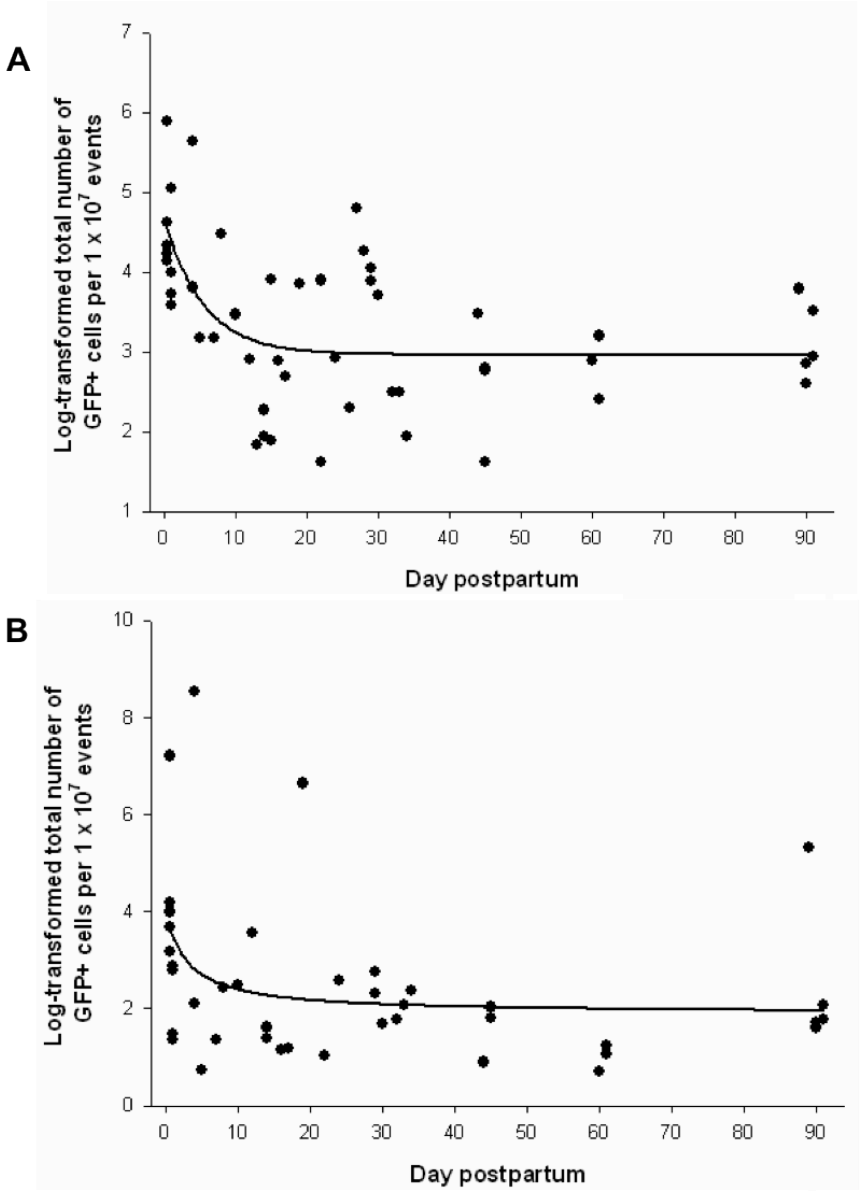

Figure 29: Ratio of Live to Dead Cells in Postpartum Maternal Organs

Ratio of log-transformed normalized live to dead cells in the maternal **A)** lung and **B)** bone marrow during the postpartum period. Horizontal lines represent median, box represents 25th to 75th percentile, and whiskers represent 10th to 90th percentile.

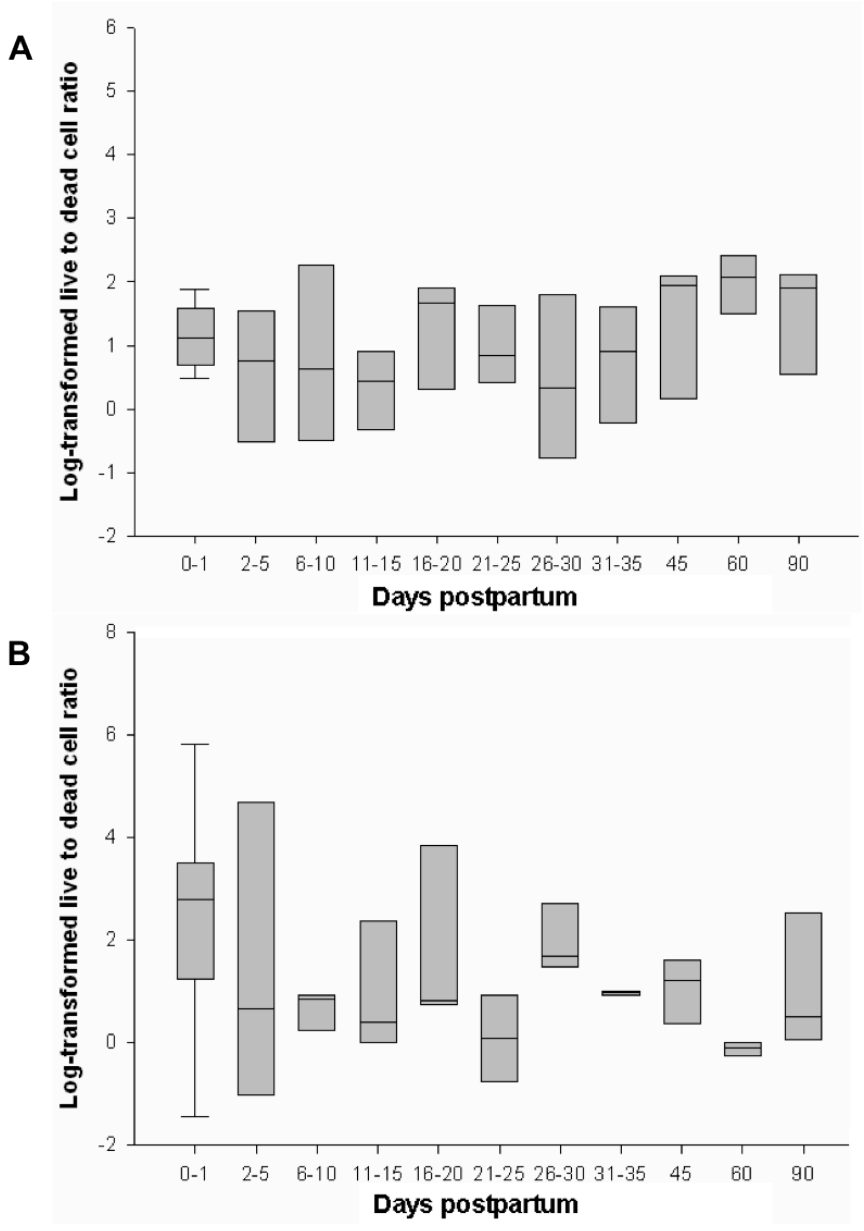

DISCUSSION

This thesis aimed to address four main knowledge gaps: (1) Limited data on fetal cell phenotype(s); (2) Unknown effects of fetomaternal histocompatibility on phenotype; (3) Uncertain physiologic impact on maternal health; and (4) Limited knowledge of postpartum fetal cell kinetics.

LIMITED DATA ON FETAL CELL PHENOTYPE(S)

Investigators studying microchimerism have long sought to understand the origin and identity of microchimeric fetal cells, as their phenotype and differentiation status may impact long-term maternal health. Because fetal cells are relatively rare within maternal organs, their characterization presents significant challenges. For the last several years, our laboratory has focused on optimizing the mouse models used for fetal cell microchimerism research. In 2008 we reported that flow cytometry is the most sensitive and specific method for detection of rare microchimeric fetal cells (Fujiki et al., 2008b). We also published a study of the broad patterns of fetal cell trafficking during pregnancy, showing that fetal cells were most prevalent in the maternal lung immediately before delivery (Fujiki et al., 2008a). We subsequently discovered elevated microchimerism in the lungs of pregnant females in allogeneic compared to syngeneic matings (Kallenbach et al., 2011a). Here we built on our previous advances with a novel technique that combines flow cytometry and multidimensional gene expression microarray analysis to examine the question of fetal cell phenotype.

Our innovative approach allowed identification of relevant genes and biological pathways to highlight fetal cell phenotypes. Our multidimensional analysis suggested that fetal cells in the maternal lung are primarily trophoblasts, cells of the immune

system, and mesenchymal stem cells (MSCs), and that these cells may be involved in the development of maternal immune tolerance during pregnancy (Chapter Two). Our results also add additional evidence that microchimeric fetal cells have stem cell-like properties (Table 14).

We endeavored to further characterize fetal MSCs and immune cells in the maternal organs (Chapters Four and Six). Unfortunately these studies were hindered by the limited numbers of cells present, underscoring the challenges of working with these rare cells.

We did not further investigate the presence of placental cells for several reasons. First, trophoblasts are known to be cleared rapidly from the mother after delivery (Attwood and Park, 1961; Chamley et al., 2011). Second, although the placenta contains stem cells, we did not see specific evidence for the presence of placental stem cells such as the expression of *Cdx2*. Many other cells in the placenta are post-mitotic and unlikely to have a long-term impact on maternal health. Finally, although markers exist to distinguish the different placental layers and their constituent cell types from one another, to our knowledge there are no readily available antibodies that target all placental cells, but do not cross-react with lung tissue. To confirm the presence of trophoblasts or other placental cells, a tetraploid complementation assay could be performed using wildtype embryonic stem cells and $GFP^{+/+}$ tetraploid embryos. In this experimental system, all extra-embryonic tissues would express GFP while the embryo proper would not. An alternative experiment would involve expression of *Egfp* under the control of a placental-specific promoter. However, this may have associated complications due to temporal expression differences in each placental cell type or expression in non-placental tissues if the promoter is not completely specific.

Unknown Effects of Fetomaternal Histocompatibility on Phenotype

Murine models of fetal cell trafficking typically use syngeneic matings (Fujiki et al., 2008a; Fujiki et al., 2009; Huu et al., 2007; Kara et al., 2012; Pritchard et al., 2012b). However, such models do not appropriately address the important fetomaternal immunologic differences present in human pregnancies. It has already been demonstrated in both humans and mice that histocompatibility between the mother and her fetus(es) influences the quantity of microchimeric fetal cells as well as the specific cell types (Adams Waldorf et al., 2010; Kallenbach et al., 2011a; Khosrotehrani et al., 2005).

Our results show that key differences exist between fetal cells in syngeneic and allogeneic pregnancies. Primarily, the fetal cells appear to have a more primitive phenotype, which may influence their role in maternal health and disease. We also confirm our earlier studies, which showed elevated fetal cell trafficking in the maternal lungs during allogeneic matings (Kallenbach et al., 2011a). Because of these differences, we recommend that future experiments use allogeneic matings wherever possible for the study of fetal microchimerism.

The other experiments presented in this thesis were performed concurrent or prior to this discovery and thus could not be done with an allogeneic model. Future experiments should determine whether postpartum kinetics follow a similar pattern in allogeneic pregnancies or whether fetal cell expression of non-shared MHC antigens facilitates more rapid clearance.

UNCERTAIN PHYSIOLOGIC IMPACT ON MATERNAL HEALTH

Fetal cells in both humans and mice are able to respond to tissue injury in a variety of organs. These cells fully integrate within the maternal tissue structures, identifiable as fetal only by the presence of an inherited paternal marker (Pritchard et al., 2011; Pritchard et al., 2012b). Although histological involvement has been described on numerous occasions, to our knowledge no published research has demonstrated significant physiologic contribution of microchimeric fetal cells to injury response. We hypothesized that pregnant or postpartum females would recover more quickly or more fully than would nulliparous females. We used two disease models, unilateral pneumonectomy (Chapter Five) and contact hypersensitivity (Chapter Six) to test this hypothesis. We used functional measurements to quantify maternal recovery.

In our pilot study, we did not observe significant differences in pulmonary function tests between virgin and postpartum female mice after pneumonectomy. It is highly likely that fetal cells do not play a role in every disease or injury and unilateral pneumonectomy may be one such model. Previous work demonstrated that partial hepatectomy did not increase fetal cell presence in the maternal liver while induction of liver fibrosis by carbon tetrachloride did (Khosrotehrani et al., 2007). This may be because liver lobe regrowth involves replication of hepatocytes, while CCl_4 injury is capable of recruiting bone marrow stem cells to the liver. This suggests that an inflammatory reaction and recruitment of bone marrow cells may be a necessary step for fetal cell trafficking to the injured tissue.

Contact hypersensitivity (CHS) is a delayed-type immune reaction mediated by CD8+ T lymphocytes. It has been previously demonstrated that microchimeric fetal cells preferentially traffic to injured skin in contact hypersensitivity induced during pregnancy (Huu et al., 2007). To enhance potential fetal cell contribution in tissue repair, we used a

$B2m^{-/-}$ mouse, which has impaired CHS reaction (Bour et al., 1995). Our preliminary experiments did not confirm diminished CHS response, however. This may be due to our use of a different chemical, or the higher than expected presence of CD8+ cells at baseline.

It is essential to determine whether fetal cells in the maternal organs result in any significant physiologic improvement following injury. We encourage researchers to include functional evaluation of pregnant, postpartum, and virgin female mice. The precise injury or disease studied may dictate how much influence, if any, fetal cells have on recovery.

LIMITED KNOWLEDGE OF POSTPARTUM FETAL CELL KINETICS

As fetal cells are most prevalent immediately prior to delivery, most animal work to date has focused on disease and injury induction during or immediately following pregnancy (Dubernard et al., 2009; Huu et al., 2007; Huu et al., 2009; Kara et al., 2012; Nassar et al., 2012). In a clinical setting, however, most diseases occur postpartum. More research is needed at this important stage. While preparing our study of fetal cell participation in compensatory lung growth following unilateral pneumonectomy (Chapter Five), we noticed a surprising deficiency in the understanding of microchimerism patterns following parturition. Other groups have examined fetal cell presence at specific time-points postpartum (Bonney and Matzinger, 1997; Sunami et al., 2010; Vernochet et al., 2007; Zeng et al., 2010) but no detailed analysis has been published to guide experimental design.

In our postpartum kinetics study (Chapter Seven), we demonstrated an initial two and a half-week rapid clearance, followed by a trend of gradual decrease in both lungs and bone marrow. We consequently suggest that murine injury experiments should

begin no earlier than day postpartum 17-18 to allow the initial clearance to complete. In humans, trophoblasts are found in the maternal lung during pregnancy but are quickly cleared such that they are undetectable by two weeks postpartum (Attwood and Park, 1961; Chamley et al., 2011). It is therefore possible that the rapid postpartum decline represents the disappearance of trophoblasts, while the longer-term persistent cells observed after days 17-18 may be fetal MSCs and/or immune cells. Future work should establish what cell types comprise the postpartum fetal cell population to test if this is true. Attempts in our laboratory to obtain sufficient fetal cells from the postpartum maternal lung and bone marrow for analysis were unsuccessful. Use of an allogeneic mating model may permit collection of adequate numbers of cells.

An observed increase in the ratio of live to dead cells within the lung over time suggests that these cells may replicate in vivo. Our microarray analyses also suggest that fetal cells proliferate by demonstrating enrichment of pathways involved in protein synthesis (Chapters Two and Three). In our experiments, propidium iodide was used as a marker of cellular viability. At higher concentrations, PI can determine cellular DNA content for cell cycle analysis. In the context it was used here, it did not directly evaluate proliferation. Although it is generally assumed that fetal cells proliferate due to their lifelong persistence (Dawe et al., 2007), the percent of replicating cells should be more concretely determined by future experimentation.

STRENGTHS OF THE STUDY

DEVELOPED TECHNIQUE CAN BE WIDELY EXPANDED

We demonstrate for the first time here that gene expression data can be collected from small numbers of fetal cells acquired by FACS from maternal organs. The technique developed here will permit endless variations to explore the fetal cell

population. Specific fetal cells can be sorted based on their surface markers, so that only cells of a specific sub-type are collected. Using a fluorescent protein under the control of a cell type-specific promoter can also identify specific fetal cell groups for analysis. This technique can also be used to investigate fetal cells in other organs, in postpartum tissues, or at sites of disease, among others.

Discovery Driven Approach

Previous work in the field has focused on identifying cell surface markers displayed by fetal cells. These studies are limited by the ability to examine only a few proteins at a time and must be based on pre-existing knowledge. They are also biased by assumptions made regarding the fetal cells. For example, a focus on CD45+ cells is based on the presumption that at least some of the fetal cells are lymphocytes. As such, only cells expressing that marker can be discerned; the phenotypic features of other cells remain undiscovered.

The unbiased nature of whole transcriptome studies removes many of these limitations. The presence of trophoblasts in the murine maternal lungs was unexpected and novel. This finding, if confirmed, will allow the use of mouse models to study the role of trophoblast deportation in diseases of pregnancy like recurrent spontaneous abortion and preeclampsia.

In silico Verification of Results

Accepted in silico gene expression validation techniques were applied to the results in Chapters Two and Three (Chuaqui et al., 2002). Strict statistical cutoffs were used to limit false positives and the Benjamini-Hochberg correction for multiple testing was applied where appropriate. We also compared our results with information available

in the literature. For example, other groups have reported fetal immune cells and MSCs in the maternal blood; these external findings corroborate our results. Finally, we used a multidimensional analysis to minimize the specific biases of each analysis type. The consistency within the different analysis types strengthens our conclusions.

Reproducibility

The gene expression studies of fetal cells in the maternal lung during syngeneic and allogeneic matings were performed nearly two years apart. Slight alterations in technique and the use of a different mouse strain did not change the key conclusions. This indicates consistency of the technique as well as underscores the veracity of our findings.

Limitations of The Study

Inherent Diversity Within Fetal Cell Population

The complexity of the microchimeric fetal cell population makes it equally interesting and difficult to study. Interpretation of our microarray data is complicated by this intrinsic diversity. We used numerous analysis methods in order to capture the heterogeneous cell types and molecular pathways. Now that the broad cell types have been identified, future experiments can use cell surface markers to characterize fetal cell subgroups and focus analyses within a more homogenous population.

An additional source of diversity is the gestational ages of the pups at the time of maternal euthanasia. In both of our array studies fetal cells were collected from females at the end of pregnancy over the course of three gestational days. This represents a considerable span of time in murine fetal development. We recognize that there may be differences in the fetal cell population over the course of gestation (Adams Waldorf et al.,

2010; Guthrie et al., 2010; Nelson, 2012) and future experiments should aim to characterize these differences.

META-ANALYSIS LIMITATIONS

Despite the fact that the principal component analyses were performed using similar datasets, the results did not entirely overlap in either the syngeneic or allogeneic mating studies. This is partially due to the way PCA is performed, and the reason why performing a similar analysis using two different datasets provides more information about reproducibility than using only one external dataset or combining all the data together. Another source of variability is that each GEO dataset only included two to three replicates. Moreover, the external datasets' use of whole organs that are made of a mixture of heterogeneous cell types may have led to variability between the two datasets. Lastly, the methods used by each group differ (compare references (Lattin et al., 2008) and (Thorrez et al., 2008)), further introducing discrepancies.

The presence of lung transcripts in several of the analyses could suggest contamination with maternal cells. However, our flow cytometry gates were established using a virgin female control and were drawn very conservatively. We also had a gate based on pulse width in order to eliminate any adherent cells. The placenta expresses surfactant proteins (Sati et al., 2010) and participates in gas exchange (Mess and Ferner, 2010), making it somewhat similar in function to the lung. Thus, transcripts currently annotated as specific for the adult mouse lung may actually be present in the placenta as well. Alternatively, these results may indicate differentiation of the fetal cells within the lung parenchyma. We have previously shown microchimeric fetal cells that have integrated within the alveolar septum (Johnson et al., 2012). Whether fetal cells truly differentiate in the lung and on what timeframe will need further investigation.

Annotation Bias within Analysis Tools

Extensive annotation of gene expression and function in murine (or human) fetal tissues is not available. Much of our analysis thus necessarily relies on gene expression patterns from adult normal and diseased tissues, particularly tumor samples. However, many genes considered as oncogenic in adults are expressed as part of normal fetal development. We used the Eurexpress Atlas to partially address this issue, although the atlas does not include any extraembryonic tissues, such as placenta. Additionally, tissues studied in this Atlas were only collected at one time point during embryonic life (Diez-Roux et al., 2011). Detailed annotation of the role of genes involved in fetal development is critical for the study of microchimerism and other fetal and obstetric conditions. Our collaborators are currently addressing this work in the Department of Computer Science, through the Developmental Functional Annotation at Tufts project (DFLAT) at http://dflat.cs.tufts.edu.

Quantitative PCR Validation of Microarray Results

A common concern of microarray analysis is the inherent false discovery rate. Many authors and manuscript reviewers request qPCR validation of genes of interest. However, the necessity and utility of qPCR validation is controversial and no clear guidelines exist (Rockett and Hellmann, 2004). In the work presented here we used strict statistical criteria in the analysis of our data to reduce the likelihood of false positives. The presence of the transcripts on all experimental replicates suggests a high degree of reproducibility and reduces the chance that the results are due to non-specific hybridization. Furthermore, because the main focus is on the broad pattern of gene

expression, such as those shown by principal component analysis, small differences in individual probes would have little impact on the overall results.

Small Sample Sizes

Although our sample sizes were small in the microarray studies, the results were highly consistent among arrays. A prior report investigating microarray result stability with increasing replicates found that a minimum of five replicates was needed to produce stable results. By eight to ten replicates near-maximal levels of stability were achieved (Pavlidis et al., 2003). In addition, the GFP+ fetal cell microarrays clustered together in all principal component analyses, further supporting the reproducibility and validity of our results.

Our postpartum kinetics study also used relatively small sample sizes (as few as three animals per time point). This especially limited the conclusions we could draw about the impact of litter size on microchimerism levels and persistence. As mentioned above, the use of delivered pups as the sole metric is not necessarily a true reflection of litter size throughout the pregnancy. In order to more completely address this question, sonographic assessment of the number of pups, combined with measurement of the number of fetal cells in maternal blood, would need to be performed repeatedly during gestation. This question may also be explored through human studies. Serial blood samples could be acquired from women pregnant with multiples and compared to singleton pregnancies. Paternal antigens inherited by the fetuses should be used to quantify fetal cells; the use of Y chromosome sequences would require all fetuses to be male and significantly limit study enrollment.

FUTURE WORK

As discussed in the introduction of this thesis, there are multiple factors that have been proposed to impact fetal cell microchimerism, including gestational age at delivery, time since parturition, organ location, and disease. Using the technique developed here, some of these factors could be considered in future studies. For example, cells could be collected at earlier gestational ages or in different maternal organs than the ones studied here. Work is currently ongoing to examine fetal cells in the livers of females in both allogeneic and syngeneic matings.

It is also important to identify how the fetal cell population changes in the postpartum female. Most of the diseases in which microchimerism is thought to play a role occur in the postpartum period. Our attempts to collect sufficient fetal cells from postpartum maternal organs were unsuccessful. It may be necessary to pool cells from multiple animals. Alternatively, postpartum injury experiments could take advantage of the fact that allogeneic matings produce more microchimerism than syngeneic matings. Future experiments should look to see whether this hold true in the postpartum period or whether fetal expression of non-shared MHC antigens facilitates a more rapid clearance.

Table 14: Added Evidence of the Stem Cell Properties of Microchimeric Fetal Cells

Evidence from our studies suggests that microchimeric fetal cells may be stem cells or have stem-like properties. HSCs = Hematopoietic stem cells; MSC = Mesenchymal stem cell; EPC = Endothelial progenitor cell. *Result only present in the syngeneic core transcriptome. **Result only present in the allogeneic core transcriptome.

	HSC	MSC	EPC
OUR STUDIES	Similarity on PCA to cells of the immune system including macrophages	Expression of genes upregulated in mesenchymal tissue including V*im and Ctnnb1*	Expression of genes important in angiogenesis including Epas1, *Tek*,* thrombomodulin*, and Cd36**
	Expression of B-cell specific genes including *Aicda** and immunoglobulins	Genes in fetal core transcriptome highly expressed in mesenchyme of day e14.5 mouse embryos	
	Inflammatory response as top biologic pathway	Similarity on PCA to bone, osteoblasts and adipose	
	Expression of Cxcr4**		
	mTOR pathway enriched in fetal cell core transcriptome		

SUMMARY OF KEY FINDINGS

- Low numbers of fetal cells can be flow-sorted from the maternal organs and reproducible gene expression information can be obtained from them.
- In syngeneic pregnancies, fetal cells in the maternal lung are primarily trophoblasts, mesenchymal stem cells, and cells of the immune system.
- Similar types of fetal cells are present in the maternal lung during allogeneic pregnancies, but the fetal cells appear to be less differentiated.
- We recommend that future mouse studies of fetal cell microchimerism should use allogeneic matings wherever possible, as this is closer to human reproduction.
- Fetal cell clearance in postpartum maternal organs is a two-stage process.
- Future murine injury experiments investigating the potential postpartum effects of fetal cells on maternal tissue repair should start at a minimum of 17-18 days after delivery to be sure that the initial clearance stage has been completed.

BUFFER RECIPES

FLOW CYTOMETRY BUFFER

In 500mL DPBS:

- 10g BSA (2%)
- 0.5g NaN_3 (0.1%)

HEPES BUFFER

In 500mL dH_2O:

- 4.38g NaCl (150mM)
- 0.186g KCl (5mM)
- 48mg $MgCl_2$ (1mM)
- 0.999g $CaCl_2$ (1.8mM)
- 5mL 1M HEPES (10mM)

Bring to pH 7.4 with NaOH

KREBS-RINGER BUFFER

In 500mL dH_2O:

- 4.5g NaCl (154mM)
- 0.21g KCl (5.6mM)
- 0.5g Glucose (5.5mM)
- 1.05g $NaHCO_3$ (25mM)
- 10.05mL 1M HEPES (20.1mM)

Bring to pH 7.4 with NaOH

Lysis Buffer

In 500mL dH_2O:

- 4.012g NH_4Cl (0.15M)
- 50mg $KHCO_3$ (1.0mM)
- 17mg Na_2-EDTA

PEB Buffer

In 500mL DPBS:

- 2.5g BSA
- 2mL 0.5M EDTA

LIST OF REFERENCES

Abumaree, M.H., Chamley, L.W., Badri, M., and El-Muzaini, M.F. (2012). Trophoblast debris modulates the expression of immune proteins in macrophages: a key to maternal tolerance of the fetal allograft? J Reprod Immunol 94, 131-141.

Adams Waldorf, K.M., Gammill, H.S., Lucas, J., Aydelotte, T.M., Leisenring, W.M., Lambert, N.C., and Nelson, J.L. (2010). Dynamic changes in fetal microchimerism in maternal peripheral blood mononuclear cells, CD4+ and CD8+ cells in normal pregnancy. Placenta 31, 589-594.

Adams, K.M., Lambert, N.C., Heimfeld, S., Tylee, T.S., Pang, J.M., Erickson, T.D., and Nelson, J.L. (2003). Male DNA in female donor apheresis and CD34-enriched products. Blood 102, 3845-3847.

Affymetrix. (2001). Affymetrix technical note: new statistical algorithms for monitoring gene expression on GeneChip probe arrays. (Santa Clara, CA: Affymetrix).
Albrecht, E.D., and Pepe, G.J. (1990). Placental steroid hormone biosynthesis in primate pregnancy. Endocr Rev 11, 124-150.

Al-Mufti, R., Hambley, H., Albaiges, G., Lees, C., and Nicolaides, K. (2000). Increased fetal erythroblasts in women who subsequently develop pre-eclampsia. Hum Reprod 15, 1624-1628.

Al-Mufti, R., Hambley, H., Farzaneh, F., and Nicolaides, K.H. (2003). Distribution of fetal erythroblasts in maternal blood after chorionic villous sampling. BJOG 110, 33-38.

Aluvihare, V.R., Kallikourdis, M., and Betz, A.G. (2004). Regulatory T cells mediate maternal tolerance to the fetus. Nat Immunol 5, 266-271.

Aractingi, S., Sibilia, J., Meignin, V., Launay, D., Hachulla, E., Le Danff, C., Janin, A., and Mariette, X. (2002). Presence of microchimerism in labial salivary glands in systemic sclerosis but not in Sjogren's syndrome. Arthritis Rheum 46, 1039-1043.

Araki, K., Ellebedy, A.H., and Ahmed, R. (2011). TOR in the immune system. Curr Opin Cell Biol 23, 707-715.

Ariga, H., Ohto, H., Busch, M.P., Imamura, S., Watson, R., Reed, W., and Lee, T.H. (2001). Kinetics of fetal cellular and cell-free DNA in the maternal circulation during and after pregnancy: implications for noninvasive prenatal diagnosis. Transfusion 41, 1524-1530.

Artlett, C.M., Cox, L.A., Ramos, R.C., Dennis, T.N., Fortunato, R.A., Hummers, L.K., Jimenez, S.A., and Smith, J.B. (2002). Increased microchimeric CD4(+) T lymphocytes in peripheral blood from women with systemic sclerosis. Clin Immunol 103, 303-308.

Artlett, C.M. (2005). Pathophysiology of fetal microchimeric cells. Clin Chim Acta 360, 1-8.

Askelund, K.J., and Chamley, L.W. (2011). Trophoblast deportation part I: Review of the evidence demonstrating trophoblast shedding and deportation during human pregnancy. Placenta 32, 716-723.

Attwood, H.D., and Park, W.W. (1961). Embolism to the lungs by trophoblast. J Obstet Gynaecol Br Commonw 68, 611-617.

Baker, J., Liu, J.P., Robertson, E.J., and Efstratiadis, A. (1993). Role of insulin-like growth factors in embryonic and postnatal growth. Cell 75, 73-82.

Bayes-Genis, A., Bellosillo, B., de La Calle, O., Salido, M., Roura, S., Ristol, F.S., Soler, C., Martinez, M., Espinet, B., Serrano, S., de Luna, A.B., and Cinca, J. (2005). Identification of male cardiomyocytes of extracardiac origin in the hearts of women with male progeny: male fetal cell microchimerism of the heart. J Heart Lung Transplant 24, 2179-2183.

Beaman, K.D., Ntrivalas, E., Mallers, T.M., Jaiswal, M.K., Kwak-Kim, J., and Gilman-Sachs, A. (2012). Immune etiology of recurrent pregnancy loss and its diagnosis. Am J Reprod Immunol 67, 319-325.

Beer, A.E., Semprini, A.E., Zhu, X.Y., and Quebbeman, J.F. (1985). Pregnancy outcome in human couples with recurrent spontaneous abortions: HLA antigen profiles; HLA antigensharing; female serum MLR blocking factors; and paternal leukocyte immunization. Exp Clin Immunogenet 2, 137-153.

Bianchi, D.W. (2004). Fetomaternal cell traffic, pregnancy-associated progenitor cells, and autoimmune disease. Best Pract Res Clin Obstet Gynaecol 18, 959-975.

Bianchi, D.W., Zickwolf, G.K., Weil, G.J., Sylvester, S., and DeMaria, M.A. (1996). Male fetal progenitor cells persist in maternal blood for as long as 27 years postpartum. Proc Natl Acad Sci USA 93, 705-708.

Bianchi, D.W. (2012). From prenatal genomic diagnosis to fetal personalized medicine: progress and challenges. Nat Med 18, 1041-1051.

Bianchi, D.W., and Fisk, N.M. (2007). Fetomaternal cell trafficking and the stem cell debate: gender matters. JAMA 297, 1489-1491.

Bianchi, D.W., Platt, L.D., Goldberg, J.D., Abuhamad, A.Z., Sehnert, A.J., Rava, R.P., and MatErnal BLood IS Source Accuratel. (2012). Genome-wide fetal aneuploidy detection by maternal plasma DNA sequencing. Obstet Gynecol 119, 890-901.

Bianchi, D. (2000). Fetal cells in the mother: from genetic diagnosis to diseases associated with fetal cell microchimerism. Eur J Obstet Gynecol Reprod Biol 92, 103-108.

Bianchi, D., Farina, A., Weber, W., Delli-Bovi, L., DeRiso, M., Williams, J., and Klinger, K. (2001). Significant fetal-maternal hemorrhage after termination of pregnancy: implications for development of fetal cell microchimerism. Am J Obstet Gynecol 184, 703-706.

Bianchi, D., Williams, J., Sullivan, L., Hanson, F., Klinger, K., and Shuber, A. (1997). PCR quantitation of fetal cells in maternal blood in normal and aneuploid pregnancies. Am J Hum Genet 61, 822-829.

Bonney, E.A., and Matzinger, P. (1997). The maternal immune system's interaction with circulating fetal cells. J Immunol 158, 40-47.

Bou-Gharios, G., Amin, F., Hill, P., Nakamura, H., Maxwell, P., and Fisk, N.M. (2011). Microchimeric fetal cells are recruited to maternal kidney following injury and activate collagen type I transcription. Cells Tissues Organs 193, 379-392.

Bour, H., Peyron, E., Gaucherand, M., Garrigue, J., Desvignes, C., Kaiserlian, D., Revillard, J., and Nicolas, J. (1995). Major histocompatibility complex class I-restricted CD8+ T cells and class II-restricted CD4+ T cells, respectively, mediate and regulate contact sensitivity to dinitrofluorobenzene. Eur J Immunol 25, 3006-3010.

Brody, A.R., Salazar, K.D., and Lankford, S.M. (2010). Mesenchymal stem cells modulate lung injury. Proc Am Thorac Soc 7, 130-133.

Bromberg, Y.M., Salzberger, M., and Abrahamov, A. (1956). Transplacental transmission of fetal erythrocytes with demonstration of fetal hemoglobin in maternal circulation. Obstet Gynecol 7, 672-674.

Burton, G.J., and Jones, C.J.P. (2009). Syncytial knots, sprouts, apoptosis, and trophoblast deportation from the human placenta. Taiwan J Obstet Gynecol 48, 28-37.

Campbell, D., MacGillivray, I., and Carr-Hill, R. (1985). Pre-eclampsia in second pregnancy. Br J Obstet Gynaecol 92, 131-140.

Cha, D., Khosrotehrani, K., Kim, Y., Stroh, H., Bianchi, D., and Johnson, K. (2003). Cervical cancer and microchimerism. Obstet Gynecol 102, 774-781.

Chamberlain, G., Fox, J., Ashton, B., and Middleton, J. (2007). Concise review: Mesenchymal stem cells: their phenotype, differentiation capacity, immunological features, and potential for homing. Stem Cells 25, 2739-2749.

Chamley, L.W., Chen, Q., Ding, J., Stone, P.R., and Abumaree, M. (2011). Trophoblast deportation: just a waste disposal system or antigen sharing? J Reprod Immunol 88, 99-105.

Chan, W.F.N., Gurnot, C., Montine, T.J., Sonnen, J.A., Guthrie, K.A., and Nelson, J.L. (2012). Male microchimerism in the human female brain. PLoS One 7, e45592.

Chandra, A., Martinez, G.M., Mosher, W.D., Abma, J.C., and Jones, J. (2005). Fertility, family planning, and reproductive health of U.S. women: data from the 2002 National Survey of Family Growth. Vital Health Stat 23 1-160.

Chen, S., Liu, Y., and Sytwu, H. (2012). Immunologic regulation in pregnancy: from mechanism to therapeutic strategy for immunomodulation. Clin Dev Immunol 2012, 258391.

Cheng, C., Lian, W., Hsiao, F.S., Liu, I., Lin, S., Lee, Y., Chang, C., Xiao, G., Huang, H., Cheng, C., Cheng, W.T., and Wu, S. (2012). Isolation and characterization of novel murine epiphysis derived mesenchymal stem cells. PLoS One 7, e36085.

Chiu, R.W.K., Akolekar, R., Zheng, Y.W.L., Leung, T.Y., Sun, H., Chan, K.C.A., Lun, F.M.F., Go, A.T.J.I., Lau, E.T., To, W.W.K., et al. (2011). Non-invasive prenatal assessment of trisomy 21 by multiplexed maternal plasma DNA sequencing: large scale validity study. Br Med J 342, c7401.

Chiu, R.W.K., and Lo, Y.M.D. (2013). Clinical applications of maternal plasma fetal DNA analysis: translating the fruits of 15 years of research. Clin Chem Lab Med 51, 197-204.

Chua, S., Wilkins, T., Sargent, I., and Redman, C. (1991). Trophoblast deportation in preeclamptic pregnancy. Br J Obstet Gynaecol 98, 973-979.

Chuaqui, R., Bonner, R., Best, C., Gillespie, J., Flaig, M., Hewitt, S., Phillips, J., Krizman, D., Tangrea, M., Ahram, M., et al. (2002). Post-analysis follow-up and validation of microarray experiments. Nat. Genet. 32, 509-514.

Chung, J., Grammer, T., Lemon, K., Kazlauskas, A., and Blenis, J. (1994). PDGF- and insulin-dependent pp70S6k activation mediated by phosphatidylinositol-3-OH kinase. Nature 370, 71-75.

Ciaranfi, A., Curchod, A., and Odartchenko, N. (1977). Post partum survival of fetal cells in maternal blood. Schweiz Med Wochenschr 107, 134-138.

Cirello, V., Recalcati, M.P., Muzza, M., Rossi, S., Perrino, M., Vicentini, L., Beck-Peccoz, P., Finelli, P., and Fugazzola, L. (2008). Fetal cell microchimerism in papillary thyroid cancer: a possible role in tumor damage and tissue repair. Cancer Res 68, 8482-8488.

Clayton, E., Feldhaus, W., and Robertson, J. (1962). Antepartum and postpartum detection of fetal erythrocytes in maternal circulation. Obstet Gynecol 20, 608-610.

Cohen, F., Evans, M., Gustafson, D., and Zuelzer, W. (1964). Mechanisms of isoimmunization .I. Transplacental passage of fetal erythrocytes in homospecific pregnancies. Blood 23, 621-646.

Dawe, G.S., Tan, X.W., and Xiao, Z. (2007). Cell migration from baby to mother. Cell Adh Migr 1, 19-27.

Dezso, Z., Nikolsky, Y., Sviridov, E., Shi, W., Serebriyskaya, T., Dosymbekov, D., Bugrim, A., Rakhmatulin, E., Brennan, R.J., Guryanov, A., et al. (2008). A comprehensive functional analysis of tissue specificity of human gene expression. BMC Biol 6, 49.

Diez-Roux, G., Banfi, S., Sultan, M., Geffers, L., Anand, S., Rozado, D., Magen, A., Canidio, E., Pagani, M., Peluso, I., et al. (2011). A high-resolution anatomical atlas of the transcriptome in the mouse embryo. PLoS Biol 9, e1000582.

Dominici, M., Le Blanc, K., Mueller, I., Slaper-Cortenbach, I., Marini, F.C., Krause, D.S., Deans, R.J., Keating, A., Prockop, D.J., and Horwitz, E.M. (2006). Minimal criteria for

defining multipotent mesenchymal stromal cells. The International Society for Cellular Therapy position statement. Cytotherapy 8, 315-317.

Dubernard, G., Aractingi, S., Oster, M., Rouzier, R., Mathieu, M., Uzan, S., and Khosrotehrani, K. (2008). Breast cancer stroma frequently recruits fetal derived cells during pregnancy. Breast Cancer Res 10, R14.

Dubernard, G., Oster, M., Chareyre, F., Antoine, M., Rouzier, R., Uzan, S., Aractingi, S., and Khosrotehrani, K. (2009). Increased fetal cell microchimerism in high grade breast carcinomas occurring during pregnancy. Int J Cancer 124, 1054-1059.

Dumont, D., Fong, G., Puri, M., Gradwohl, G., Alitalo, K., and Breitman, M. (1995). Vascularization of the mouse embryo: a study of flk-1, tek, tie,
and vascular endothelial growth factor expression during development. Dev Dyn 203, 80-92.

Dutta, P., and Burlingham, W.J. (2011). Microchimerism: tolerance vs. sensitization. Curr Opin Organ Transplant 16, 359-365.

Dutta, P., Dart, M.L., Schumacher, S.M., and Burlingham, W.J. (2010). Fetal microchimerism persists at high levels in c-kit+ stem cells in sensitized mothers. Chimerism 1, 51-55.

Dye, J.F., Jablenska, R., Donnelly, J.L., Lawrence, L., Leach, L., Clark, P., and Firth, J.A. (2001). Phenotype of the endothelium in the human term placenta. Placenta 22, 32-43.

Evans, P.C., Lambert, N., Maloney, S., Furst, D.E., Moore, J.M., and Nelson, J.L. (1999). Long-term fetal microchimerism in peripheral blood mononuclear cell subsets in healthy women and women with scleroderma. Blood 93, 2033-2037.

Flowers, M.E.D., Pepe, M.S., Longton, G., Doney, K.C., Monroe, D., Witherspoon, R.P., Sullivan, K.M., and Storb, R. (1990). Previous donor pregnancy as a risk factor for acute graft-versus-host disease in patients with aplastic anemia treated by allogeneic marrow transplantation. Br J Haematol 74, 492-496.

Fugazzola, L., Cirello, V., and Beck-Peccoz, P. (2011). Fetal microchimerism as an explanation of disease. Nat Rev Endocrinol 7, 89-97.

Fugazzola, L., Cirello, V., and Beck-Peccoz, P. (2010). Fetal cell microchimerism in human cancers. Cancer Lett 287, 136-141.

Fujiki, Y., Johnson, K.L., Peter, I., Tighiouart, H., and Bianchi, D.W. (2009). Fetal cells in the pregnant mouse are diverse and express a variety of progenitor and differentiated cell markers. Biol Reprod 81, 26-32.

Fujiki, Y., Johnson, K.L., Tighiouart, H., Peter, I., and Bianchi, D.W. (2008a). Fetomaternal trafficking in the mouse increases as delivery approaches and is highest in the maternal lung. Biol Reprod 79, 841-848.

Fujiki, Y., Tao, K., Bianchi, D.W., Giel-Moloney, M., Leiter, A.B., and Johnson, K.L. (2008b). Quantification of green fluorescent protein by in vivo imaging, PCR, and flow cytometry: comparison of transgenic strains and relevance for fetal cell microchimerism. Cytometry A 73A, 111-118.

Gadi, V.K. (2009). Fetal microchimerism and cancer. Cancer Lett 276, 8-13.

Gadi, V.K., Malone, K.E., Guthrie, K.A., Porter, P.L., and Nelson, J.L. (2008). Case-control study of fetal microchimerism and breast cancer. PLoS One 3, e1706.

Gadi, V.K., and Nelson, J.L. (2007). Fetal microchimerism in women with breast cancer. Cancer Res 67, 9035-9038.

Gammill, H.S., Guthrie, K.A., Aydelotte, T.M., Waldorf, K.M.A., and Nelson, J.L. (2010). Effect of parity on fetal and maternal microchimerism: interaction of grafts within a host? Blood 116, 2706-2712.

Georgiades, P., Ferguson-Smith, A., and Burton, G. (2002). Comparative developmental anatomy of the murine and human definitive placentae. Placenta 23, 3-19.

Gimpl, G., and Fahrenholz, F. (2001). The oxytocin receptor system: structure, function, and regulation. Physiol Rev 81, 629-683.

Goodell, M.A., Brose, K., Paradis, G., Conner, A.S., and Mulligan, R.C. (1996). Isolation and functional properties of murine hematopoietic stem cells that are replicating in vivo. J Exp Med 183, 1797-1806.

Gratwohl, A., Hermans, J., Niederwieser, D., van Biezen, A., van Houwelingen, H.C., Apperley, J., and Chronic Leukemia Working Party of the European Group for Blood and Marrow Transplantation EBMT. (2001). Female donors influence transplant-related mortality and relapse incidence in male recipients of sibling blood and marrow transplants. Hematol J 2, 363-370.

Griswold, M.D., and Oatley, J.M. (2013). Concise Review: defining characteristics of mammalian spermatogenic stem cells. Stem Cells 31, 8-11.

Grove, J.E., Lutzko, C., Priller, J., Henegariu, O., Theise, N.D., Kohn, D.B., and Krause, D.S. (2002). Marrow-derived cells as vehicles for delivery of gene therapy to pulmonary epithelium. Am J Respir Cell Mol Biol 27, 645-651.

Guetta, E., Gordon, D., Simchen, M.J., Goldman, B., and Barkai, G. (2003). Hematopoietic progenitor cells as targets for non-invasive prenatal diagnosis: detection of fetal CD34+cells and assessment of post-delivery persistence in the maternal circulation. Blood Cells Mol Dis 30, 13-21.

Guillot, P.V., Gotherstrom, C., Chan, J., Kurata, H., and Fisk, N.M. (2007). Human first-trimester fetal MSC express pluripotency markers and grow faster and have longer telomeres than adult MSC. Stem Cells 25, 646-654.

Guillot, P.V., O'Donoghue, K., Kurata, H., and Fisk, N.M. (2006). Fetal stem cells: betwixt and between. Semin Reprod Med 24, 340-347.

Gussoni, E., Soneoka, Y., Strickland, C.D., Buzney, E.A., Khan, M.K., Flint, A.F., Kunkel, L.M., and Mulligan, R.C. (1999). Dystrophin expression in the *mdx* mouse restored by stem cell transplantation. Nature 401, 390-394.

Guthrie, K.A., Dugowson, C.E., Voigt, L.F., Koepsell, T.D., and Nelson, J.L. (2010). Does pregnancy provide vaccine-like protection against rheumatoid arthritis? Arthritis Rheum 62, 1842-1848.

Herzenberg, L.A., Bianchi, D.W., Schroder, J., Cann, H.M., and Iverson, G.M. (1979). Fetal cells in the blood of pregnant women: detection and enrichment by fluorescence-activated cell sorting. Proc Natl Acad Sci USA 76, 1453-1455.

Holzgreve, W., Ghezzi, F., Di Naro, E., Ganshirt, D., Maymon, E., and Hahn, S. (1998). Disturbed feto-maternal cell traffic in preeclampsia. Obstet Gynecol 91, 669-672.

Hui, L., and Bianchi, D.W. (2013). Recent advances in the prenatal interrogation of the human fetal genome. Trends Genet 29, 84-91.

Hui, L., Slonim, D.K., Wick, H.C., Johnson, K.L., and Bianchi, D.W. (2012). The amniotic fluid transcriptome: a source of novel information about human fetal development. Obstet Gynecol 119, 111-118.

Hunkapiller, N.M., Gasperowicz, M., Kapidzic, M., Plaks, V., Maltepe, E., Kitajewski, J., Cross, J.C., and Fisher, S.J. (2011). A role for Notch signaling in trophoblast endovascular invasion and in the pathogenesis of pre-eclampsia. Development 138, 2987-2998.

Huu, S.N., Dubernard, G., Aractingi, S., and Khosrotehrani, K. (2006). Feto-maternal cell trafficking: a transfer of pregnancy associated progenitor cells. Stem Cell Rev 2, 111-116.

Huu, S.N., Oster, M., Avril, M., Boitier, F., Mortier, L., Richard, M., Kerob, D., Maubec, E., Souteyrand, P., Moguelet, P., Khosrotehrani, K., and Aractingi, S. (2009). Fetal microchimeric cells participate in tumour angiogenesis in melanomas occurring during pregnancy. Am J Pathol 174, 630-637.

Huu, S.N., Oster, M., Uzan, S., Chareyre, F., Aractingi, S., and Khosrotehrani, K. (2007). Maternal neoangiogenesis during pregnancy partly derives from fetal endothelial progenitor cells. Proc Natl Acad Sci USA 104, 1871-1876.

Ichinohe, T., Teshima, T., Matsuoka, K., Maruya, E., and Saji, H. (2005). Fetal-maternal microchimerism: impact on hematopoietic stem cell transplantation. Curr Opin Immunol 17, 546-552.

Ichinohe, T., Uchiyama, T., Shimazaki, C., Matsuo, K., Tamaki, S., Hino, M., Watanabe, A., Hamaguchi, M., Adachi, S., Gondo, H., et al. (2004). Feasibility of HLA-haploidentical hematopoletic stem cell transplantation between noninherited maternal antigen (NIMA)-mismatched family members linked with long-term fetomatemal microchimerism. Blood 104, 3821-3828.

Imaizumi, M., Pritsker, A., Unger, P., and Davies, T.F. (2002). Intrathyroidal fetal microchimerism in pregnancy and postpartum. Endocrinology 143, 247-253.

Iniguez, G., Gonzalez, C.A., Argandona, F., Kakarieka, E., Johnson, M.C., and Cassorla, F. (2010). Expression and protein content of IGF-I and IGF-I receptor in placentas from small, adequate and large for gestational age newborns. Horm Res Paediatr 73, 320-327.

Ishizawa, K., Kubo, H., Yamada, M., Kobayashi, S., Numasaki, M., Ueda, S., Suzuki, T., and Sasaki, H. (2004). Bone marrow-derived cells contribute to lung regeneration after elastase-induced pulmonary emphysema. FEBS Lett. 556, 249-252.

Jarvenpaa, J., Vuoristo, J.T., Savolainen, E., Ukkola, O., Vaskivuo, T., and Ryynanen, M. (2007). Altered expression of angiogenesis-related placental genes in pre-eclampsia associated with intrauterine growth restriction. Gynecol Endocrinol 23, 351-355.

Jimenez, D., Leapley, A., Lee, C., Ultsch, M., and Tarantal, A. (2005). Fetal CD34(+) cells in the maternal circulation and long-term microchimerism in rhesus monkeys (Macaca mulatta). Transplantation 79, 142-146.

Jimenez, D., and Tarantal, A. (2003). Quantitative analysis of male fetal DNA in maternal serum of gravid rhesus monkeys (Macaca mulatta). Pediatr Res 53, 18-23.

Johansen, M., Redman, C.W.G., Wilkins, T., and Sargent, I.L. (1999). Trophoblast deportation in human pregnancy--its relevance for pre-eclampsia. Placenta 20, 531-539.

Johnson, K.L., and Bianchi, D.W. (2004). Fetal cells in maternal tissue following pregnancy: what are the consequences? Hum Reprod Update 10, 497-502.

Johnson, K.L., Nelson, J.L., Furst, D.E., McSweeney, P.A., Roberts, D.J., Zhen, D.K., and Bianchi, D.W. (2001). Fetal cell microchimerism in tissue from multiple sites in women with systemic sclerosis. Arthritis Rheum 44, 1848-1854.

Johnson, K.L., Samura, O., Nelson, J.L., McDonnell, W.M., and Bianchi, D.W. (2002). Significant fetal cell microchimerism in a nontransfused woman with hepatitis C: evidence of long-term survival and expansion. Hepatology 36, 1295-1297.

Johnson, K.L., Stroh, H., Tadesse, S., Norwitz, E.R., Richey, L., Kallenbach, L.R., and Bianchi, D.W. (2012). Fetal cells in the murine maternal lung have well-defined characteristics and are preferentially located in alveolar septum. Stem Cells Dev 21, 158-165.

Johnson, K.L., Tao, K., Stroh, H., Kallenbach, L., Peter, I., Richey, L., Rust, D., and Bianchi, D.W. (2010). Increased fetal cell trafficking in murine lung following complete pregnancy loss from exposure to lipopolysaccharide. Fertil Steril 93, 1718-1721.

Kallenbach, L.R., Bianchi, D.W., Peter, I., Stroh, H., and Johnson, K.L. (2011a). Maternal background strain influences fetal-maternal trafficking more than maternal immune competence in mice. J Reprod Immunol 90, 188-194.

Kallenbach, L.R., Johnson, K.L., and Bianchi, D.W. (2011b). Fetal cell microchimerism and cancer: a nexus of reproduction, immunology, and tumor biology. Cancer Res 71, 8-12.

Kara, R.J., Bolli, P., Karakikes, I., Matsunaga, I., Tripodi, J., Tanweer, O., Altman, P., Shachter, N.S., Nakano, A., Najfeld, V., and Chaudhry, H.W. (2012). Fetal cells traffic to injured maternal myocardium and undergo cardiac differentiation. Circ Res 110, 82-93.

Khakoo, A.Y., and Finkel, T. (2005). Endothelial progenitor cells. Annu Rev Med 56, 79-101.

Khosrotehrani, K., and Bianchi, D.W. (2005). Multi-lineage potential of fetal cells in maternal tissue: a legacy in reverse. J Cell Sci 118, 1559-1563.

Khosrotehrani, K., Johnson, K.L., Cha, D.H., Salomon, R.N., and Bianchi, D.W. (2004). Transfer of fetal cells with multilineage potential to maternal tissue. JAMA 292, 75-80.

Khosrotehrani, K., Johnson, K.L., Guegan, S., Stroh, H., and Bianchi, D.W. (2005). Natural history of fetal cell microchimerism during and following murine pregnancy. J Reprod Immunol 66, 1-12.

Khosrotehrani, K., Reyes, R.R., Johnson, K.L., Freeman, R.B., Salomon, R.N., Peter, I., Stroh, H., Guegan, S., and Bianchi, D.W. (2007). Fetal cells participate over time in the response to specific types of murine maternal hepatic injury. Hum Reprod 22, 654-661.

Khosrotehrani, K., and Aractingi, S. (2009). Fetal cell microchimerism in cancer: a meaningful event? Future Oncol 5, 1441-1448.

Khosrotehrani, K., Leduc, M., Bachy, V., Huu, S.N., Oster, M., Abbas, A., Uzan, S., and Aractingi, S. (2008). Pregnancy allows the transfer and differentiation of fetal lymphoid progenitors into functional T and B cells in mothers. J Immunol 180, 889-897.

Kitada, M. (2012). Mesenchymal cell populations: development of the induction systems for Schwann cells and neuronal cells and finding the unique stem cell population. Anat Sci Int 87, 24-44.

Koelman, C., Coumans, A., Nijman, H., Doxiadis, I., Dekker, G., and Claas, F. (2000). Correlation between oral sex and a low incidence of preeclampsia: a role for soluble HLA in seminal fluid? J Reprod Immunol 46, 155-166.

Kolialexi, A., Tsangaris, G.T., Antsaklis, A., and Mavrou, A. (2004). Rapid clearance of fetal cells from maternal circulation after delivery. Ann N Y Acad Sci 1022, 113-118.

Koller, B.H., Marrack, P., Kappler, J.W., and Smithies, O. (1990). Normal development of mice deficient in beta 2M, MHC Class I proteins, and CD8+ T cells. Science 248, 1227-1230.

Kollman, C., Howe, C.W.S., Anasetti, C., Antin, J.H., Davies, S.M., Filipovich, A.H., Hegland, J., Kamani, N., Kernan, N.A., King, R., et al. (2001). Donor characteristics as risk factors in recipients after transplantation of bone marrow from unrelated donors: the effect of donor age. Blood 98, 2043-2051.

Koopmans, M., Hovinga, I.C.L.K., Baelde, H.J., Harvey, M.S., de Heer, E., Bruijn, J.A., and Bajema, I.A. (2008). Chimerism occurs in thyroid, lung, skin and lymph nodes of women with sons. J Reprod Immunol 78, 68-75.

Lambert, N.C., and Reed, A.M. (2006). Maternal-fetal aspects of autoimmune disease. In Handbook of Systemic Autoimmune Diseases. Volume 4: Reproductive and Hormonal Aspects of Systemic Autoimmune Diseases, Lockshin, M. Branch,DW ed., (Amsterdam: Elsevier Science) pp. 11-28.

Lapaire, O., Holzgreve, W., Oosterwijk, J.C., Brinkhaus, R., and Bianchi, D.W. (2007). Georg Schmorl on trophoblasts in the maternal circulation. Placenta 28, 1-5.

Lattin, J.E., Schroder, K., Su, A.I., Walker, J.R., Zhang, J., Wiltshire, T., Saijo, K., Glass, C.K., Hume, D.A., Kellie, S., and Sweet, M.J. (2008). Expression analysis of G Protein-Coupled Receptors in mouse macrophages. Immunome Res 4, 5.

Leduc, M., Guegan, S., Roy, E., Oster, M., Aractingi, S., and Khosrotehrani, K. (2010). Limited functional capacity of microchimeric fetal hematopoietic progenitors acquired by mothers during pregnancy. Exp Hematol 38, 852-853.

Lee, E.S.M., Bou-Gharios, G., Seppanen, E., Khosrotehrani, K., and Fisk, N.M. (2010). Fetal stem cell microchimerism: natural-born healers or killers? Mol Hum Reprod 16, 869-878.

Lepez, T., Vandewoestyne, M., Hussain, S., Van Nieuwerburgh, F., Poppe, K., Velkeniers, B., Kaufman, J., and Deforce, D. (2011). Fetal microchimeric cells in blood of women with an autoimmune thyroid disease. PLoS One 6, e29646.

Liegeois, A., Escourrou, J., Ouvre, E., and Charreire, J. (1977). Microchimerism: stable state of low-ratio proliferation of allogeneic bonemarrow. Transplant Proc 9, 273-276.

Liegeois, A., Gaillard, M.C., Ouvre, E., and Lewin, D. (1981). Microchimerism in pregnant mice. Transplant Proc 13, 1250-1252.

Lissauer, D., Piper, K.P., Moss, P.A.H., and Kilby, M.D. (2007). Persistence of fetal cells in the mother: friend or foe? BJOG 114, 1321-1325.

Lo, Y.M.D., Chan, K.C.A., Sun, H., Chen, E.Z., Jiang, P., Lun, F.M.F., Zheng, Y.W., Leung, T.Y., Lau, T.K., Cantor, C.R., and Chiu, R.W.K. (2010). Maternal plasma DNA sequencing reveals the genome-wide genetic and mutational profile of the fetus. Sci Transl Med 2, 61ra91.

Lo, Y., Leung, T., Tein, M., Sargent, I., Zhang, J., Lau, T., Haines, C., and Redman, C. (1999). Quantitative abnormalities of fetal DNA in maternal serum in preeclampsia. Clin Chem 45, 184-188.

Loubiere, L.S., Lambert, N.C., Flinn, L.J., Erickson, T.D., Yan, Z., Guthrie, K.A., Vickers, K.T., and Nelson, J.L. (2006). Maternal microchimerism in healthy adults in lymphocytes, monocyte/macrophages and NK cells. Lab Invest 86, 1185-1192.

Lubinski, J., Vrdoljak, V., Beaman, K., Kwak, J., Beer, A., and Gilman-Sachs, A. (1993). Characterization of antibodies induced by paternal lymphocyte immunization in couples with recurrent spontaneous abortion. J Reprod Immunol 24, 81-96.

Lv, F., Lu, M., Cheung, K.M.C., Leung, V.Y.L., and Zhou, G. (2012). Intrinsic properties of mesemchymal stem cells from human bone marrow, umbilical cord and umbilical cord blood comparing the different sources of MSC. Curr Stem Cell Res Ther 7, 389-399.

Malassine, A., Frendo, J., and Evain-Brion, D. (2003). A comparison of placental development and endocrine functions between the human and mouse model. Hum Reprod Update 9, 531-539.

Marder, W. and Somers, E.C. (2014) Is pregnancy a risk factor for rheumatic autoimmune diseases? Curr Opin Rheumatol 26, 321-328.

Massy, W. (1965). Principal components regression in exploratory statistical research. J Am Stat Assoc 60, 234-256.

Matthay, M.A., Thompson, B.T., Read, E.J., McKenna, D.H.,Jr., Liu, K.D., Calfee, C.S., and Lee, J.W. (2010). Therapeutic potential of mesenchymal stem cells for severe acute lung injury. Chest 138, 965-972.

Mazzone, A., and Ricevuti, G. (1995). Leukocyte CD11/CD18 integrins: biological and clinical relevance. Haematologica 80, 161-175.

McNallan, K.T., Aponte, C., el-Azhary, R., Mason, T., Nelson, A.M., Paat, J.J., Crowson, C.S., and Reed, A.M. (2007). Immunophenotyping of chimeric cells in localized scleroderma. Rheumatology 46, 398-402.

Medawar, P.B. (1953). Some immunological and endocrinological problems raised by the evolution of viviparity in vertebrates. Symp Soc Exp Biol 7, 320-338.

Meleti, D., Caetano, A.C.R., Boute, T., de Oliveira, L.G., Araujo, E., Jr., Nardozza, L.M.M., and Moron, A.F. (2012). Assessment of fetomaternal hemorrhage by Kleihauer-Betke test, flow cytometry and alpha-fetoprotein after invasive obstetric procedures. Clin Exp Obstet Gynecol 39, 303-306.

Mess, A.M., and Ferner, K.J. (2010). Evolution and development of gas exchange structures in Mammalia: the placenta and the lung. Respir Physiol Neurobiol 173, S74-S82.

Michaelsson, J., Mold, J.E., McCune, J.M., and Nixon, D.F. (2006). Regulation of T cell responses in the developing human fetus. J Immunol 176, 5741-5748.

Mikhail, M.A., M'Hamdi, H., Welsh, J., Levicar, N., Marley, S.B., Nicholls, J.P., Habib, N.A., Louis, L.S., Fisk, N.M., and Gordon, M.Y. (2008). High frequency of fetal cells within a primitive stem cell population in maternal blood. Hum Reprod 23, 928-933.

Mold, J.E., Michaelsson, J., Burt, T.D., Muench, M.O., Beckerman, K.P., Busch, M.P., Lee, T., Nixon, D.F., and McCune, J.M. (2008). Maternal alloantigens promote the development of tolerogenic fetal regulatory T cells in utero. Science 322, 1562-1565.

Morrison, S.J., and Spradling, A.C. (2008). Stem cells and niches: mechanisms that promote stem cell maintenance throughout life. Cell 132, 598-611.

Nassar, D., Droitcourt, C., Mathieu-d'Argent, E., Kim, M.J., Khosrotehrani, K., and Aractingi, S. (2012). Fetal progenitor cells naturally transferred through pregnancy participate in inflammation and angiogenesis during wound healing. FASEB J 26, 149-157.

Nelson, J.L. (2001). Microchimerism: expanding new horizon in human health or incidental remnant of pregnancy? Lancet 358, 2011-2012.

Nelson, J.L. (1996). Maternal-fetal immunology and autoimmune disease: is some autoimmune disease auto-alloimmune or allo-autoimmune? Arthritis Rheum 39, 191-194.

Nelson, J.L. (2012). The otherness of self: microchimerism in health and disease. Trends Immunol 33, 421-427.

Nelson, J.L. (2008). Your cells are my cells. Sci Am 298, 64-71.

Nelson, J. (2003). Microchimerism in human health and disease. Autoimmunity 36, 5-9.

Nelson, J., Furst, D., Maloney, S., Gooley, T., Evans, P., Smith, A., Bean, M., Ober, C., and Bianchi, D. (1998). Microchimerism and HLA-compatible relationships of pregnancy in scleroderma. Lancet 351, 559-562.

Ngo, S.T., Steyn, F.J., and McCombe, P.A. (2014). Gender differences in autoimmune disease. Front Neuroendocrinol 35(3), 347-369.

Nijagal, A., Wegorzewska, M., Jarvis, E., Le, T., Tang, Q., and MacKenzie, T.C. (2011). Maternal T cells limit engraftment after in utero hematopoietic cell transplantation in mice. J Clin Invest 121, 582-592.

Nolen-Walston, R.D., Kim, C.F., Mazan, M.R., Ingenito, E.P., Gruntman, A.M., Tsai, L., Boston, R., Woolfenden, A.E., Jacks, T., and Hoffman, A.M. (2008). Cellular kinetics and modeling of bronchioalveolar stem cell response during lung regeneration. Am J Physiol Lung Cell Mol Physiol 294, L1158-L1165.

O'Donoghue, K., Chan, J., de la Fuente, J., Kennea, N., Sandison, A., Anderson, J.R., Roberts, I.A.G., and Fisk, N.M. (2004). Microchimerism in female bone marrow and bone decades after fetal mesenchymal stem-cell trafficking in pregnancy. Lancet 364, 179-182.

O'Donoghue, K., Choolani, M., Chan, J., de la Fuente, J., Kumar, S., Campagnoli, C., Bennett, P.R., Roberts, I.A.G., and Fisk, N.M. (2003). Identification of fetal mesenchymal stem cells in maternal blood: implications for non-invasive prenatal diagnosis. Mol Hum Reprod 9, 497-502.

O'Donoghue, K., Sultan, H.A., Ai-Allaf, F.A., Anderson, J.R., Wyatt-Ashmead, J., and Fisk, N.M. (2008). Microchimeric fetal cells cluster at sites of tissue injury in lung decades after pregnancy. Reprod Biomed Online 16, 382-390.

Okabe, M., Ikawa, M., Kominami, K., Nakanishi, T., and Nishimune, Y. (1997). 'Green mice' as a source of ubiquitous green cells. FEBS Lett 407, 313-319.

Osada, H., Doi, S., Fukushima, T., Nakauchi, H., Seki, K., and Sekiya, S. (2001). Detection of fetal HPCs in maternal circulation after delivery. Transfusion 41, 499-503.

Parant, O., Dubernard, G., Challier, J., Oster, M., Uzan, S., Aractingi, S., and Khosrotehrani, K. (2009). CD34+cells in maternal placental blood are mainly fetal in origin and express endothelial markers. Lab Invest 89, 915-923.

Parolini, O., Alviano, F., Bergwerf, I., Boraschi, D., De Bari, C., De Waele, P., Dominici, M., Evangelista, M., Falk, W., Hennerbichler, S., et al. (2010). Toward cell therapy using placenta-derived cells: disease mechanisms, cell biology, preclinical studies, and regulatory aspects at the round table. Stem Cells Dev 19, 143-154.

Pavlidis, P., Li, Q.H., and Noble, W.S. (2003). The effect of replication on gene expression microarray experiments. Bioinformatics 19, 1620-1627.

Paxson, J.A., Parkin, C.D., Iyer, L.K., Mazan, M.R., Ingenito, E.P., and Hoffman, A.M. (2009). Global gene expression patterns in the post-pneumonectomy lung of adult mice. Respir Res 10, 92.

Peister, A., Mellad, J., Larson, B., Hall, B., Gibson, L., and Prockop, D. (2004). Adult stem cells from bone marrow (MSCs) isolated from different strains of inbred mice vary in surface epitopes, rates of proliferation, and differentiation potential. Blood 103, 1662-1668.

Pritchard, S., Hoffman, A.M., Johnson, K.L., and Bianchi, D.W. (2011). Pregnancy-associated progenitor cells: an under-recognized potential source of stem cells in maternal lung. Placenta 32, S298-S303.

Pritchard, S., Peter, I., Johnson, K.L., and Bianchi, D.W. (2012a). The natural history of fetal cells in postpartum murine maternal lung and bone marrow: a two-stage phenomenon. Chimerism 3, 59-64.

Pritchard, S., Wick, H.C., Slonim, D.K., Johnson, K.L., and Bianchi, D.W. (2012b). Comprehensive analysis of genes expressed by rare microchimeric fetal cells in the maternal mouse lung. Biol Reprod 87, 42.

Rak, J.M., Maestroni, L., Balandraud, N., Guis, S., Boudinet, H., Guzian, M.C., Yan, Z., Azzouz, D., Auger, I., Roudier, C., et al. (2009). Transfer of the shared epitope through microchimerism in women with rheumatoid arthritis. Arthritis Rheum 60, 73-80.

Randolph, S., Gooley, T., Warren, E., Appelbaum, F., and Riddell, S. (2004). Female donors contribute to a selective graft-versus-leukemia effect in male recipients of HLA-matched, related hematopoietic stem cell transplants. Blood 103, 347-352.

Reed, E., Beer, A., Hutcherson, H., King, D., and Suciufoca, N. (1991). The alloantibody response of pregnant women and its suppression by soluble HLA antigens and antiidiotypic antibodies. J Reprod Immunol 20, 115-128.

Rieger, L., Hofmeister, V., Probe, C., Dietl, J., Weiss, E.H., Steck, T., and Kammerer, U. (2002). Th1- and Th2-like cytokine production by first trimester decidual large granular lymphocytes is influenced by HLA-G and HLA-E. Mol Hum Reprod 8, 255-261.

Rockett, J., and Hellmann, G. (2004). Confirming microarray data--is it really necessary? Genomics 83, 541-549.

Rudek, Z., and Kwiatkowska, L. (1983). The possibility of detecting fetal lymphocytes in the maternal blood of the domestic pig, Sus scrofa. Cytogenet Cell Genet 36, 580-583.

Saadai, P., Lee, T., Bautista, G., Gonzales, K.D., Nijagal, A., Busch, M.P., Kim, C.J., Romero, R., Lee, H., Hirose, S., et al. (2012). Alterations in maternal-fetal cellular trafficking after fetal surgery. J Pediatr Surg 47, 1089-1094.

Salamone, G., Fraccaroli, L., Gori, S., Grasso, E., Paparini, D., Geffner, J., Perez Leiros, C., and Ramhorst, R. (2012). Trophoblast cells induce a tolerogenic profile in dendritic cells. Hum. Reprod. 27, 2598-2606.

Santos, M.A., O'Donoghue, K., Wyatt-Ashmead, J., and Fisk, N.M. (2008). Fetal cells in the maternal appendix: a marker of inflammation or fetal tissue repair? Hum Reprod 23, 2319-2325.

Sati, L., Seval-Celik, Y., and Demir, R. (2010). Lung surfactant proteins in the early human placenta. Histochem Cell Biol 133, 85-93.

Sawaya, H.H.B., Jimenez, S.A., and Artlett, C.M. (2004). Quantification of fetal microchimeric cells in clinically affected and unaffected skin of patients with systemic sclerosis. Rheumatology 43, 965-968.

Schaible, B., Schaffer, K., and Taylor, C.T. (2010). Hypoxia, innate immunity and infection in the lung. Respir Physiol Neurobiol 174, 235-243.

Scherjon, S., Lashley, L., van der Hoorn, M.-., and Claas, F. (2011). Fetus specific T cell modulation during fertilization, implantation and pregnancy. Placenta 32, S291-S297.

Schroder, J. (1975). Transplacental passage of blood cells. J Med Genet 12, 230-242.

Schroder, J., and Chapelle, A.D. (1972). Fetal lymphocytes in the maternal blood. Blood 39, 153-162.

Schroder, J., Tiilikai.a, and Chapelle, A.D. (1974). Fetal leukocytes in maternal circulation after delivery .1. Cytological aspects. Transplantation 17, 346-354.

Seppanen, E., Fisk, N.M., and Khosrotehrani, K. (2013). Pregnancy-acquired fetal progenitor cells. J Reprod Immunol 97, 27-35.

Seppanen, E.J., Hodgson, S.S., Khosrotehrani, K., Bou-Gharios, G., and Fisk, N.M. (2012). Fetal Microchimeric Cells in a Fetus-Treats-Its-Mother Paradigm Do Not Contribute to Dystrophin Production in Serially Parous mdx Females. Stem Cells Dev. 21, 2809-2816.

Srinivasan, A., Bianchi, D.W., Huang, H., Sehnert, A.J., and Rava, R.P. (2013). Noninvasive detection of fetal subchromosome abnormalities via deep sequencing of maternal plasma. Am J Hum Genet 92, 167-176.

Srivatsa, B., Srivatsa, S., Johnson, K.L., Samura, O., Lee, S.L., and Bianchi, D.W. (2001). Microchimerism of presumed fetal origin in thyroid specimens from women: a case-control study. Lancet 358, 2034-2038.

Stevens, A.M., McDonnell, W.M., Mullarkey, M.E., Pang, J.M., Leisenring, W., and Nelson, J.L. (2004). Liver biopsies from human females contain male hepatocytes in the absence of transplantation. Lab Invest 84, 1603-1609.

Strumpf, D., Mao, C.A., Yamanaka, Y., Ralston, A., Chawengsaksophak, K., Beck, F., and Rossant, J. (2005). Cdx2 is required for correct cell fate specification and differentiation of trophectoderm in the mouse blastocyst. Development 132, 2093-2102.

Sugiyama, T., Kohara, H., Noda, M., and Nagasawa, T. (2006). Maintenance of the hematopoietic stem cell pool by CXCL12-CXCR4 chemokine signaling in bone marrow stromal cell niches. Immunity 25, 977-988.

Summer, R., and Fine, A. (2008). Mesenchymal progenitor cell research: limitations and recommendations. Proc Am Thorac Soc 5, 707-710.

Summer, R., Fitzsimmons, K., Dwyer, D., Murphy, J., and Fine, A. (2007). Isolation of an adult mouse lung mesenchymal progenitor cell population. Am J Respir Cell Mol Biol 37, 152-159.

Sunami, R., Komuro, M., Yuminamochi, T., Hoshi, K., and Hirata, S. (2010). Fetal cell microchimerism develops through the migration of fetus-derived cells to the maternal organs early after implantation. J Reprod Immunol 84, 117-123.

Sung, J.F., Fan, X., Dhal, S., Dwyer, B.K., Jafari, A., El-Sayed, Y.Y., Druzin, M.L., and Nayak, N.R. (2011). Decreased circulating soluble Tie2 levels in preeclampsia may result from inhibition of vascular endothelial growth factor (VEGF) signaling. J Clin Endocrinol Metab 96, E1148-E1152.

Sverzellati, N., Calabrò, E., Randi, G., La Vecchia, C., Marchianò, A., Kuhnigk, J.M., Zompatori, M., Spagnolo, P., and Pastorino, U. (2009). Sex differences in emphysema phenotype in smokers without airflow obstruction. Eur Respir J. 33, 1320-1328.

Taglauer, E.S., Waldorf, K.M.A., and Petroff, M.G. (2010). The hidden maternal-fetal interface: events involving the lymphoid organs in maternal-fetal tolerance. Int J Dev Biol 54, 421-430.

Tan, X.W., Liao, H., Sun, L., Okabe, M., Xiao, Z.C., and Dawe, G.S. (2005). Fetal microchimerism in the maternal mouse brain: a novel population of fetal progenitor or stem cells able to cross the blood-brain barrier? Stem Cells 23, 1443-1452.

Tanaka, A., Lindor, K., Gish, R., Batts, K., Shiratori, Y., Omata, M., Nelson, J.L., Ansari, A., Coppel, R., Newsome, M., and Gershwin, M.E. (1999). Fetal microchimerism alone does not contribute to the induction of primary biliary cirrhosis. Hepatology 30, 833-838.

Tarleton, R.L., Koller, B.H., Latour, A., and Postan, M. (1992). Susceptibility of beta-2-microglobulin-deficient mice to Trypanosoma cruzi infection. Nature 356, 338-340.

Tarnok, A., Ulrich, H., and Bocsi, J. (2010). Phenotypes of stem cells from diverse origin. Cytometry A 77A, 6-10.

Thaxton, J.E., and Sharma, S. (2010). Interleukin-10: a multi-faceted agent of pregnancy. Am J Reprod Immunol 63, 482-491.

Theiler, K. (1989). The House Mouse: Atlas of Embryonic Development.(New York: Springer-Verlag).

Thorrez, L., Van Deun, K., Tranchevent, L., Van Lommel, L., Engelen, K., Marchal, K., Moreau, Y., Van Mechelen, I., and Schuit, F. (2008). Using ribosomal protein genes as reference: a tale of caution. PLoS One 3, e1854.

Toda, I., Kuwana, M., Tsubota, K., and Kawakami, Y. (2001). Lack of evidence for an increased microchimerism in the circulation of patients with Sjogren's syndrome. Ann Rheum Dis 60, 248-253.

Tokita, K., Terasaki, P., Maruya, E., and Saji, H. (2001). Tumour regression following stem cell infusion from daughter to microchimeric mother. Lancet 358, 2047-2048.

Tse, W.W., Zang, S.L., Bunting, K.D., and Laughlin, M.J. (2008). Umbilical cord blood transplantation in adult myeloid leukemia. Bone Marrow Transplant 41, 465-472.

Turin, L., Invernizzi, P., Woodcock, M., Grati, F.R., Riva, F., Tribbioli, G., and Laible, G. (2007). Bovine fetal microchimerism in normal and embryo transfer pregnancies and its implications for biotechnology applications in cattle. Biotechnol J 2, 486-491.

van Rood, J., Loberiza, F., Zhang, M., Oudshoorn, M., Claas, F., Cairo, M., Champlin, R., Gale, R., Ringden, O., Hows, J., and Horowitz, M. (2002). Effect of tolerance to noninherited maternal antigens on the occurrence of graft-versus-host disease after bone marrow transplantation from a parent or an HLA-haploidentical sibling. Blood 99, 1572-1577.

Vernochet, C., Caucheteux, S.M., and Kanellopoulos-Langevin, C. (2007). Bi-directional cell trafficking between mother and fetus in mouse placenta. Placenta 28, 639-649.

von Garnieir, C., and Nicod, L.P. (2009). Immunology taught by lung dendritic cells. Swiss Med Wkly 139, 186-192.

Wagner, W., Saffrich, R., and Ho, A.D. (2008). The stromal activity of mesenchymal stromal cells. Transfus Med Hemother 35, 185-193.

Walknows.J, Conte, F.A., and Gumbach, M.M. (1969). Practical and theoretical implications of fetal/maternal lymphocyte transfer. Lancet 1, 1119-1122.

Wang, C., Su, P., Du, X., Kuo, M., Lin, C., Yang, C., Chan, H., Chang, S., Kuo, C., Seo, K., Leung, L.L., and Chuan, Y. (2010). Thrombospondin type I domain containing 7A (THSD7A) mediates endothelial cell migration and tube formation. J Cell Physiol 222, 685-694.

Wang, Y., Iwatani, H., Ito, T., Horimoto, N., Yamato, M., Matsui, I., Imai, E., and Hori, M. (2004). Fetal cells in mother rats contribute to the remodeling of liver and kidney after injury. Biochem Biophys Res Commun 325, 961-967.

Wataganara, T., Gratacos, E., Jani, J., Becker, J., Lewi, L., Sullivan, L., Bianchi, D., and Deprest, J. (2005). Persistent elevation of cell-free fetal DNA levels in maternal plasma after selective laser coagulation of chorionic plate anastomoses in severe midgestational twin-twin transfusion syndrome. Am J Obstet Gynecol 192, 604-609.

Wegmann, T., Lin, H., Guilbert, L., and Mosmann, T. (1993). Bidirectional cytokine interactions in the maternal-fetal relationship: is successful pregnancy a TH2 phenomenon? Immunol Today 14, 353-356.

Williams, Z., Zepf, D., Longtine, J., Anchan, R., Broadman, B., Missmer, S.A., and Hornstein, M.D. (2009). Foreign fetal cells persist in the maternal circulation. Fertil Steril 91, 2593-2595.

Wognum, A., Eaves, A., and Thomas, T. (2003). Identification and isolation of hematopoietic stem cells. Arch Med Res 34, 461-475.

Wu, C., Orozco, C., Boyer, J., Leglise, M., Goodale, J., Batalov, S., Hodge, C.L., Haase, J., Janes, J., Huss, J.W.,III, and Su, A.I. (2009). BioGPS: an extensible and customizable portal for querying and organizing gene annotation resources. Genome Biol 10, R130.

Yamada, M., Kubo, H., Kobayashi, S., Ishizawa, K., Numasaki, M., Ueda, S., Suzuki, T., and Sasaki, H. (2004). Bone marrow-derived progenitor cells are important for lung repair after lipopolysaccharide-induced lung injury. J Immunol 172, 1266-1272.

Yan, Z., Aydelotte, T., Gadi, V.K., Guthrie, K.A., and Nelson, J.L. (2011). Acquisition of the rheumatoid arthritis HLA shared epitope through microchimerism. Arthritis Rheum 63, 640-644.

Zenclussen, A. (2005). CD4(+)CD25(+) T regulatory cells in murine pregnancy. J Reprod Immunol 65, 101-110.

Zeng, X.X., Tan, K.H., Yeo, A., Sasajala, P., Tan, X., Xiao, Z.C., Dawe, G., and Udolph, G. (2010). Pregnancy-associated progenitor cells differentiate and mature into neurons in the maternal brain. Stem Cells Dev 19, 1819-1830.

Zhang, J., and Patel, G. (2007). Partner change and perinatal outcomes: a systematic review. Paediatr Perinat Epidemiol 21, 46-57.

Zhong, J.F., and Weiner, L.P. (2007). Role of fetal stem cells in maternal tissue regeneration. Gene Regul Syst Bio 1, 111-115.

Zhong, X., Holzgreve, W., Li, J., Aydinli, K., and Hahn, S. (2000). High levels of fetal erythroblasts and fetal extracellular DNA in the peripheral blood of a pregnant woman with idiopathic polyhydramnios: case report. Prenat Diagn 20, 838-841.

Zipursky, A., Hull, A., White, F.D., and Israels, L.G. (1959). Foetal erythrocytes in the maternal circulation. Lancet 1, 451-452.